UNITED NATIONS UNIVERSITY
GEOTHERMAL TRAINING PROGRAMME
Orkustofnun, Grensásvegur 9,
IS-108 Reykjavík, Iceland

Reports 2008
Number 3

FEASIBILITY STUDY OF GEOTHERMAL UTILIZATION OF YANGBAJAIN FIELD IN TIBET AUTONOMOUS REGION, P.R. CHINA

MSc thesis
Department of Mechanical and Industrial Engineering
University of Iceland

by

Sun Caixia
Beijing Institute of Geo-Exploration and Technology
No. A2. Lishuigiao, Chaoyang District
Beijing
P.R. CHINA
susan616128@hotmail.com

United Nations University
Geothermal Training Programme
Reykjavík, Iceland
Published in December 2008

ISBN 978-9979-68-249-3
ISSN 1670-7427

This MSc thesis has also been published in June 2008 by the
Faculty of Engineering – Department of Mechanical and Industrial Engineering,
University of Iceland

INTRODUCTION

The Geothermal Training Programme of the United Nations University (UNU) has operated in Iceland since 1979 with six month annual courses for professionals from developing countries. The aim is to assist developing countries with significant geothermal potential to build up groups of specialists that cover most aspects of geothermal exploration and development. During 1979-2008, 402 scientists and engineers from 43 countries have completed the six month courses. They have come from Asia (44%), Africa (26%), Central America (15%), and Central and Eastern Europe (15%). There is a steady flow of requests from all over the world for the six month training and we can only meet a portion of the requests. Most of the trainees are awarded UNU Fellowships financed by the UNU and the Government of Iceland.

Candidates for the six month specialized training must have at least a BSc degree and a minimum of one year practical experience in geothermal work in their home countries prior to the training. Many of our trainees have already completed their MSc or PhD degrees when they come to Iceland, but several excellent students have made requests to come again to Iceland for a higher academic degree. In 1999, it was decided to start admitting UNU Fellows to continue their studies and study for MSc degrees in geothermal science or engineering in co-operation with the University of Iceland. An agreement to this effect was signed with the University of Iceland. The six month studies at the UNU Geothermal Training Programme form a part of the graduate programme. Six UNU-GTP MSc Fellows completed their MSc degree in 2008, the biggest group to date.

It is a pleasure to introduce the first woman and the thirteenth UNU Fellow to complete the MSc studies at the University of Iceland under the co-operation agreement, Ms. Sun Caixia of the Beijing Institute of Geo-Exploration and Technology – BIGET. She has a BSc in Mechanical Engineering from the Inner Mongolia University of Science and Technology and completed the six month specialized training in Geothermal Utilization at the UNU Geothermal Training Programme in October 2005. Her research report was entitled “A different approach for an existing geothermal utilization project in Beijing”. A year later, in September 2006, she came back to Iceland for MSc studies in Mechanical Engineering at the Department of Mechanical and Industrial Engineering, within the Faculty of Engineering of the University of Iceland. In May 2008, she defended her MSc thesis presented here, entitled “Feasibility study of geothermal utilization of Yangbajain field in Tibet Autonomous Region, P.R. China”. Her studies in Iceland were financed by a fellowship from the Government of Iceland through the UNU Geothermal Training Programme. We congratulate Ms. Sun Caixia on her achievements and wish her all the best for the future. We thank the Department of Mechanical and Industrial Engineering of the University of Iceland for the co-operation, and her supervisors for the dedication.

Finally, I would like to mention that Caixia’s MSc thesis with the figures in colour is available for downloading on our website at page *www.unugtp.is/yearbook/2008.*

With warmest wishes from Iceland,

Ingvar B. Fridleifsson, director
United Nations University
Geothermal Training Programme

ACKNOWLEDGEMENTS

I would like to express my gratitude to all those who gave me the possibility to complete this thesis. I want to acknowledge United Nations University - Geothermal Training Programme for the financial support to my MSc study in the University of Iceland. I sincerely want to express my appreciation to the director of UNU-GTP, Dr. Ingvar B. Fridleifsson, and the deputy director, Mr. Lúdvík S. Georgsson for giving me this precious study opportunity and their selfless dedication.

I am deepest and sincerest grateful to my supervisor Dr. Páll Valdimarsson for his excellent and generous technical help and the heartfelt support and encouragement during my thesis study. Also I want to express my sincerest gratitude to Dr. Thorleikur Jóhannesson from Fjarhitun Consulting Engineering for sharing his deep knowledge and great help. I would also like to thank Thorbjörg Saemundsdóttir from Enex Consulting Engineering for her kindly help in financial study of the thesis.

My devout thanks to the professors in Engineering Faculty of the University of Iceland for their patient teaching and sharing their knowledge and experiences during these two years study. I would also like to thank all the fellows in UNU-GTP for the memorable friendship the experience. I would like to thank all staff and our assistants from Orkustofnun (Nation Energy Authority of Iceland) and ISOR (Icelandic Geo-Survey) for their kindness.

Finally, I would like to express my deepest appreciation to my family, my parents and sister for their moral supports. Especially, I want to express my heartfelt gratitude to my husband whose love and encouragement enabled me to complete this work.

ABSTRACT

This study investigates the feasibility of the renewable energy utilization in Tibet, which is known as the “world roof” with highest elevation and splendid natural scenery. Based on the available energy assessment and market analysis, a technical and economic feasibility study is carried out on geothermal utilization of Yangbajain field with the objective of solving both electricity shortage and lack of space heating so as to improve the Tibetan people’s living condition.

The technical feasibility study is to set up thermodynamic model of proposed different power generation scenarios and long distance district heating system to analyze and optimize each scenario by using EES and Matlab programmes. Four alternative scenarios optimized for new power plant design are double flash cycle (Scenario 1), hybrid single flash and ORC cycle with isopentane as working fluid (Scenario 2), pure ORC cycle with isobutane as working fluid (Scenario 3), and hybrid single flash and Kalina cycle (Scenario 4). The conceptual design of district heating system with about 90km distance from Yangbajain to Lhasa is as well carried out. The results indicate that all power cycles are technically feasible at different efficiency and heating system can be put up under appropriate design and construction.

A financial viability evaluation is performed for all scenarios using engineering economic Present Worth (PW) value analysis method with objective to figure out Internal Rate of Return (IRR) of each system. The most optimum power cycle scenario is Scenario 1 with IRR value of 31.84%, followed by Scenario 2 with IRR value of 22.15%. The district heating system has low IRR value of 3.13% due to the high investment cost of long distance transmission pipeline. However, as an entire system of CHP power plant, the optimum system can yield 8.92% IRR value at pure commercial investment level. Since it will be a subsidized programme from the central government, it can reach 10.78% of IRR value without loan interest payment. If the expected IRR of the investment company is 10.00%, it proves this project is economically feasible.

The environmental protection in Tibet is the most important to be emphasized to carry out such a big infrastructure project. As a renewable energy application, this project will benefit the region and local people. At the same time, environmental protection should be conducted during the whole process of proposal, designing and implementation for sustainable development.

TABLE OF CONTENTS

Page

Page

LIST OF FIGURES

Page

LIST OF TABLES

Page

1. INTRODUCTION

1.1 Main concerns of the study

This study deals with two main concerns, which is about power supply and district heating system in Tibet. It is widely known that energy is substantial basis of the economic and social development of a country or region. It relates to the infrastructure construction, public service supply and basically the quality of life. Due to the special geographic location and historical reasons, Tibet remains behind of other regions or provinces in different aspects of development. However, the central government has been giving special support and aid especially since the reform and opening up policies started in 1979. The local people's life has been improved significantly. In this report, the main emphasis is focusing on how to make good and full use of the local energy potential especially geothermal energy to work on improving people's standard of living.

First of all, the local energy status of potential and utilization is discussed. There are very few conventional resources in Tibet but abundant renewable energy such as hydro, geothermal, solar and biomass energy, etc. Hydro power is the main support of power supply in Tibet. But it has disadvantage that the water flow is in shortage in winter. Geothermal is an important supplement, especially during winter time. Since there's big potential in Yangbajain field, this report is focusing on the full use of the geothermal utilization to solve the problem.

1.2 An overview of the present work

The work of this study is primarily about the geothermal energy utilization performance analysis and feasibility research. The final objective is to work out the most technical and economic feasible solution to meet the power and district heating system demand in Tibet. Geothermal potential from Yangbajain field as a substantial support to hydropower in Tibet plays significant role in supplying electricity for Lhasa especially in winter, as well as the direct use application. The present work focuses on the multi-use of geothermal energy which is structured as follows:

Chapter 2 is a literature review and status of energy assessment and utilization. The related studies of the energy project are discussed such as the hydropower, geothermal energy, solar and wind, as well as the bio-energy utilization. Chapter 3 presents market analysis and proposed project background. Chapter 4, 5, 6 as the main part of the study deals with feasibility study of the utilization of Yangbajain geothermal potential. Different alternatives are carried out to make comparison based on the technical and economic analysis. The final and optimum solution will be drawn out. Therein chapter 4 concerns power generation study on the basis of latest reservoir assessment. Chapter 5 is to continue the regeneration part supplying district heating system for Lhasa. Chapter 6 gives the economic evaluation and analysis for both power generation and districting heating system. Based on the above studies, the comprehensive and viable solution is recommended. It is followed by the environmental and sustainable concerns study in Chapter 7. The conclusions and recommendations are given in Chapter 8.

2. LITERATURE REVIEW AND ENERGY ASSESSMENT

2.1 Brief introduction of Tibet and Lhasa

Tibet, as the second largest Autonomous Region in China, is located at main section of Qinghai-Tibet plateau, the southwest frontier of China. The total area is about 1.22 million km^2. About 100 million years ago, this place was a sea. With continuous collisions between the Indian Continent and the Eurasian Continent, it was then gradually transformed into today's "world roof" with the average elevation of over 4,000 m. Tibet is China's southwest barrier (Figure 1). Tibet Plateau is the main body of the Qinghai-Tibet Plateau, consisting of high mountains and great rivers, prairie and gorges. It is also one of the regions in the world with the most gorges. The region has over 1500 lakes including 47 with over 100 km^2. Lake area stands at 24,183km^2, representing over one-third of the total lake area in China. It has complicated and unique climate. Main features are thin air, low atmospheric pressure, scant oxygen, high elevation, strong sunlight, long sunlight radiation, low temperature with small annual difference but big daily difference, distinct dry season and rainy season, much night rain, and complicated climate categories with big vertical changes.

FIGURE 1: Tibet Autonomous Region in China

Tibet has a population of 2.74 million, including Tibetan, Han, Hui, Menba, Geba, Nu and Naxi people and as Deng and Xiaerba ethnic groups. Tibetan people make up 96.5% of total population. Lhasa is the capital city as a political, economic and cultural centre. The average altitude is 3648 meters, and the average yearly temperature is 8.5°C with 3021 hours of sunshine because of which it is named Sunshine City. The total area of Lhasa region is nearly 30,000km^2, therein the downtown area is 523km^2. At present, the public transportation system in Tibet has been developing steadily. There are domestic flights to major big cities and international flights to Kathmandu Nepal. The highway condition is getting better and better. The new Qinghai-Tibet railway opened on July 1st, 2006 has significantly facilitated the economic and social development of the entire region.

Tibet lags behind other regions or provinces in many areas, including economy, literacy rates, life expectancy and average per-capita income, which is under $250 a year in rural areas. However, since the implementation of reform and opening-up policy in China, the region's economy has been developing, the society has been stable, and the living standard has been improving. The central government and the local government are making great effort to change the behind situation in Tibet. Even though, there are still 42% of the population have no access to electricity. The application of space heating system is still very old. There is no more than 10% of the construction area with heating system which is normally coal burning boiler system. In order to improve the local people's life quality, the central government has decided to support the new energy projects to solve these basic problems in the period of "11th Five Year Plan" (2005-2010) and "12th Five Year Plan"(2011-2015).

2.2 Energy assessment and utilization

2.2.1 Main energy resource assessment

The energy in Tibet is weak in conventional resource, but rich in renewable energy. The total reservoir of coal including explored and potential is no more than 0.3 billion ton. The potential of oil resource

has not yet been proven. However, the potential of hydro resource reservoir is 200 GW, accounting for 29% of the total amount of the whole country and rating the first in the country. Therein, reservoirs can be used to build hydro power plant with more than 500kW capacity is about 110 GW, accounting for 25% of the total amount of the whole country and rating the second in the country. Wind and geothermal energy are also abundant. The potential of geothermal for electricity generation is about 800 MW, and the potential of wind energy is 93 billion kWh. The solar energy in Tibet is the most abundant among all provinces or regions in the country. The radiation duration is totally more than 3000 hours in many areas, and the energy capacity of radiation is around 6000-8000 MJ/m^2/year. In addition, the biomass energy in Tibet is also rich. The total amount of forest residue amounts to 2.7 million ton coal equivalent, rating the first in the country. The yearly production of dry dung amounts to 1.7 million son coal equivalent, which the primary fuel in the rural area.

Generally, the proportion of renewable energy is larger than the conventional and the energy is distributed unbalanced. The southeast of the region is more abundant than the northwest. The low level of resource exploration influenced the exploitation and utilization.

2.2.2 General energy utilization and status

Since the special geographic location and the high elevation with average 4000m, as well as the low population density in the region, it is relatively difficult to explore the energy potential and construct the infrastructure. However, the central government has been giving high attention to its economic and social development. There have been 222 supporting projects for Tibet since 1984 to 2001. Therein, energy project was always the emphasis, and accounted for the majority of all the projects.

The electric power generation construction is the most important and basic application of energy and also influences people's lives significantly. The primary energy to generate electric power in Tibet is hydro power due to the abundant potential. Since the region's liberation, the central government has invested billions of yuan cumulatively to construct medium-small scale hydro power plants. In the period of "9^{th} Five Year Planning (1995-2000)", many large scale power plants have been built such as Yanghu, Wokahe and Manla projects. In addition, the geothermal power plants also have generated electricity around 28 MW. The power grid has been completed in the middle of Tibet.

Till the end of 2004, the total installation capacity of electric power throughout the region was 500 MW, the yearly power production was nearly 1.2 billion kWh. Therein, the installation capacity for towns or cities were 330 MW, yearly production was 1 billion kWh. The small scale capacity was around 160 MW, yearly production was 0.2 billion kWh. The capacity per capita of the region was 180 W, and the yearly electricity consumption per capita was 450 kWh. The total electricity consumers were around 1.6 million, which accounted for 60%. The electrified rate of the town and village were 71% and 41% respectively. The electric power grid has covered 30 counties with the consumers of 1.2 million.

2.2.3 Utilization of conventional energy

As stated before, the potential of conventional energy in Tibet is very limited. There's very rare coal in Tibet according to the exploration. The potential in the whole region are mainly distributed in Changdu, Naqu and Ali areas. The production in 1991 was only 10,000 tons, and it only increased to twice in 2003. Up to now the most production is 25,000 tons which can never meet the demand. Therefore, the main solution is to import from other provinces. The annual imported coal is about 100,000 tons. Because of the high transportation cost, the local coal price is roughly double to that of the other areas.

Oil resource is still under exploration, the potential has not been evaluated yet. The annually imported oil by transportation and Golmud-Lhasa oil transmission pipeline is about 150,000~200,000 tons/year to fulfil the transportation and living needs. There's no natural gas proven yet. But in the neighbour province it is abundant. Therefore, it is also possible to import from the others. Due to the shortage of fossil energy resource, until now, most of the coal, oil and LPG (liquefied petroleum gas) are

transported from elsewhere at least 1,000km away by road or pipeline. Since the opening of new railway, the transportation has been facilitated. The main purpose of conventional energy is that coal is mostly used for cement industry, and the oil is for transportation and LPG for cooking.

2.2.4 Utilization of hydropower

Tibet is Asia's principal watershed and the source of its major rivers. A substantial proportion of river flows in Tibet are stable or base flows coming from ground water and glacial sources. This is in marked contrast to river flows in most neighbour countries, which are determined by seasonal rainfall patterns. 90% of Tibet's river run-off flows down across its borders, internal use accounting for less than 1% of total river run-off. Steep slopes and abundant river flows give Tibet an exploitable hydropower potential of 250,000 MW, the highest of any country in the world. Since 1980s, hydro power has been developed very rapidly in Tibet. The total installed capacity in 1990 and 2000 has been the double of 10 years before. After entering the "Tenth Five Year Plan" (From 2001 to 2005), the development is even faster with average annually increase of 0.12 billion kWh.

Due to the specific geographic and population distribution features, small hydro power plant plays an important role in Tibet's rural electrification. 48.4% of townships, 37.1% of villages and 25.9% of families are electrified by small hydro power plants. A central government sponsored program called "Sending Electricity to Villages" has been launched in Tibet to provide electricity to the remaining villages, which have no access to electricity grid.

The first generating unit in a 100 MW hydropower project has been finally in operation in late 2006, which is the biggest hydropower project in Tibet. The hydropower plant, with four generating units, each with a capacity of 25 MW, started construction in May 2003. The project has 80% of its 1.34 billion yuan (about US$165 million) investment from state coffers. Apart from power generation, the hydropower project will also have a role to play in flood control and irrigation. The hydro resource been used in this power plant is the Lhasa River, which originates in the southern foot of the towering Nyainqentanglha Range, flows through the eastern suburbs of Lhasa, and then joins the Yarlung Tsangpo River, which is also known as Brahmaputra as it flows out of China.

According to a survey of potential hydropower resources across China, Tibet could turn out 110 GW of hydropower and is second only to Sichuan in view of unexploited energy potential. So far, hydropower facilities with a total installed capacity of roughly 500MW have been built across rivers in Tibet. Hydro power is the main support of electric construction in Tibet with the high proportion almost 90%.

2.2.5 Utilization of solar and wind energy

Tibet possesses the world's highest solar energy potential followed by the Sahara. **S**ince 1980s, the utilization of solar energy has been introduced in primary energy construction in rural areas of Tibet and gradually some other programmes have implemented such as Sunshine, the Shine of Science and Electricity and Solar in Ali area plan. These projects have solved the problem of the lack of electricity for some pastoral areas. Tibet has the largest numbers of photovoltaic power plants using solar energy in China with totally 300 projects with the gross capacity 7000 kW mainly in the remote areas. The heat utilization of solar energy is also used widely, especially using for cooking in households.

In addition, there are 1000 small-scale wind power generators installed in the rural areas to meet the basic electricity demand. Wind power cannot work in most areas of Tibet, due to variable winds and thin air, plus difficulty covering distances to do maintenance.

2.2.6 Utilization of biomass energy

Due to the long distance transportation and the high cost of the fossil energy, energy consumption in Tibet is dominated by traditional biomass. In 2003, the total amount of energy consumption is about 2 million tons of coal equivalents (tce), of which the traditional biomass accounts for 70%. At present,

utilization of the biomass in Tibet is of low efficiency and proceeds in a way that rapidly degrades the environment and causes desertification. The local residents almost entirely depend on the traditional biomass for cooking and space heating. Most of the biomass is directly burned as fuel for cooking. Due to shortage of oxygen in Tibet and use of outdated stoves, the burning efficiency is very low, utilizing less 10 percent of the potential energy of biomass.

Traditional space heating consumes a lot of traditional biomass, which include straw, firewood and animal dung. Cattle dung and straw, in particular, are used as the main fuels in the rural area as well as in towns. Excessive utilization of straw and animal dung has degraded the local environment. In 2003, about 24,300 km^2 of grassland was degraded by desertification, accounting for 3% of all grassland in Tibet. As the vegetation cover rate has dropped greatly, sandstorms and droughts occur more frequently.

In recent years, some new utilization has been developed like biogas. Biogas is a fuel source produced by the decomposition, or digestion, of organic matter. In both Tibet and in Changshui, GEI (Global Environmental Institute) uses "continuous feeding systems", where farmers add manure and other organic matter to two underground basins. They then add water to break down the material and pump it into an airtight "digester" through a pipe. From the digester, the biogas travels through a hose straight to appliances in the farmers' homes, where it can be used as fuel for cooking and heating - and even to generate electricity. It has been developed quite well.

2.2.7 Utilization of geothermal energy

Tibet is famous for the most abundant high temperature geothermal resource in China. There are around 672 geothermal active areas (spots) appeared on Tibet Plateau including geysers, hydrothermal explosions, steaming grounds, fumaroles, and boiling springs. The estimated reservoir temperatures vary from 170 to 270℃. High temperature geothermal fields in Tibet are located mostly along the two sides of the Yarlung Zangbo River, which runs along the junction of the Eurasian and Indian Plates.

The most well-known field, Yangbajain geothermal field is located at the foot of Nyenchen Tanglha Mountain which is about 90 km to the northwest of Lhasa City, capital of Tibet. The elevation is between 4300 and 4500 m. The field has a total area of about 15 km^2, although the accessible part of the upper reservoir from which hot fluids can be produced covers only about 4 km^2. The field is controlled by a crisscross of fault systems. There are three northeast compression shear faults and three perpendicular northwest tension shear faults to form the boundaries of the field. There is dense and hard granite in the basement of Yangbajain. The faults extend deep into the reservoir and there are basement faults passing through the reservoir. The hot water flows up along the faults in the basement to the Quaternary grit layer to form a shallow reservoir.

Exploration of geothermal resources initiated in 1976. Geological studies, geophysical exploration and drilling program have been carried out in 5 geothermal fields. Until 1993, geothermal power plant has been built in Yangbajain, Nagqu and Langjiu geothermal fields respectively with total installed capacity of 27.18MWe. Geothermal power plant has been built in Nagqu with total installed capacity of 1 MWe, however, it's out of operations due to the scaling problem. The other power plant was built in Langjiu with installed capacity of 2MWe and is running only 1MWe.

Based on the geological conditions and the results of geophysical exploration, the reservoir can be divided into upper and lower two sections in Yangbajain field. From 1976 to 1984, reconnaissance has been carried out, including geological studies, geophysical and geochemical exploration as well as reservoir engineering testing. Information about straight graphics, tectonic activity, major hydro thermal activity and reservoir features, parameter of thermal fluid have been obtained, which provide basic data for development and utilization of geothermal field. Also some production wells have been drilled for establish of geothermal power plant. Based on the result of geophysical exploration and feature of geo-tectonics, the geothermal field can be divided into two areas, northern area and southern area with total area about 13.6km^2. From 1985 to 1991, based on the data obtained, development of upper geothermal resources has been carried out during this period, mainly for drilling of production

wells and providing thermal fluid to geothermal power plant for expending installed capacity. Until the end of 1991, 80 wells have been drilled of the depth for single well ranging from 90 to 600 m and total depth obtained about 20 km. The maximum downhole temperature was 172°C and total flow rate of steam and water of 1400 t/h.

Since 1977, a number of Chinese and foreign geothermal experts have come to Yangbajain and built a power plant. The United Nations Development Programme (UNDP) and the Italian government sent technicians and financial resources to Yangbajain power plant since July 1982, and with their help, the station was equipped with power generators with installed capacity of 10,000 kW in total in 1985. The Central Government has also invested 230 million yuan into Yangbajain until 1990, building it into a station that provides almost half of electricity that Lhasa needs. Lhasa relies on the Yangbajain geothermal station mostly during the winter when hydroelectricity stations couldn't generate enough power. It plays an important role for mitigating the pressure of electricity use in Lhasa. Yangbajain provides 41% of the electrical needs of Lhasa City, 60% in winter. Waste thermal water has been used to heat greenhouses with floor space of 50,000 m^2.

In 2000 the Japan International Cooperation Agency, a government body, also began to help to fund the power plant and worked out a plan to exploit geothermal energy deeper into the earth, which enables the power station to work for another 30 years. This work has taken 5 years from 2001 to 2006. They drilled an exploration well CJZK3001 for the survey work. Meanwhile, they did some geophysical and geochemical work in the existing well ZK4001 to assess the lower geothermal reservoir. According to their final assessment report, the total reasonable exploitation capacity of the steam in Yangbajain geothermal field could be 200 t/h in the following 30 years including both the upper and lower reservoirs.

In general, Tibet is weak in conventional recourses like coal, oil and natural gas but rich in the renewable energy like hydro, geothermal, bio-energy, etc. According to the statistics, the majority of the electricity is supplied by the hydropower plant, followed by the geothermal and solar. Solar energy research has been carried out for some years, which have proved positive results both for generating electricity and space heating. The most potential energy expected to be utilized is geothermal energy, which is presently an important electricity generation supplement for Lhasa especially in winter when the hydropower plant cannot ensure the full need. The estimated geothermal potential of geothermal is about 3096.45×10^{15} kJ.

3. ENERGY MARKET ANALYSES AND PROPOSED PROJECT BACKGROUND

3.1 Energy market analysis

According to the present energy potential and utilization status, the energy market in Tibet is still under exploration. Electricity is in serious shortage in Lhasa area which has a network output capacity very limited especially during winter. This is severely affecting the overall economic development of the region. Moreover, the natural environment is progressively being damaged by increasing forest cutting and use of animal waste. Except for a few major cities (Lhasa, Xigaze, Nagqu), the 2 million inhabitants of Tibet live in small rural centres scattered over a surface area of 1.5 million square kilometres at an average altitude of more than 4,000 meters. Due to such severe geographic and climatic conditions, communication is extremely difficult and consequently electricity distribution in Tibet is still limited.

Although fossil fuels are costly to import into the region, the consumption is growing and will continue to grow in the future by necessity, causing future stress to the overall economy and the very fragile environment of the Tibetan plateau. Further development of the hydroelectric potential might not result a cost-effective option with the current technology, due to Tibet's environment and social-economic conditions. Wood and animal excrement are to be preserved for ecological reasons.

Tibet is potentially rich in geothermal resources for both power generation and direct uses. In fact evidences of thermal anomalies in the shallow crust (thermal spring, hot grounds, and steaming vents) are scattered throughout Southern and Central Tibet. Shallow exploration wells drilled in the past by the Regional Government in several locations have yielded fluids of potential interest, both for direct uses and electricity generation. It is believed that geothermal energy could account for the majority of Tibet's energy needs.

The power generation structure is shown in Figure 2. It shows that the majority of the power is supplied by hydro power which makes up 87.8% of total supply. However, the total electricity has not been able to meet the local demand ever since. There are 4,850 villages, 0.21 million families and 1.1 million people without power supply (Zheng, 2002).

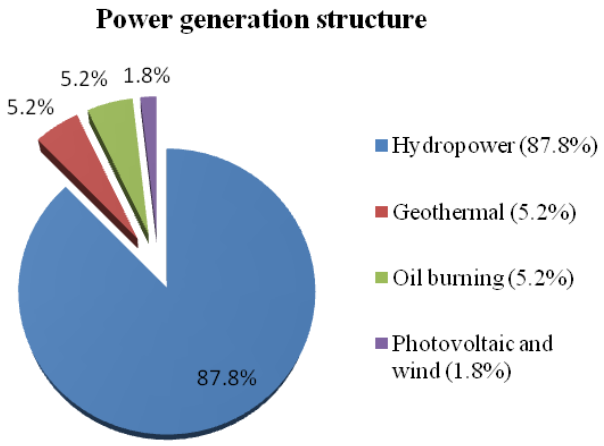

FIGURE 2: Power generation structure in Tibet

The power consumption structure in Tibet is shown in following Figure 3. It reveals clearly that the majority consumed part of the energy is residential consumption. Even though, the power is still not enough for all the people especially in the rural area.

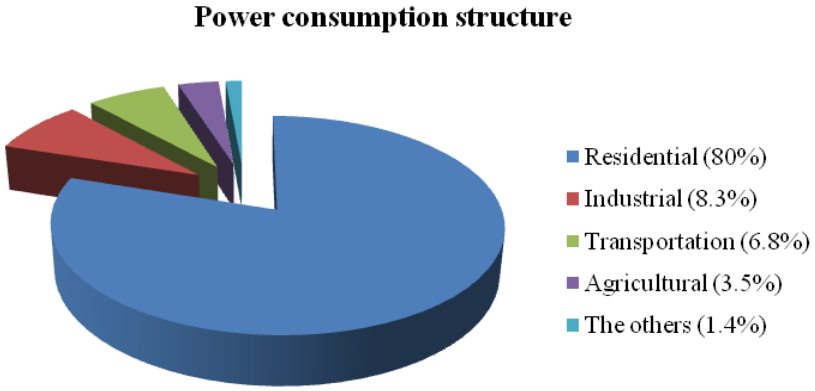

FIGURE 3: Power consumption structure in Tibet

3.1.1 Shortage of living energy in rural areas

In rural areas, the energy structure is shown in Table 1 below, it is shown that the energy used here is still very primal, even lots of people have to suffer from the cold in winter due to lack of heating energy. Besides, people burn a lot of animal excrement and turf to get heat. The consequence is the ecological balance of the soil, plant and grazing was broken, and has directly influenced the development of agriculture. Furthermore, it would be a big threat of the sustainable economic and social development of Tibet.

TABLE 1: Energy consumption status in rural areas of Tibet

Item	Amount (ton)	Percentage
Animal excrement	1,200,000	45%
Firewood	900,000	30%
Turf	400,000	17%
The others	-	8%

3.1.2 Shortage of power supply in cities and towns

The main energy for generating electricity in the cities and towns of Tibet is hydropower and geothermal. Some oil and coal are also used by transporting from Qinghai province and Xinjiang Autonomous Region, and mainly used in the transportation and public constructions. The power supplied is mostly for living energy, which accounts for 80% as stated above. And the majority of the consumers are the residents in the cities and towns. Even though, the supply is still tense. For instance, in the capital, Lhasa, the limited power using time is about 20-40%. Sometimes even illuminating power is not guaranteed.

3.1.3 Shortage of energy for heating system

There is no district heat supply in winter in Tibet and most of the local residents depend on the individual traditional space heating. Due to the long duration of cold winter, traditional space heating consumes a lot of traditional biomass, which include straw, firewood and animal dung. The cattle dung and straw, in particular, are used as the main fuels in the rural area as well as in towns. Excessive utilization of straw and animal dung has degraded the local environment. In 2003, about 2.43 million of grassland was degraded by desertification, accounting for 3% of all grassland in Tibet. As the vegetation cover rate has dropped greatly, sandstorms and droughts occur more frequently.

Meanwhile, the common form of heating system for public buildings is just using the gas or coal burning boiler as well as small solar system for households. All the renewable energy utilizing systems have been studied and tested for couples of years. The government has been trying to solve the problem and set the goal in the “Eleventh Five-Year Plan” to fulfil the heating system construction step by step.

Generally, the power supply of the Tibet is in shortage and basic district heating system construction is also urgently required.

3.2 Background of the proposed project

According to the energy utilization status, there are still 42% of the population has no access to electricity in Tibet, and only 10% of the building in Lhasa has heating system. The living standard of local people is far behind the other provinces or regions. However, a lot of changes have happened especially during last “Five Year Plan” from 2001 to 2005. The infrastructure development in Tibet has increased very fast such as the urban area has reached to 54 km^2 which is 18 times than 50 years before. Now it is already in the “Eleventh Five Year Plan”, there are more requirements and challenges to face. According to the energy development goal for “Eleventh Five Year Plan”, the energy

construction will be the emphasis of development. The main task is to develop renewable energy based on the electricity grid, and hydropower will still be the focus due to the abundant resource potential. Try to develop city district heating system to supply better living condition for the residence. The development goal is to solve the power supply problem in rural area and change the unbalance and shortage of power distribution situation, and improve the building heating condition in cities and towns by 2010.

Tibet as an important part of the country, the Central Government attaches importance to improving the standard of living of local people and developing the whole region. Energy supply as stated before is the most significant issue related to the regional development not only for the economy but also for the people's living quality. It is proposed to fulfil the district heating demand in Lhasa before the end of 2008 with majority of the government's support.

In long term development point of view, the hydro power and the geothermal energy will be the focus of large scale project construction. The energy construction project as the basic solution to improve the local people's living level will be the subsidized programme continuing supported by the central government. The proposed project is to make comprehensive use of Yangbajain geothermal potential to meet the power and space heating demand. The feasibility study is discussed in following chapters.

4. TECHNICAL FEASIBILITY STUDY OF POWER GENERATION

As stated previously, the most accessible and available energy in Tibet is hydro and geothermal energy. Hydro power is developing steadily and still accounts for the majority of total power supply in the region. But there's a disadvantage of hydro power which is lack of resource in winter. Geothermal energy as a renewable energy is abundant in Tibet especially in Yangbajain field and it has been supplying Lhasa electricity demand mostly in winter up to almost 50%. According to the survey report and practical experience, the existing power plants are already very old with non-efficient power output while the power demand in Tibet is still much more than it can offer. In this chapter in order to make the sustainable long term development of Yangbajain geothermal utilization, the upper and lower sections of the reservoir will be exploited simultaneously. Since there are many different approaches to generate power, this study considers four alternative scenarios with respect to the electricity generation and heating system supply.

4.1 Primary power cycle overview

In theory, unless there are specific exploitation restrictions that must be considered, the most economic generation of electricity from high temperature geothermal recourses is generally achieved from conventional steam turbine plants (i.e. Single/Double flash system). Therein, double flash cycle is most used in this field which accounts for roughly 25% of the world's total installation capacities. For low to medium temperature geothermal resource, the binary fluid technology has been developed primarily to generate electricity. This binary system utilizes a secondary working fluid, typically isobutane, isopentane or some mixture of them, which has a low boiling point and high vapor pressure at low temperature compared with steam. The secondary fluid is operated through an ORC (Organic Rankine Cycle) or another modification form, known as Kalina cycle which utilized a water/ammonia mixture for the process fluid.

4.1.1 Flash cycle system

Flash cycle is the simplest and conventional form for high temperature geothermal power generation. Most geothermal wells produce two phase fluids, consisting of brine and steam. Sometimes the fluids also contain non condensable gases and solid particles. The water and solid particles are separated from the steam and gases using a separator. The separator works by principle of centrifugal forces and density differences. The isobaric process takes place in the separator, where geothermal fluid first go through a throttling valve which can create pressure drop so as to maintain the required separation pressure. It can be assumed that the enthalpy of geothermal fluid flowing up from the well is constant, which means it is isenthalpic process by assuming there's no heat loss from the well to the surroundings. Thus, the state of separation geothermal fluid can be calculated based on the enthalpy and pressure. The process of ideal separator is relatively simple since the outlets are saturated steam and saturated brine. The saturated steam will direct to the turbine which is coupled with generator to produce power. The steam quality of the fluid is given by the equation:

$$h_1 = h_2 \tag{1}$$

$$\dot{m}_{steam} = x_2 \cdot \dot{m}_{mixture} \tag{2}$$

$$x_2 = \frac{h_2 - h_5}{h_3 - h_5} \tag{3}$$

where h is the enthalpy at each state point, kJ/kg;
x_2 is the steam quality of the geothermal mixture entering the separator.

According to different exhaust condition of turbine, flash system can be roughly divided into two types; Atmospheric exhaust (back-pressure) steam turbines and condensing exhaust steam turbines.

Atmospheric exhaust (back pressure) turbines are the simplest, and have the lowest capital cost, of all geothermal cycles. With this type of plant, steam is separated from geothermal discharge and fed through a conventional axial flow steam turbine that exhausts directly to the atmosphere. Such turbines consume about twice as much steam per kilowatt of output (for the same inlet pressure) as condensing plants, and are therefore wasteful of energy and costly in wells. However, it is commonly used as a pilot plant for generating electricity from the discharge of test wells during field development. The most important influential part of this cycle is the altitude at which the turbine is operated. It affects the power output which is produced from a given inlet pressure and steam mass flow. At higher altitudes the lower exhaust pressure, corresponding to the lower atmospheric pressure, results in greater power generations (Hudson, 1988).

A simplified schematic diagram of an atmospheric exhaust plant is shown in Figure 4. Separated steam is transmitted through insulated steam pipes to the turbine. The turbine is the prime mover and the most important part of a power plant. The turbine transforms some of the energy in the steam into mechanical energy which is used to drive the generator to produce electrical energy.

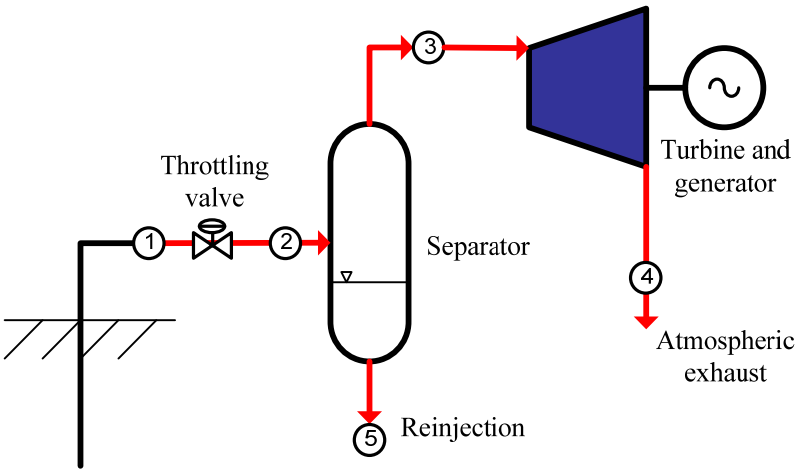

FIGURE 4: Schematic diagram for atmospheric exhaust turbine flash system

The steam enters into the turbine at inlet conditions (3) of inlet pressure P_3, quality (x=1) and enthalpy h_3, then expands through turbine to the exhaust side (4) which is kept at a lower pressure P_4 The turbine is made of rotating blades which are fixed to the turbine rotor and stationary blades often called diaphragms. The stationary blades guide the steam into next row of rotating blades.

The work done by the steam on turbine is given by the enthalpy drop across the turbine and the process efficiency. Under ideal conditions, the steam expands in isentropic process through turbine and exits with the same entropy as at inlet. Nevertheless, in actual case, the expansion is irreversible and the steam exits with higher entropy. Some basic calculation equations are given as follows:

$$W_{actual} = (h_3 - h_4) \cdot m_s \cdot \eta_{generator} \tag{4}$$

$$\eta_{is,turb} = \frac{h_3 - h_4}{h_3 - h_{4,s}} \tag{5}$$

where W_{actual} is the actual power output of the turbo-generator, kW;
h_3 is the enthalpy of the steam at inlet of the turbine, kJ/kg;
h_4 is the enthalpy of the steam at actual outlet of the turbine, kJ/kg;
$h_{4,s}$ is the isentropic enthalpy of the steam at outlet of the turbine, kJ/kg;
$h_{is,turb}$ is the isentropic efficiency of the turbine;
$\eta_{generator}$ is the isentropic efficiency of the generator.

Condensing exhaust steam turbine plant is a thermodynamic improvement on the atmospheric exhaust design, and is by far the most common plant concept employed for geothermal power generation. Instead of the steam from the turbine being discharged to the atmosphere, it is discharged to a condensing chamber that is maintained at a very low absolute pressure, typically about 0.10bar. As stated in the atmospheric exhaust turbine part, it can produce approximately twice as much power as that at typical inlet conditions because of the greater pressure drop across the condensing turbine.

However, the addition of a condenser and associated cooling towers and pumping equipment significantly increases the cost of the plant construction. In addition, power consumption is required for the main cooling water pumps and cooling tower fans with total station auxiliary power consumption being typically approximately 4.6 percent of the gross generation (Hudson, 1988).

The condensers can be direct-contact or indirect-contact and can be dry or wet types. It works by transferring heat from the exhaust steam into the cooling fluid thereby causing the steam to condense. This creates a vacuum in the condenser due to collapse of steam and creates a driving force for the steam flow. The effect is higher output from the turbine. As there's no need to recover the condensate for reuse in the process cycle, direct contact condensers are generally preferred since they have lower initial capital costs and less maintenance work. A simplified schematic diagram of a condensing exhaust turbine plant is shown in Figure 5.

Since geothermal steam contains varying quantities of non-condensable gases which come with the geothermal fluid. When the steam condenses, the NCGs remain in the condenser. A build up of the NCGs in the condenser will create a back pressure which lowers the performance of the turbine. These gases have to be removed from the condenser in order to maintain in the performance of the turbine and this requires some work input. The appropriate equipment to be used for gas extraction is dependent on the proportion of NCGs present with the steam. At low gas contents (less than 1.5 percent by weight), steam venturi gas ejectors are generally the most economic choice. At high gas contents, the high steam consumption of the comparatively inefficient steam ejectors leads to the selection of higher capital cost, lower auxiliary consumption alternatives. Generally, for NCG contents between approximately 1 and 3.5 percent by weight, the most economic option will be a hybrid system involving first-stage steam venturi ejectors with liquid-ring vacuum pumps for the second-stage compression. At NCG contents above approximately 3.5 percent by weight it is generally more economic to use multi-stage centrifugal compressors. For NCG contents exceeding about 12 percent mass of the steam, it is generally more economic to use a back-pressure turbine plant because of the large amount of power required to extract the gases from the condenser.

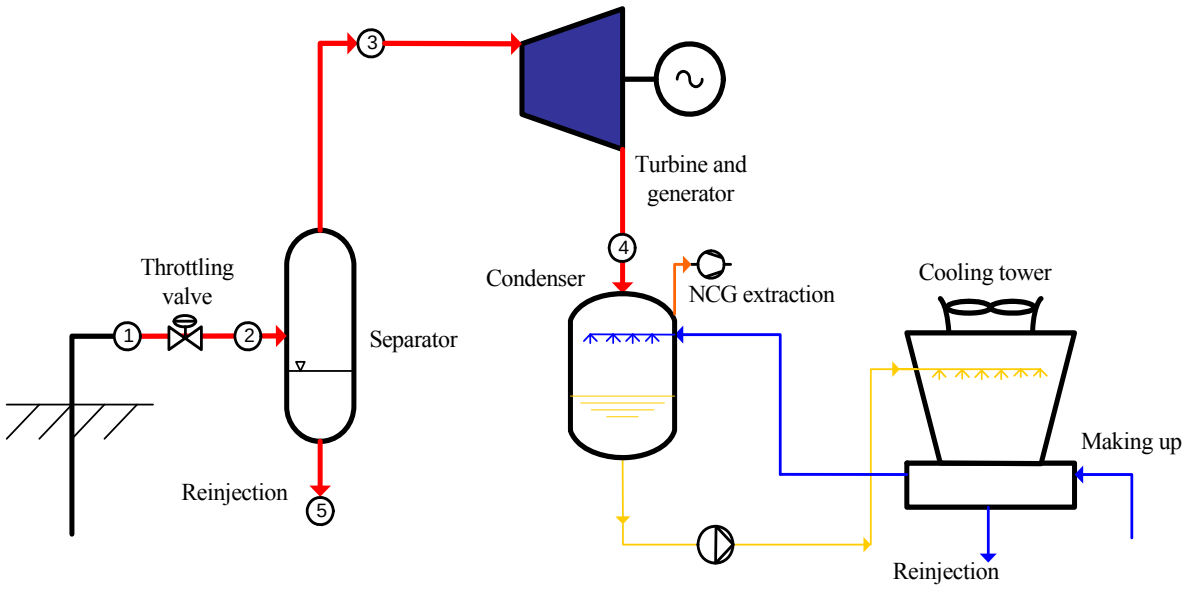

FIGURE 5: Schematic diagram for flash system with condensing turbine

The proper condenser design depends on many factors like the availability of cooling water, economic analysis of the plant, and the environment concerns. The temperature difference between cooling water outlet and exhaust steam temperature inlet is the pinch point of condenser design calculation. A large pinch results in a smaller condenser area but higher cooling water flow, vice versa. It is recommended that this pinch should not be less than 2.8 ºC and usually could be between 11 and 17 ºC.

A wet cooling tower (Figure 6) is commonly used in condensing exhaust power cycles. The calculations of cooling tower are performed based on these assumptions:

- Steady operating conditions where the mass flow rate of dry air remains constant during the entire process;
- The kinetic and potential energy changes are neglected;
- The cooling tower is adiabatic.

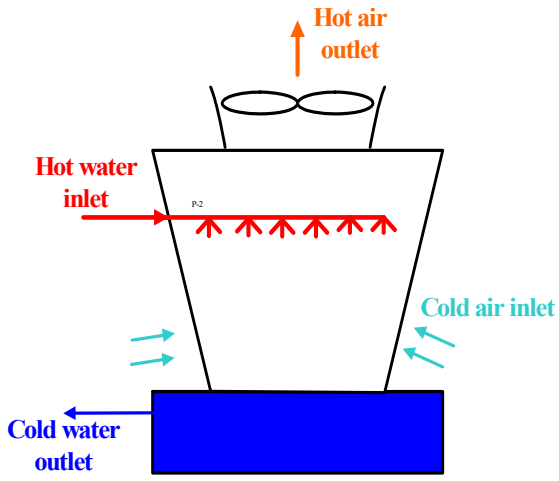

FIGURE 6: Schematic diagram of a cooling tower

Applying the mass and energy balances on the cooling tower gives:

Dry mass air balance

$$\dot{m}_{a,in} = \dot{m}_{a,out} = \dot{m}_a \tag{6}$$

Water mass balance

$$\dot{m}_{w,in} + \dot{m}_{a,in} \cdot \omega_{a,in} = \dot{m}_{w,out} + \dot{m}_{a,out} \cdot \omega_{a,out} \tag{7}$$

Energy balance

$$\dot{m}_{w,in} \cdot h_{a,in} + \dot{m}_{a,in} \cdot h_{a,in} = \dot{m}_{w,out} \cdot h_{w,out} + \dot{m}_{a,out} \cdot h_{a,out} \tag{8}$$

Solving for $\dot{m}_a$ gives,

$$\dot{m}_a = \frac{\dot{m}_{w,in}(h_{w,in} - h_{w,out})}{(h_{a,out} - h_{a,in}) - (\omega_{a,out} - \omega_{a,in}) \cdot h_{w,out}} \tag{9}$$

Volume flow rate of air into the cooling tower is:

$$\dot{V}_{a,in} = \frac{\dot{m}_a}{\rho_{a,in}} \tag{10}$$

The mass flow rate of the required makeup water is determined from:

$$\dot{m}_{makeup} = \dot{m}_a(\omega_{a,out} - \omega_{a,in}) \tag{11}$$

where $h_{a,in}$ is the enthalpy of the cold dry air (kJ/kg dry air), from psychometric chart;
$h_{a,out}$ is the enthalpy of the hot dry air (kJ/kg dry air), from psychometric chart;
ω is the ratio of water vapour to dry air in a particular height of air, expressed as a ratio of kilograms of water vapour per kilogram of dry air, from psychometric chart;
$\dot{m}_{a,in} \cdot \omega_{a,in}$ is the water content in incoming air stream;
$\dot{m}_{a,out} \cdot \omega_{a,out}$ is the water content in leaving air stream;
h_w is the enthalpy of saturated liquid water, from steam table.

Power of cooling tower fan is:

$$P_{fan} = \frac{\dot{V}_a \cdot \Delta P}{\eta_{fan}} \tag{12}$$

The power of pumping the circulating cooling water between condenser and cooling tower is

calculated by the equation below:

$$P_{pump} = \frac{\dot{V}_{cooling} \cdot \Delta P}{\eta_{pump}} \quad (13)$$

where $V_{cooling}$ is the volume flow rate of circulating cooling water, m^3/kg;
ΔP is the pressure difference, kPa;
η_{pump} is the efficiency of circulating pump.

4.1.2 Binary cycle system

The binary cycle power plant is developed for low and medium geothermal resources. Generally there are mainly two types of binary cycles shown below which are ORC and Kalina cycle.

By selecting the appropriate working fluid, the ORC system can be designed to operate with inlet temperatures in the range 85 to 170 ºC. The upper temperature limit is restricted by the thermal stability of the organic binary fluids (working fluid). The lower temperature limit is primarily restricted by practical and economic considerations, as the required heat exchanger size for a given capacity becomes impractical. Heat is transferred from the geothermal fluid to the binary cycle via heat exchangers, where the working fluid is heated and vaporized before being expanded through a turbine to some lower pressure and temperature. A schematic diagram of ORC system is shown in Figure 7.

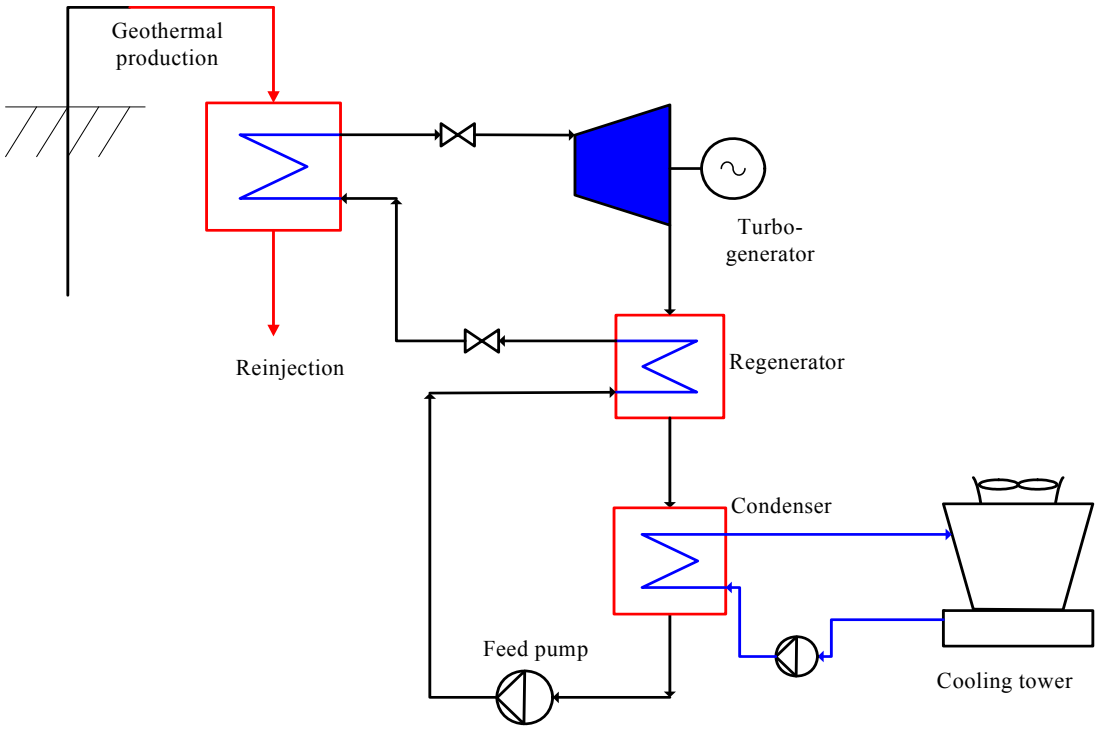

FIGURE 7: Schematic diagram of ORC binary cycle

There are two cycles of this system, the first one is the geothermal heat exchange cycle where the working fluid absorbs heat from geothermal fluid via the heat exchanger; the second one is the ORC working cycle. These two cycles are separated, only the heat transfer is taking place via the heat exchangers, normally the shell-and-tube heat exchangers are applied. By using the low boiling point nature of working fluid, the ORC cycle can work in a comparatively lower temperature range. The working fluid is mostly isobutane, or isopentane or the mixture of them. According to the experiences, generally, isobutane gives more power output compared with isopentane. In addition, the mixtures can be tailored to effectively match the characteristics of the resource geothermal fluid better than virtually

any pure fluid choice for the working fluid. Thus, the working fluid is selected both from the optimizing power output view and requirement of the critical temperatures. The Table 2 below shows the critical temperature and pressure of some main working fluid applying in ORC cycle which must fit the geothermal fluid heat source.

TABLE 2: Critical temperatures and pressures of different working fluid in ORC cycle

Working fluid	Critical temperature (ºC)	Critical pressure (bar)
Isopentane	187.2	33.70
Isobutane	134.7	36.40
n-pentane	196.5	33.64
n-butane	152	37.96

A Kalina cycle is a modification of traditional binary ORC system using a mixture of ammonia and water as the working fluid instead of a pure working fluid. The Kalina power plant shown in Figure 8 is based on the Kalina Cycle System 34 (KCS34) license. The basic ammonia-water stream is vaporized in the evaporator and then separated into a saturated rich vapour ammonia-water mixture stream and a saturated lean liquid ammonia-water mixture stream in the separator. The basic stream reappears when the saturated liquid stream is cooled in the HT regenerator and throttled in the throttle valve, and then mixed with the saturated vapour stream passed through the turbine.

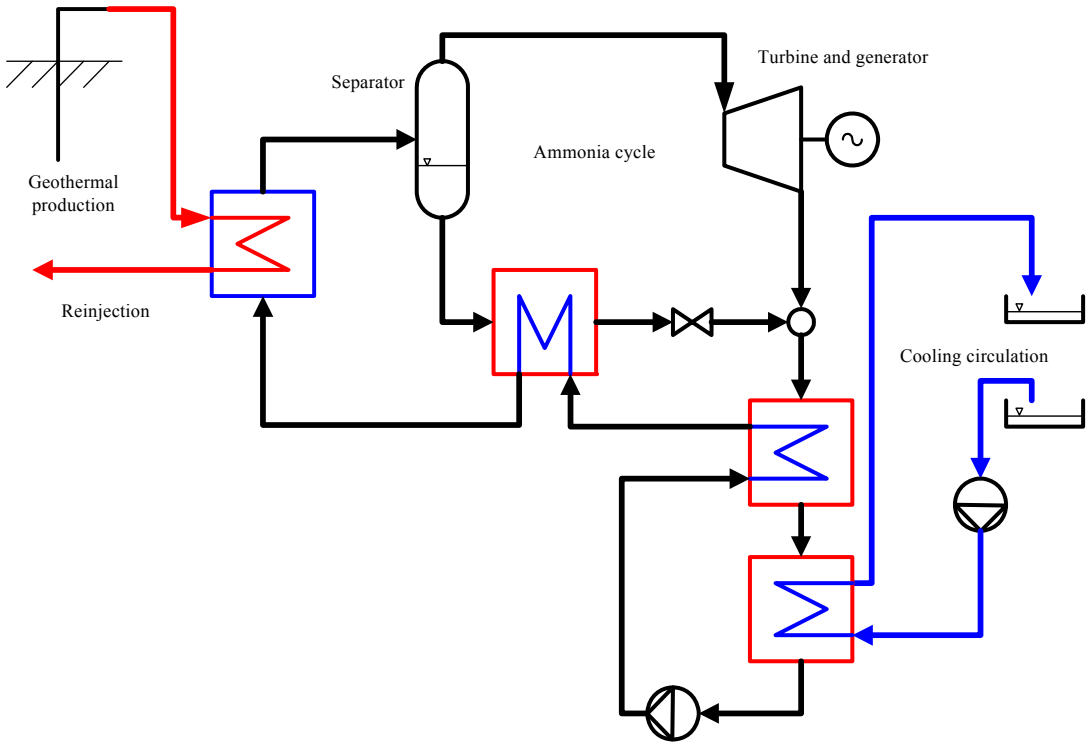

FIGURE 8: Schematic diagram for Kalina cycle

After that the basic stream is cooled in the LT regenerator and condensed in the condenser. The condensed basic stream is pressurized before re-entering the LT and HT regenerator. Here the basic stream returns to its initial state and the processes are repeated.

The main benefit of the Kalina cycle is that heat addition to the process happens at a variable temperature, and can thus be fitted to the falling temperature of a heat source with a finite heat capacity, reducing the generation of entropy in the heat exchange with the primary fluid.

4.1.3 Net power output of each cycle

Net power output of each power cycle is calculated as follows. It equals to the shaft power output which subtracts auxiliary power consumption of the cycle if exists.

Flash cycle with atmospheric exhaust steam turbine:

$$W_{net} = W_{shaft} \tag{14}$$

Flash cycle with condensing exhaust steam turbine:

$$W_{net} = W_{shaft} - P_{pump,cooling} - P_{fan} \tag{15}$$

Binary cycle (ORC or Kalina):

$$W_{net} = W_{shaft} - P_{feedpump} - P_{pump,cooling} - P_{fan} \tag{16}$$

4.2 Evaluation of the existing power plants

The present power cycle applied in existing power plants is double flash cycle. There were about 18 wells with an average depth of 200 m tapping the upper water-dominated reservoir. The power plants were constructed in two parts: the capacity of the southern plant is 10 MWe, thereof 3 units with each capacity of 3MWe and 1MWe testing unit which was retired soon. The capacity of northern plant is 15.18 MWe, thereof four units with each capacity of 3MWe and one 3.18 MWe unit. Therefore, the total capacity of the power plants is 24.18 MWe. However, the power plants have already been operated for almost 30 years, the equipments are old or at very low efficiency. The real power output now is just around 15 MWe.

The initial working condition of the cycle is as follows: the geothermal water temperature is 145ºC at wellhead. The inlet pressure of geothermal steam at first stage is 1.82 bar, and the temperature is 115ºC; the second stage inlet pressure is 0.54 bar and the temperature is 81ºC. The exhaust pressure is 0.10 bar. Total geothermal production is about 3000 m^3/h. The discharging geothermal brine from the power plants is at the temperature of 80-90ºC. Most of the water has been discharged into the local Zangbuqu River. It has been a serious pollution due to the chemical component with fluoride, boron, etc.

Performance analysis of this double flash cycle is implemented and the results show that the original power cycle has been designed under suitable working conditions with approximately optimized pressures. However, according to the new reservoir assessment, the present upper geothermal potential can no longer sustain the initial production. The present geothermal potential is about 167 t/h of the steam production.

4.3 New power plants design concept and methodology

According to the reservoir assessment to date, new power plant conceptual design is carried out here. The main objective is to make sustainable utilization of both upper and lower reservoir so as to meet the increasing power demand as well as the space heating need in Lhasa. The three basic power generation cycles are all taken into account. The combined hybrid system concept is applied in conceptual design. Based on double flash cycle, ORC cycle, and Kalina cycle three general power generation types, four different alternative scenarios are carried out to make the thermodynamic and optimization analysis with objective to get the best solution with both concerns of power generation and district heating.

This work includes the thermodynamic model calculations of each proposed scenario, the thermodynamic properties of each state of the cycles, the system optimization and performance analysis, and the examination of variations of fundamental characteristics of the cycles. The basic process model of ORC and Kalina cycle was accessed from Enex Engineering Consulting Company. In the performance and optimization analysis, optimum flashing pressures are determined in double flash cycle, the separation pressure of topping flash cycle and evaporation pressure of bottoming ORC cycle, and the separation pressure of topping flash cycle and the ammonia high pressure and the ammonia mixture strength are optimized. And the technically feasibility comparison of different scenarios are given at last.

All the thermodynamic calculations and optimization are performed in the software of Engineering Equation Solver (EES) and Matlab programme.

4.4 General assumptions and boundary conditions

4.4.1 General assumptions

Yangbajain geothermal field reservoir data were derived from the latest reservoir assessment report.

For this preliminary study, it is assumed that there is no non-condensable gas in the new design; All heat transfer losses are neglected; A shell and tube heat exchanger is applied as a condenser; A titanium plate heat exchanger is applied for the district heating supply system;

U (overall heat transfer coefficient) to calculate the area required for the heat exchanger was assumed :

U = 0.9 for the evaporator
U = 1 for the regenerator
U = 1.5 for the condenser
U = 1.5 for heat exchanger of district heating source

The efficiency of the pump and fan are 0.70, 0.60, respectively;

The efficiency of the turbine and generator is 0.85 and 0.95, respectively;

The temperature difference between cooling water entering the cooling tower and hot air leaving the cooling tower is 7ºC;

The make up water of cooling tower is from the river nearby; the average temperature is 5ºC;

A wet cooling tower is applied.

For district heating system design, snow melt water was the heating water source with inlet temperature of 5ºC and the outlet of 85ºC.

4.4.2 Boundary conditions

The boundary conditions normally hot end and cold end of a power plant. They are described detailed as follows:

Hot end (geothermal fluid):

Yangbajain field is the most important geothermal field in Tibet. The reservoir is divided into two sections, upper reservoir and lower reservoir. At present, only the upper reservoir has been utilized by the existing power plants. The Figure 9 below shows the elevation of the field and the existing plants location.

According to the reservoir assessment report, the upper reservoir potential is assessed to be 167 t/h steam production which is about 1512 t/h (i.e. 420 kg/s) total mass flow roughly.

The condition of the upper geothermal reservoir is indicated in the Table 3:

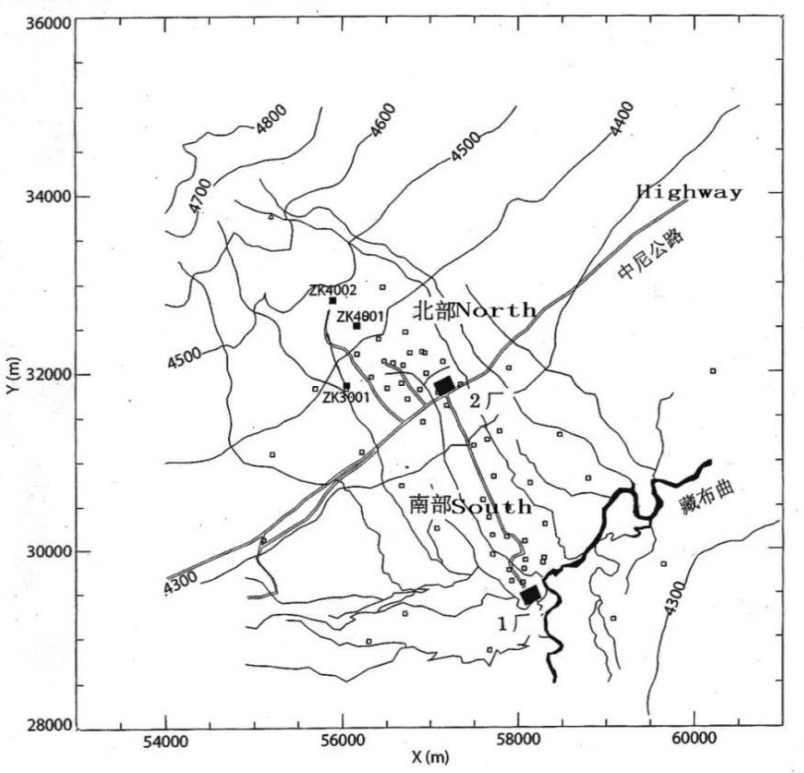

FIGURE 9: Yangbajain geothermal field and existing power plants location

TABLE 3: The typical geothermal water data of upper reservoir in Yangbajain

Properties	Value
Down hole temperature (ºC)	141-172
Wellhead temperature (ºC)	120-147
Mass flow rate per well (t/h)	72-169.7
Steam flow rate per well (t/h)	9.13-25.8
Wellhead pressure (bar)	2-4.6
TDS (mg/l)	954-1853
pH	7.7-8.89
SiO_2 (mg/l)	36.5-124.5

Project of exploration of the lower geothermal resources was initiated in 1993. Two deep wells (ZK4001, ZK4002) have been drilled in northern area with maximum downhole temperature of 328.9ºC (ZK4002/1850 m) and 252ºC (ZK4001/1450 m). Additionally, there drilled another deep well (ZK308) in the southern area with lower temperature below 150ºC. After that, a joint group of Chinese experts and Japanese International Cooperation Agency has carried out a lower geothermal reservoir assessment by 2006. It is latest reservoir assessment report which applied as the main geothermal heat source reference for this study. There was another new survey well drilled during this period which is CJZK3001 (2254.5 m). Well testing for CJZK3001 (Figure 10) shows that the condition in this well is the highest temperature got in the depth of 1405.2 m is 270.8ºC. The temperature of the depth 0-200 m is increasing sharply. Then it maintains 150ºC at the depth of 200-950 m. From 950 to 1200 m, the temperature again goes sharply highly to 220-230ºC. The pressure related to this temperature is about 13 MPaA. The stimulation work for this well failed unfortunately due to the bad condition of casing after 3 years working. The deep part was already damaged. Some results of well testing are given as follows.

The research revealed that the lower geothermal resource with high enthalpy is distributed mostly in the northern area of Yangbajain field with the temperature of more than 200ºC. Then the well testing

and stimulation have been made to well ZK4001 successfully. The main results as well as the scaling test of ZK4001are presented in Tables 4 and 5:

Then according to the reservoir modelling and simulation work (Japanese International Cooperation Agency, 2006), the final conclusions of the lower reservoir are given as follows:

- The geothermal reservoir of Yangbajain has the ability of sustaining the present production of the upper reservoir.
- The total amount of steam production can keep stable at 200 t/h in the following 30 years including the upper and lower reservoir. It involves the existing upper wells and 3 more deep wells totally.
- It is possible to produce the amount of 240t/h steam from the both upper and lower reservoir, but with associated risks.

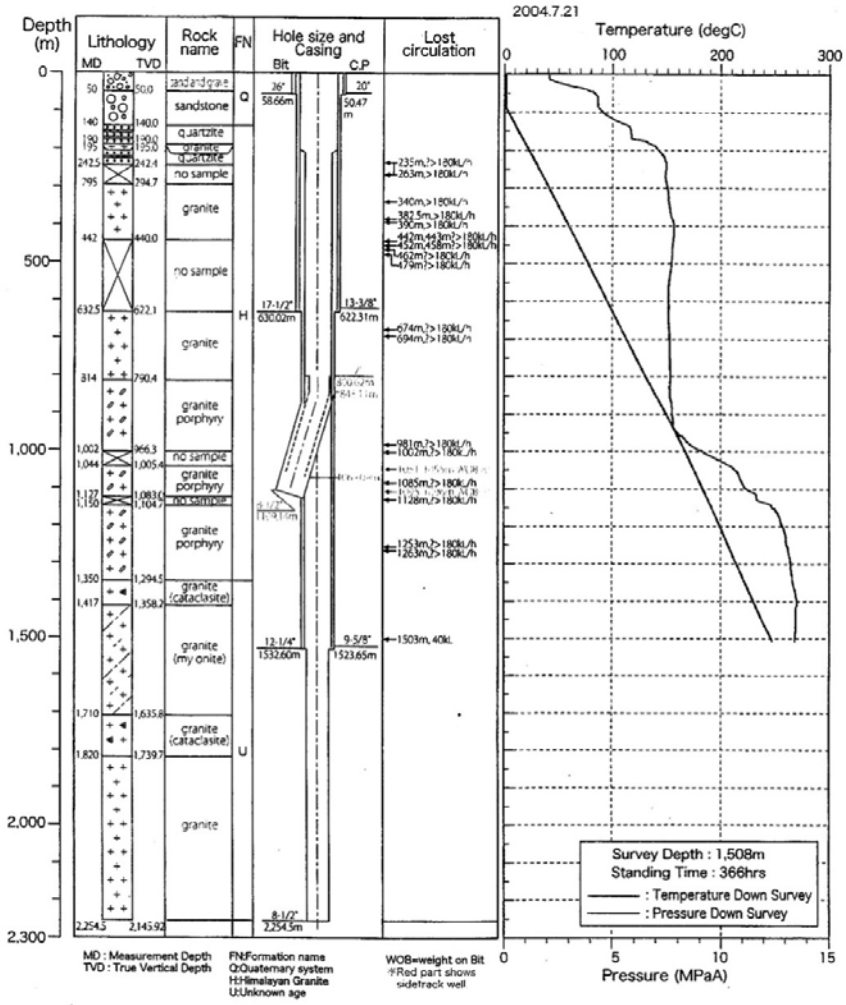

FIGURE 10: Temperature and pressure results of CJZK3001 well testing

TABLE 4: Well testing main results of ZK4001

Result item	Value
Wellhead Pressure (bar)	14.30
Mass flow rate (t/h)	280.90
Steam flow rate (t/h)	30.50
Water flow rate (t/h)	250.00
Enthalpy of the mass (kJ/kg)	1053.00

TABLE 5: Scaling testing main results of ZK4001

Sample number	1	2	3
Fluid category	Steam+ hot water	Hot water	Hot water
Flow rate	330-260 t/h	260-210 t/h	
Duration	86 days		
Installation location	Below the second wellhead valves	Below regulator valve for hot water	Hot water pipe between well and separator
Result	Minim. of scaling	None	None

Cold end:

The dry bulb temperature and wet bulb temperature duration curve are given below in Figure 11. The average wet bulb temperature in Lhasa is -4.35ºC.

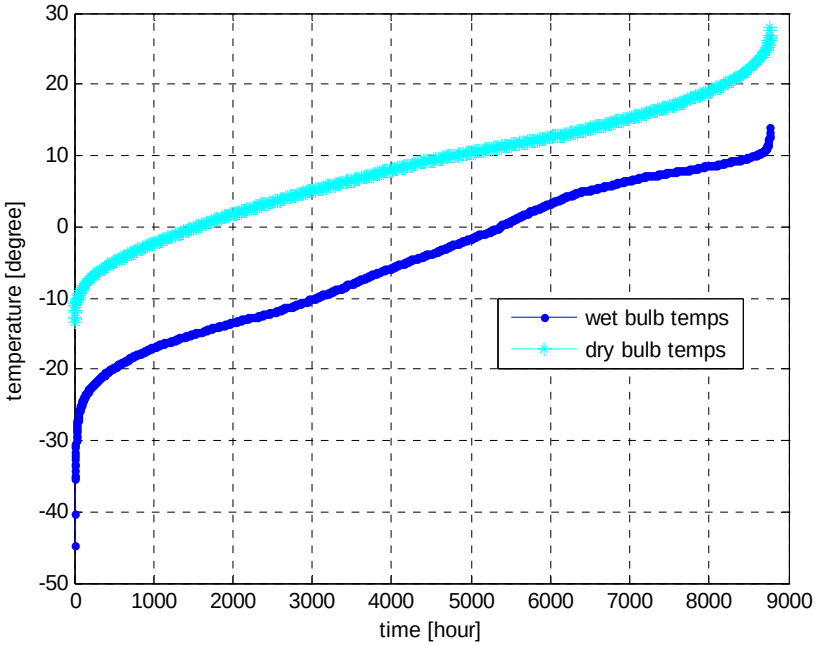

FIGURE 11: Outdoor temperature data in Lhasa of Tibet

Yangbajain geothermal field is about 90 km to the north of Lhasa with the altitude of 4300 m, is 650 m higher than Lhasa. The average outdoor dry bulb temperature is about 2.5ºC. The average river temperature is about 5ºC. The atmospheric pressure in Yangbajain field is 0.6 bar. The average water temperature of Zangbuqu River nearby Yangbajain existing power plants is 5ºC. It is an available cooling water resource for the new power plant as well.

4.5 Thermodynamic calculations and optimization of new power plant

According to the design concept, the different scenarios are performed in EES calculation procedure and Matlab programming. The main steps and processes are shown as follows:

4.5.1 Double flash cycle (Scenario 1)

Double flash cycle as the simplest and most common cycle is the first scenario to be considered for new design named as Scenario 1. The well data stated in the boundary conditions are used here for the present design. Therefore, one new deep well from the lower high enthalpy reservoir is the source of the first flash cycle. The enthalpy is 1053 kJ/kg, and the mass flow is about 78 kg/s. This high enthalpy geothermal fluid will go through the separator at the separation pressure P_1. Then the separated pure steam goes to the turbo-generator to generate electricity, while the separated brine goes to mix with the geothermal fluid from upper reservoir and after throttling valve to be lower pressure fluid for the second flash cycle. The temperature and mass flow of upper reservoir geothermal water is 145ºC and 420 kg/s, respectively. The second separation pressure is P_8 which together with P_1 are the main variables to optimize the net power output.

In Yangbajain geothermal field the highest ambient temperature all year round can reach around 25˚C with average relative humidity of air 54%. The highest wet bulb temperature is about 13˚C. The wet cooling tower is chosen for cooling condensed steam due to the high efficiency and available cooling

water source. With a wet cooling tower the "cold water" temperature approaches the "wet bulb" temperature. In this study a "cold water" temperature of 7˚C is used for all the scenarios.

The pinch point between cooling water outlet and turbine exhaust temperature is the point to be determined in the design (Figure 12). The lower pinch could get higher power output, but the capital cost will be higher because of the bigger condenser area need. To keep the exit pressure at safe and manageable level, it is designed to be around 0.08 bar, by assuming $T_{c,out}$ of 20˚C and then the pinch is 22˚C, the temperature of condensation would be 42˚C.

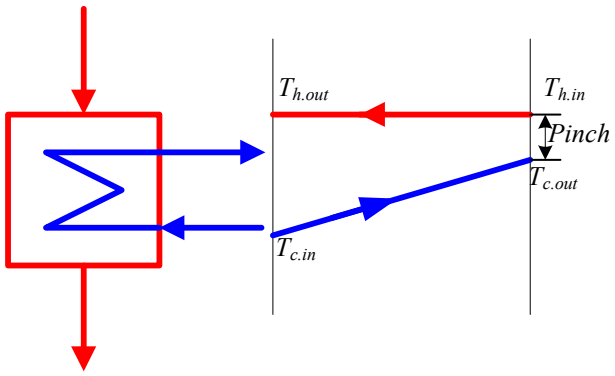

FIGURE 12: Pinch point of condenser

The detailed calculations and optimization are performed in double flash model set up in EES programme and Matlab, the schematic diagram is shown below in Figure 13.

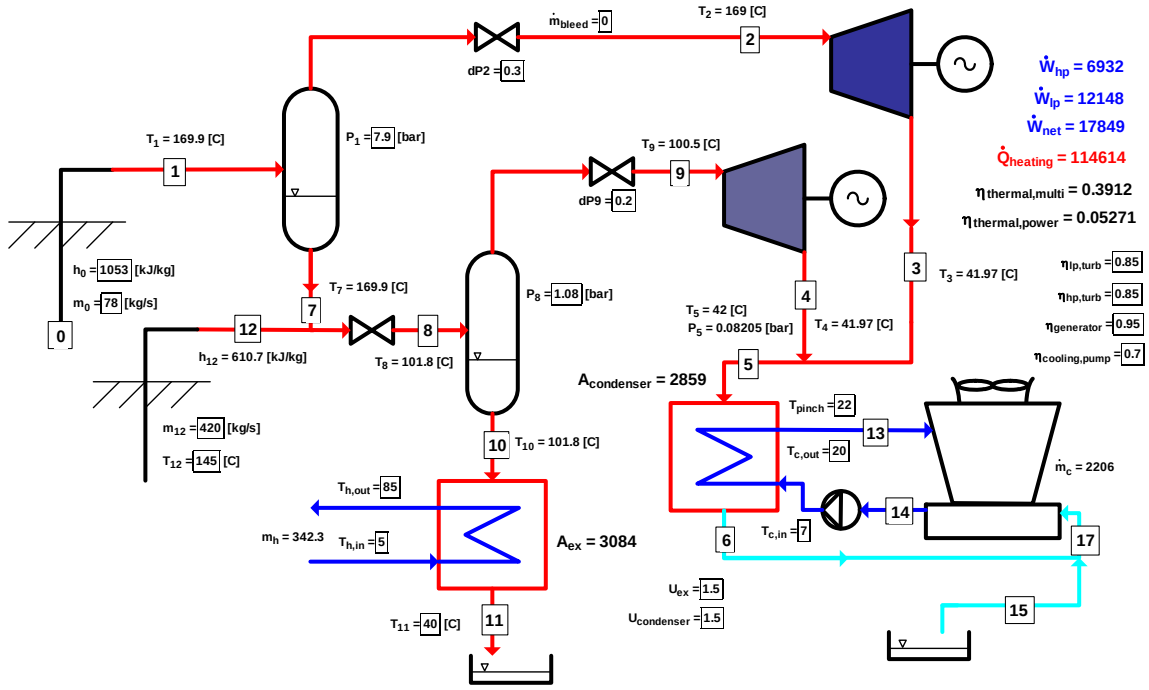

FIGURE 13: Schematic diagram of Scenario 1

The optimization work is to get the optimum separation pressures for both two separators which could maximize the net power output as well as the available discharge geothermal brine temperature for the district heating system. Therefore, the two separation pressure P_1 and P_8 are varied to seek the maximum net power output. It takes 208 runs in EES programme to get the optimum results. By using Matlab programme the optimum power output diagram is given in Figure 14 with the optimum pressures: P_1=7.9 bar; P_8=1.08 bar. The maximum power is shown on the top central area to be 17849 kW.

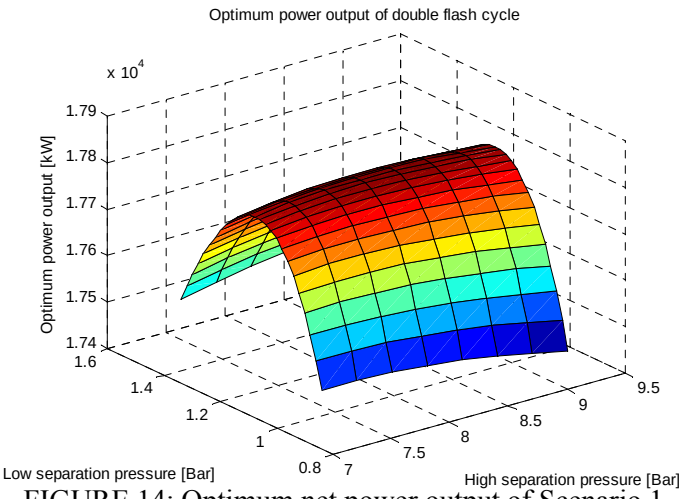

FIGURE 14: Optimum net power output of Scenario 1

On the other hand, the temperature of discharge geothermal brine for district heating system is variable according to the pressures changing. Table 6 shows the values around the optimum range which is clearly indicated there's definitely available hot water supply for the district heating system. Thus for the optimum system the supply temperature is 101.8°C.

TABLE 6: Temperature of discharge geothermal brine variation of Scenario 1

High separation P_1 [bar]	**Low separation P_8 [bar]**	**Net power output W_{net} [kW]**	**Temperature of discharge brine T_{10} [°C]**	**Heating capacity Q [kW]**
7.3	1.06	17841	101.2	113510
7.6	1.07	17847	101.5	114064
7.9	1.08	17849	101.8	114614
8.2	1.09	17848	102.0	115161
8.5	1.10	17844	102.3	115704
8.8	1.11	17837	102.6	116243
9.1	1.12	17828	102.8	116779
9.4	1.13	17816	103.1	117311
9.7	1.14	17802	103.3	117840
10.0	1.15	17786	103.6	118366

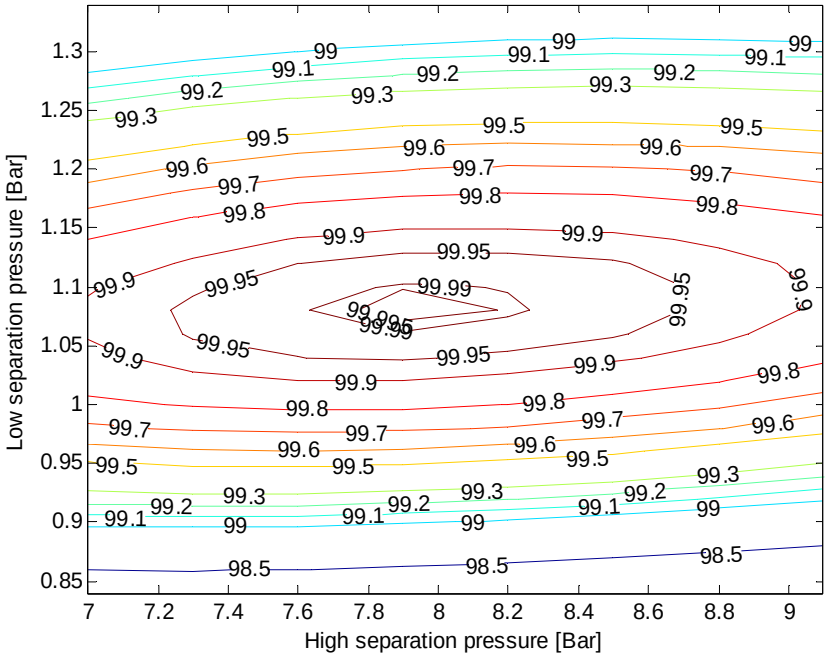

FIGURE 15: Net power output contour of Scenario 1

Figure 15 shows the net power output contour corresponding to different separation pressures. The maximum output can be determined accurately and then the optimum pressures can be figured out. It is also indicated that the pressures of high and low separation process have relatively big range resulting in the optimum power output. It means for practical operation of this system there are some flexible pressure choices which also can avoid some problems when the pressure drop happens or some other emergency cases.

The following two tables indicate the main results of the double flash cycle design calculations. The optimum net power output of this cycle is 17849 kW at separation pressure of 7.90 bar and 1.08 bar. The discharge geothermal brine which keeps high temperature is a good district heating source. The total capacity for district heating system is 114614 kW. Thus, it is known as a CHP plant gives higher utilizing efficiency of the geothermal resource. This is also a big benefit solving the lack of heating system in Lhasa. The thermodynamic properties of each process state in the optimum system are detailed tabulated below in Table 7.

TABLE 7: Thermodynamic properties of each process state of Scenario 1

Parameter	Enthalpy	Mass flow	Pressure	Entropy	Temperature	Steam quality
Unit	*h* [kJ/kg]	*m* [kg/s]	*P* [bar]	*s* [kJ/kg.°C]	*T* [°C]	*x*
[0]	1053.00	78.00	35.43	2.73	243.30	0.00
[1]	1053.00	78.00	7.90	2.80	169.90	0.16
[2]	2768.00	12.72	7.60	6.68	169.00	100.00
[3]	2195.00	12.72	0.08	7.01	41.97	0.84
[4]	2380.00	42.83	0.08	7.59	41.97	0.92
[5]	2338.00	55.55	0.08	7.46	42.00	0.90
[6]	175.90	55.55	0.08	0.60	42.00	0.00
[7]	718.90	65.28	7.90	2.04	169.90	0.00
[8]	625.30	485.30	1.08	1.86	101.80	0.09
[9]	2679.00	42.83	0.88	7.43	100.50	100.00
[10]	426.50	442.50	1.08	1.33	101.80	0.00
[11]	167.50	442.50	1.08	0.57	40.00	0.00
[12]	610.70	420.00	4.15	1.79	145.00	0.00

The overall results are summarized as in Table 8. The maximum power output of double flash cycle is 17849 kW which is only 5.27% as the thermal efficiency of the system. However, as including the district heating capacity it supplies, the efficiency increases a lot up to 39.12%. There are only two heat exchangers are used as one condenser and one plate heat exchanger for heating system. According to the calculation, the total area of the heat exchangers is about 5943 m^2.

TABLE 8: Summary of overall results of Scenario 1

No.	Item description	Units	Optimum value
1	**High separation pressure**	**bar**	**7.90**
2	**Low separation pressure**	**bar**	**1.08**
3	Shaft power output	kW	19080.00
4	High pressure cycle power output	kW	6932.00
5	Low pressure cycle power output	kW	12148.00
6	**Net power output**	**kW**	**17849.00**
7	Pumping rating, cooling water	kW	630.40
8	Power of cooling tower fan	kW	600.30
9	Condenser pressure	bar	0.08
10	Condenser cooling capacity	kW	120069.00
11	Condenser area	m^2	2859.00
12	Cooling water flow rate	kg/s	2206.00
13	Cooling water inlet temperature	°C	7.00
14	Cooling water outlet temperature	°C	20.00
15	Minimum making up water flow rate	kg/s	52.36
16	Discharge geothermal brine temperature	°C	101.80
17	**District heating power capacity**	**kW**	**114614.00**
18	Heated water inlet temperature	°C	5.00
19	Heated water outlet temperature	°C	85.00
20	Heated water mass flow	kg/s	342.3
21	Heat exchanger area	m^2	3084.00
22	Total heat exchanger area	m^2	5943.00
23	**Thermal efficiency of power cycle**	**%**	**5.27**
24	**Thermal efficiency of multi-utility cycle**	**%**	**39.12**

4.5.2 Combined flash and ORC cycle (Scenario 2)

The second scenario of the new design is a combined cycle with flash and ORC cycle named as Scenario 2 (Figure 16). This cycle is designed at the same assumption and boundary conditions as Scenario 1. The design concept is to use high enthalpy geothermal reservoir in topping flash cycle, and the separated brine combined with low enthalpy upper geothermal reservoir will be used in bottoming ORC cycle. The working fluid is isopentane. The calculations and optimization analysis are performed as follows.

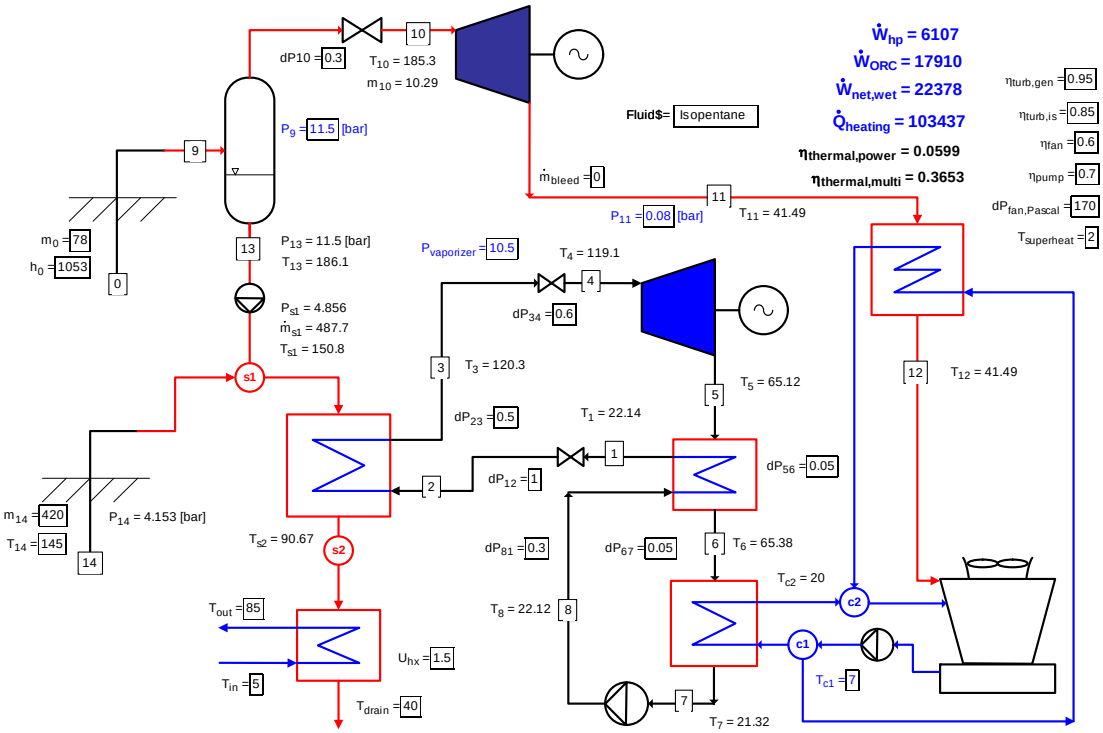

FIGURE 16: Schematic diagram of Scenario 2

The detailed calculations and optimization are performed in EES programme and Matlab, the schematic diagram is shown below in Figure 16. Similarly as designed in double flash cycle system, the geothermal fluid from deep well extracting high enthalpy geothermal resource goes into the topping flash cycle giving the power output W_{hp}. The separated brine together with the low enthalpy geothermal fluid goes to the heat exchanger of the ORC cycle which supplies the heat source of ORC bottoming cycle. The power output is denoted by W_{ORC}. The total shaft power is thus given as the work sum of these two cycles denoted by W_{shaft}. In addition, the auxiliary power input is from the cooling water circulating pump, ORC feed pump and the cooling tower fan. Therefore, the net power output W_{net} of the combined cycle is given by the Equation 16 given previously.

The optimization work is to input different values of the variables to work out which can result in the maximum power output. Here in this system, the high separation pressure P_9 for the topping flash cycle and the vaporizing pressure P_{vap} for the bottoming ORC cycle are the key input variables. In EES table calculation, the separation pressure P_9 and the vaporizing pressure P_{vap} are varied to calculate the net power output. It takes 221 runs to get the best results which show that the optimum pressures are: P_9=11.5 bar; P_{vap}=6.5 bar. Thus, the optimum results programmed then in Matlab are shown as follows. The carmine centre area of the surf diagram indicates the maximum net power output as **25388 kW** in Figure 17. And the thermal efficiency for power output is 6.6%.

In Figure 18 the net power output contour shows the maximum power output location and by which the optimum variables can be figured out. It also indicates that the separation pressure of topping flash cycle doesn't affect the final net power output too much. The more influencing factor is vaporizer pressure of ORC cycle.

This gives a good method to identify the maximum value as well as the tendency and accuracy of the value. It means for the practical operation of this system there are some flexible pressure choices as the same situation as Scenario 1.

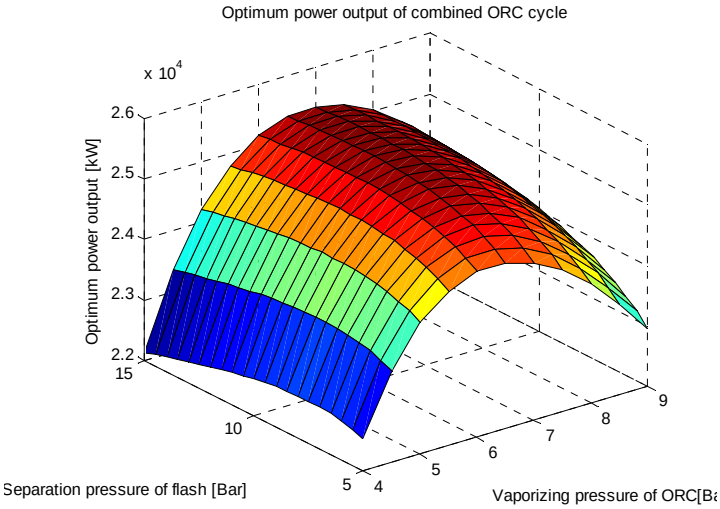

FIGURE 17: Optimum net power output of Scenario 2

Therefore, the topping cycle separation pressure is kept stable at the optimum value, the vaporizing pressure of bottoming ORC cycle is varied to seek for the available discharge geothermal brine temperature. The following Table 9 indicates the variation results which can give possibility to get available temperature for district heating system. It will thus result in some decrease of optimum power output around 3MW. However, the huge district heating capacity deserves the sacrifice of power output depreciation.

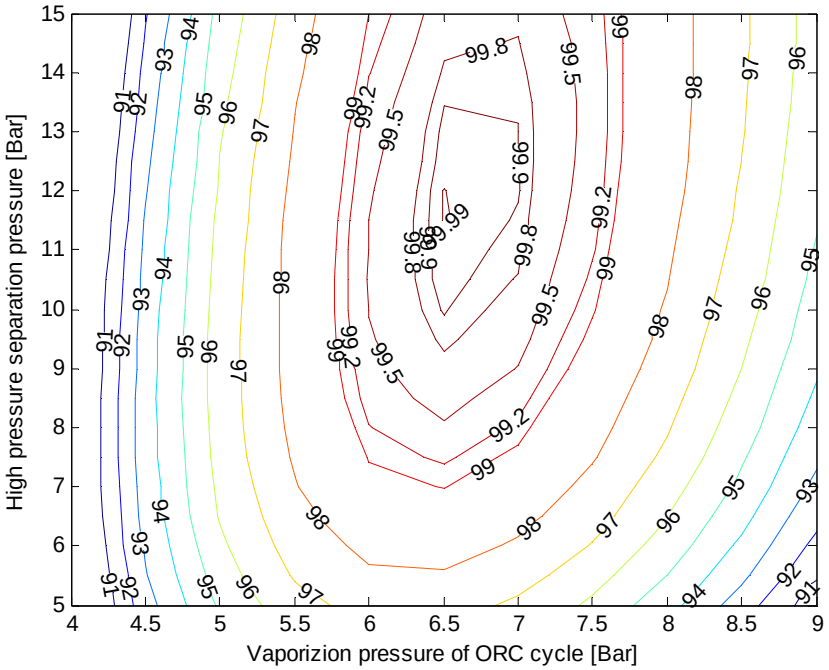

FIGURE 18: Net power output contour of Scenario 2

TABLE 9: Temperature of discharge geothermal brine variation of Scenario 2

Separation pressure P_9 [bar]	**Vaporizer pressure P_{vap} [bar]**	**Net power output W_{net} [kW]**	**Temperature of discharge brine T_{10}[°C]**
11.5	6.0	25283	59.69
11.5	6.5	25410	63.09
11.5	7.0	25381	66.49
11.5	7.5	25232	69.90
11.5	8.0	24965	73.32
11.5	8.5	24602	76.75
11.5	9.0	24156	80.20
11.5	9.5	23630	83.67
11.5	10.0	23036	87.16
11.5	10.5	22378	90.67
11.5	11.0	21664	94.20

According to the district heating design condition, the new pressures could be selected from Table 9 above. The main results of optimized system are given in Tables 10 and 11.

TABLE 10: Thermodynamic properties of each process state of Scenario 2

Parameter	Enthalpy	Mass flow	Pressure	Entropy	Temperature	Steam quality
Unit	*h* [kJ/kg]	*m* [kg/s]	*P* [bar]	*s* [kJ/kg.°C]	*T* [°C]	*x*
[0]	1053.00	78.00	35.43	2.73	243.30	0.00
[1]	-355.60	246.10	12.00	-1.72	22.14	-100.00
[2]	-355.60	246.10	11.00	-1.71	22.17	-100.00
[3]	143.10	246.10	10.50	-0.35	120.30	100.00
[4]	143.10	246.10	9.90	-0.35	119.10	100.00
[5]	66.44	246.10	0.91	-0.31	65.12	100.00
[6]	67.13	246.10	0.86	-0.30	65.38	100.00
[7]	-358.40	246.10	0.80	-1.72	21.32	0.00
[8]	-355.60	246.10	12.30	-1.72	22.12	-100.00
[9]	1053.00	78.00	11.50	2.77	186.10	0.13
[10]	2783.00	10.29	11.20	6.55	185.30	100.00
[11]	2158.00	10.29	0.08	6.90	41.49	0.83
[12]	173.70	10.29	0.08	0.59	41.49	0.00
[13]	790.10	67.71	11.50	2.20	186.10	0.00
[14]	610.70	420.00	4.15	1.79	145.00	0.00

By choosing the discharge temperature at 90.67°C, the corresponding pressures and power output are also obtained. The new vaporizing pressure is 10.5bar.

Table 11 summarized the overall results of this combined system. The optimum net power output of this cycle is 22378kW (i.e. about 22MW). The district heating system capacity is 103437kW. The thermal efficiency of pure power output is just 5.99%. By adding heating system capacity, it is increased considerably to be 36.53%.

4.5.3 ORC cycle using isobutane (Scenario 3)

Alternative scenario 3 was designed also as a combined flash and ORC cycle but with working fluid isobutane in ORC cycle in the beginning. The process of calculations and optimization was quite similar as made for scenario 2. However, the optimization results showed that the higher pressures of both cycles, the more power output it can give. It is no more necessary to keep the topping flash cycle in this system. Therefore the new concept is to design an ORC cycle which makes use of combined geothermal brine from both upper and lower reservoir.

The schematic diagram is shown below in Figure 19. It is a binary cycle that s_1 is the combination point of both reservoirs. The calculation assumptions are the same as the previous two scenarios. The shaft power is given as the work of ORC cycle using isobutane denoted by W_{shaft}. The auxiliary power input is from the cooling water circulating pump, ORC feed pump and the cooling tower fan. Therefore, the net power output W_{net} of the combined cycle is given by the Equation 16 given previously.

The optimization work is to try different vaporizing pressure P_{vap} as input variable to find out the maximum power output. In EES table calculation, it is varied to calculate the net power output. The result shows that the higher P_{vap}, the more power output the cycle gives. Considering the critical point of isobutane which is 36.4 bar, to keep the cycle at safe working level, P_{vap} at **28 bar** is chosen for the final optimum cycle. As well it indicates in Table 12 below, the temperature of discharge geothermal brine is kept always low. Therefore, there's no possibility for district heating supply.

TABLE 11: Summary of overall results of Scenario 2

No.	Item description	Units	Optimum value
1	**High separation pressure**	**bar**	**11.50**
2	**ORC vaporizing pressure**	**bar**	**10.50**
3	Shaft power output	kW	24017.00
4	High pressure cycle power output	kW	6107.00
5	Bottoming ORC cycle power output	kW	17910.00
6	**Net power output**	**kW**	**22378.00**
7	Pumping rating, cooling water	kW	328.50
8	Pumping rating of circulation of ORC	kW	685.00
9	Power of cooling tower fan	kW	625.60
10	Mass flow of isopentane working fluid	kg/s	246.10
11	Condenser pressure	bar	0.08
12	Condenser cooling capacity	kW	125129.00
13	High pressure stage condenser area	m^2	495.40
14	Low pressure stage condensers area	m^2	9575.00
15	Cooling water flow rate	kg/s	2674.30
16	Cooling water inlet temperature	°C	7.00
17	Cooling water outlet temperature	°C	20.00
18	Minimum making up water flow rate	kg/s	55.42
19	Evaporator area	m^2	7915.00
20	Regenerator area	m^2	0.00
21	Discharge geothermal brine temperature	°C	90.67
22	**District heating power capacity**	**kW**	**103437.00**
23	Heated water inlet temperature	°C	5.00
24	Heated water outlet temperature	°C	85.00
25	Heated water mass flow	kg/s	308.90
26	Heat exchanger area	m^2	4280.00
27	Total heat exchanger area	m^2	22257.00
28	**Thermal efficiency of power cycle**	**%**	**5.99**
29	**Thermal efficiency of multi-utility cycle**	**%**	**36.53**

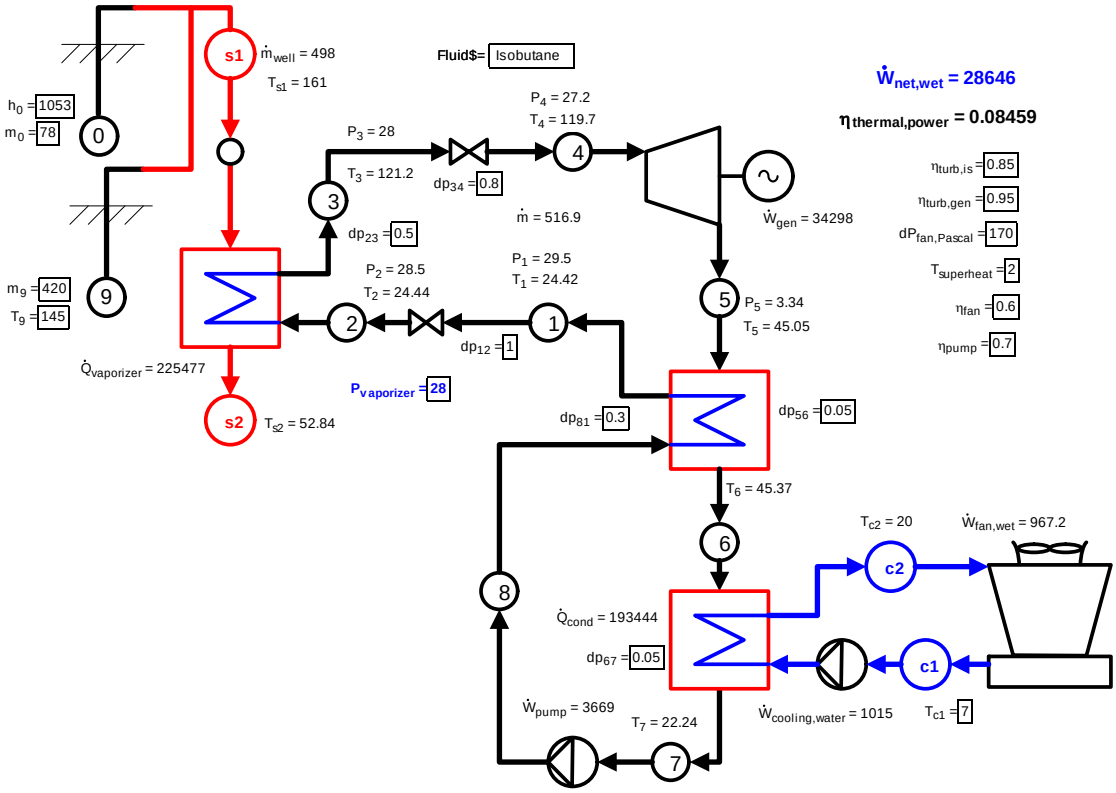

FIGURE 19: Schematic diagram of Scenario 3

TABLE 12: Optimization calculation of Scenario 3

Vaporizer pressure P_{vap} [bar]	Net power output W_{net} [kW]	Temperature of discharge brine T_{s2}[°C]
21	27458	46.13
22	27704	47.35
23	27907	48.52
24	28081	49.61
25	28232	50.61
26	28366	51.51
27	28495	52.28
28	**28646**	**52.84**
29	28820	53.2
30	29264	53.18

The main results of optimum system are given in the following two tables. The optimum net power output of this cycle is 28646 kW (i.e. about 29 MW). The discharge geothermal brine has low drain temperature which is not available for heating system. Therefore, there is not district heating system supply capacity in this system.

In Table 13, the thermodynamic properties of each process state of the schematic diagram are clearly indicated.

TABLE 13: Thermodynamic properties of each process state of Scenario 3

Parameter	Enthalpy	Mass flow	Pressure	Entropy	Temperature
Unit	h [kJ/kg]	m [kg/s]	P [bar]	s [kJ/kg.°C]	T [°C]
[0]	1053.0	78.00	35.43	2.731	243.3
[1]	259.5	516.90	29.50	1.191	24.42
[2]	259.5	516.90	28.50	1.192	24.44
[3]	695.8	516.90	28.00	2.397	121.2
[4]	695.8	516.90	27.20	2.399	119.7
[5]	625.9	516.90	3.34	2.438	45.05
[6]	626.7	516.90	3.29	2.443	45.37
[7]	252.4	516.90	3.23	1.183	22.24
[8]	259.5	516.90	29.80	1.191	24.41
[9]	610.7	420.00	4.15	1.791	145.00

Table 14 below shows the summary of overall results of this ORC cycle system. The power output is the highest to be 28646 kW. The thermal efficiency of the system is 8.46%.

4.5.4 Combined flash and Kalina cycle (Scenario 4)

The forth scenario of the new design is the combined cycle with flash and Kalina cycle named as Scenario 4. This cycle is designed as well at the same assumption and boundary condition as the former scenarios.

The detailed calculations and optimization are performed in EES programme and Matlab, the schematic diagram is shown below in Figure 20. As the similar design concept as the former scenarios, the high enthalpy reservoir is utilized in the topping flash cycle which enters the cycle at separation pressure P_{12}, the power output is W_{hp}. The bottoming one is Kalina cycle using the separated brine from the first separator mixed with the low enthalpy reservoir as the heat source of the cycle. Thus, the supply heat source is at the temperature of $T_{source,in}$ and the mass flow rate of m_{source}. The significant

TABLE 14: Summary of overall results of Scenario 3

No.	Item description	Units	Optimum value
1	**ORC vaporizer pressure**	**bar**	**28.00**
2	Shaft power output	kW	34298.00
3	**Net power output**	**kW**	**28646.00**
4	Pumping rating, cooling water	kW	1015.00
5	Pumping rating of ORC feed pump	kW	3669.00
6	Power of cooling tower fan	kW	967.20
7	Mass flow of isobutene working fluid	kg/s	468.70
8	Condenser cooling capacity	kW	193444.00
9	Condensers area	m^2	17904.00
10	Cooling water flow rate	kg/s	3555.00
11	Cooling water inlet temperature	°C	7.00
12	Cooling water outlet temperature	°C	20.00
13	Minimum making up water flow rate	kg/s	85.68
14	Evaporator area	m^2	21230.00
15	Regenerator area	m^2	0.00
16	Total heat exchanger area	m^2	39091.00
17	Discharge geothermal brine temperature	°C	52.84
18	District heating power capacity	kW	0.00
19	Thermal efficiency of power cycle	%	**8.46**

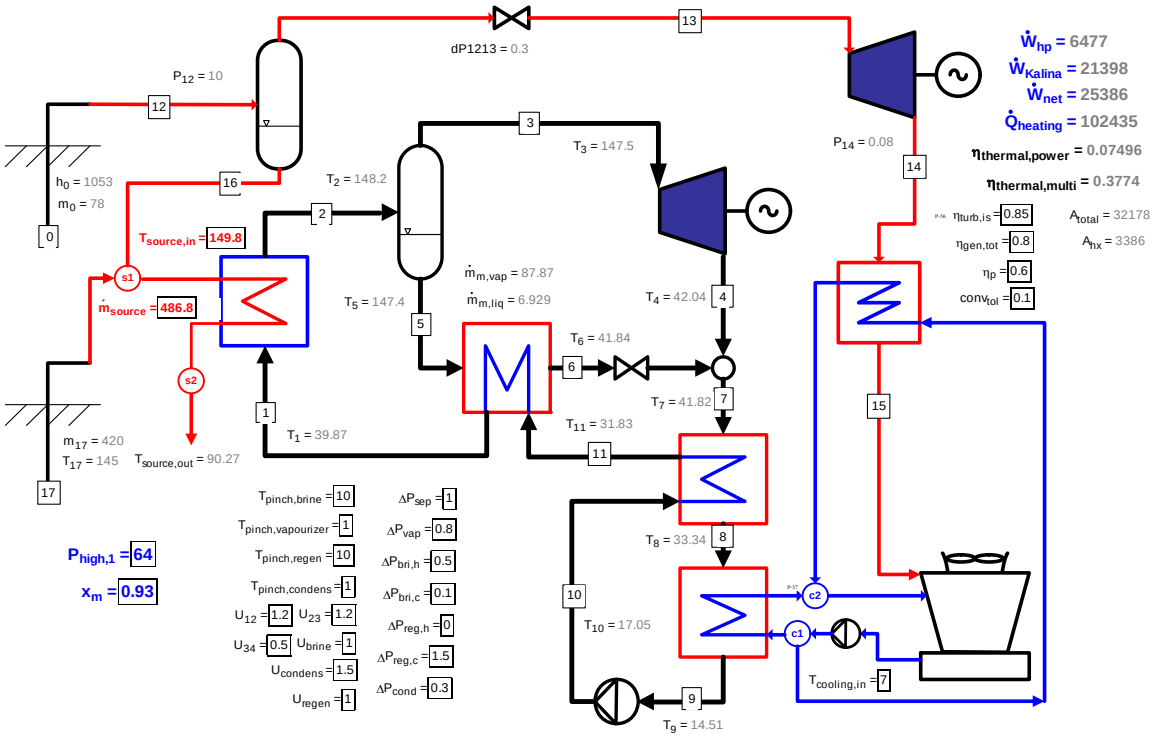

FIGURE 20: Schematic diagram of Scenario 4

factors of the Kalina cycle are the high pressure $P_{high,1}$ of working fluid of ammonia mixture and the ammonia mixture strength x_m. The power output of the Kalina cycle is denoted by W_{kalina}. Thus the total shaft power output W_{shaft} is given as the sum of these two. Additionally, the auxiliary power input is from the cooling water circulating pump, Kalina feed pump and cooling tower fan. The net power output of this combined flash and Kalina cycle is finally calculated as W_{net} also by the Equation 16.

The optimization work for this combined flash and Kalina cycle is more complicated than the former work since there are three variables to determine. They are the separation pressure P_{12} of topping flash cycle, the high inlet pressure $P_{high,1}$ for ammonia mixture and the ammonia mixture strength x_m of bottoming Kalina cycle. The method applied here is to make a calculation first for the topping flash cycle to give some variables of separation pressure P_{12}. By using different P_{12} and relative values as input parameters to the bottoming Kalina cycle, vary the other two variables so as to optimize the entire system. After a lot of trials, it gives the maximum power output of **28251 kW** at the input condition as follows: P_{12}=10 bar, $P_{high,1}$=41 bar, x_m=0.93. Thus, the surf diagram is performed in Matlab shown in Figure 21.

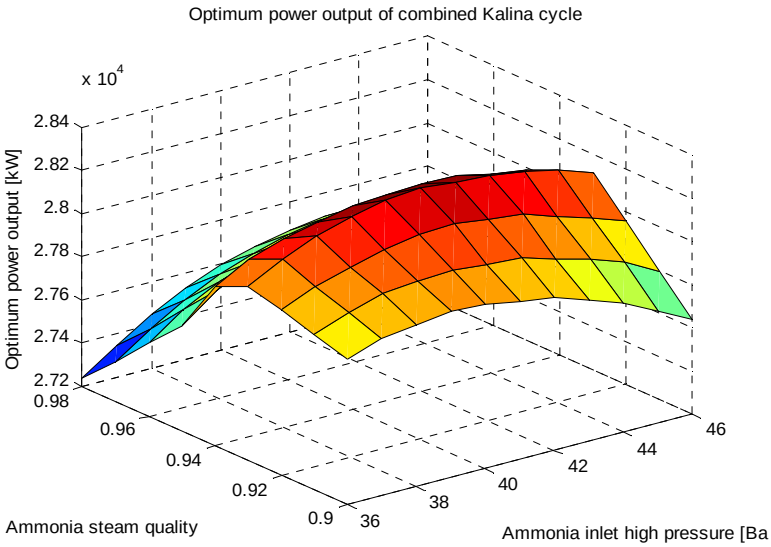

FIGURE 21: The optimum net power output of Scenario 4

The net power output contour of Scenario 4 indicates that the ammonia mixture strength has more influence to the power output than the ammonia high inlet pressure $P_{high,1}$. The net power output can be kept over 99% of the maximum value in the range of 36 to 46 of $P_{high,1}$. While by varying ammonia mixture strength, the power output can be decreased more as shown in the contour diagram of Figure 22.

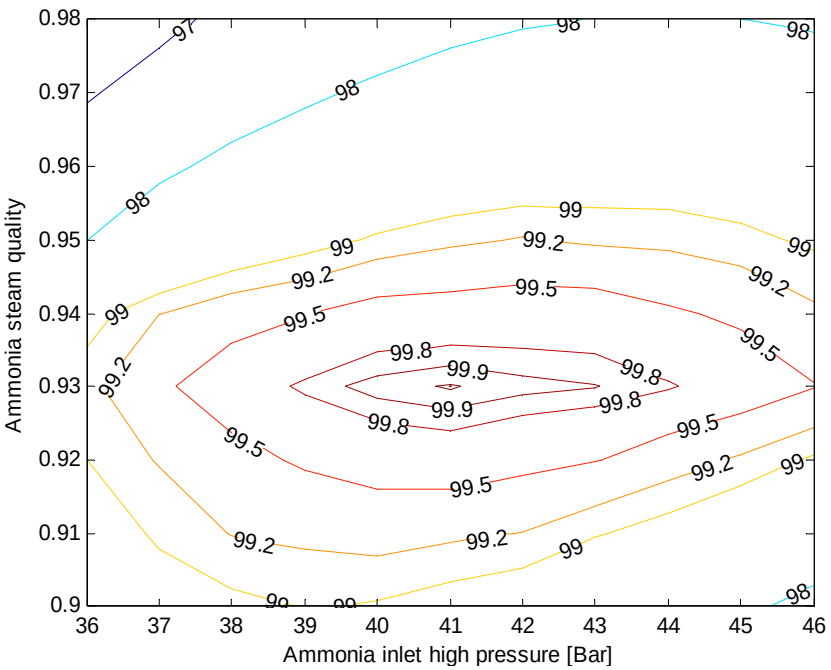

FIGURE 22: Net power output contour of Scenario 4

Figures 23, 24 and 25 indicate the relationships between three variables and net power output. The relationships between net power output and P_{12}, x_m, and $P_{hgih,1}$ respectively are showing the peak points which could result in the optimum value.

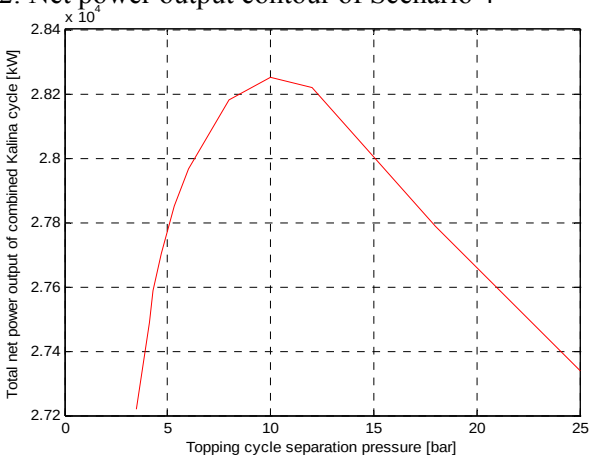

FIGURE 23: W_{net} as a function of topping cycle separation pressure P_{12}

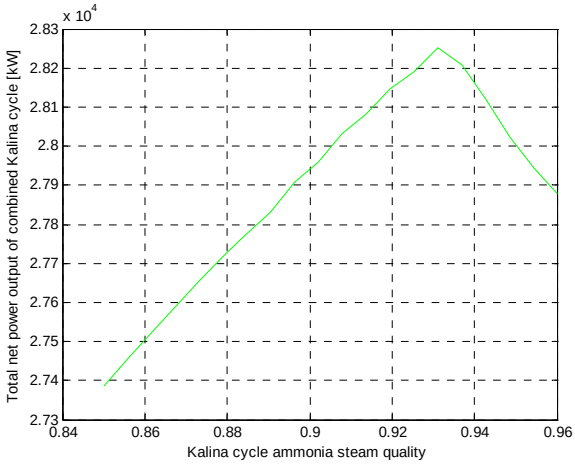

FIGURE 24: W_{net} as a function of bottoming Kalina cycle ammonia steam quality x_m

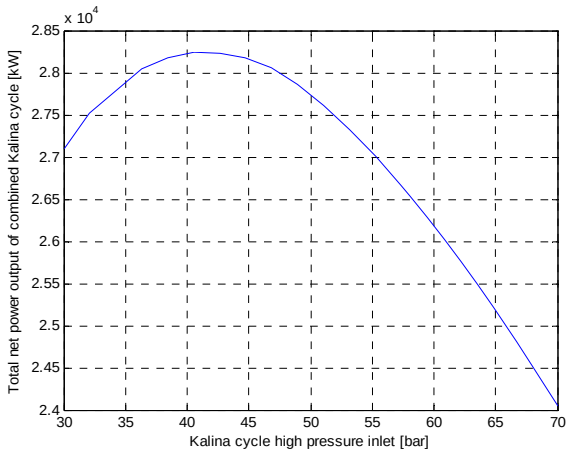

FIGURE 25: W_{net} as a function of Kalina cycle ammonia high pressure $P_{high,1}$

In order to obtain the available temperature of discharge geothermal brine $T_{source,out}$, the varied calculation of three input variable have carried out. The results show that the most sensitive input variable is the high inlet pressure of ammonia mixture $P_{high,1}$. Therefore, Table 15 indicates the results of varied calculation by changing $P_{high,1}$. Considering the feasibility of district heating system, $T_{source,out}$ =90.27 is selected. Thus, the final optimum system is determined at the condition as: P_{12}=10 bar, $P_{high,1}$ =64 bar, x_m =0.93.

TABLE 15: Temperature of discharge geothermal brine variation of Scenario 4

P_{12} [bar]	$P_{high,1}$ [bar]	x_m	W_{net} [kW]	$T_{source,out}$[°C]
10	40	0.93	28237	77.39
10	43	0.93	28224	79.50
10	46	0.93	28113	81.31
10	49	0.93	27855	82.79
10	52	0.93	27489	84.24
10	55	0.93	27060	85.69
10	58	0.93	26547	87.17
10	61	0.93	25999	88.66
10	64	0.93	25386	90.27
10	67	0.93	24744	91.91

The main results of optimum system with both power generation and district heating supply are given in the following two tables. The thermodynamic properties of each process state of the schematic diagram are shown in Table 16.

The summary of overall results of this combined flash and Kalina cycle system are indicated in Table 17. The optimum net power output of this cycle is 25,386 kW. The district heating system supply capacity is 102,435 kW.

TABLE 16: Thermodynamic properties of each process state of Scenario 4

Parameter	Enthalpy	Pressure	Temperature	Steam quality	Mass flow
Unit	h [kJ/kg]	P [bar]	T [°C]	x	m [kg/s]
[0]	1053.00	35.40	243.30	0.00	78.00
[1]	140.00	64.00	39.87	0.93	94.80
[2]	1419.00	63.20	148.20	0.93	94.80
[3]	1493.00	62.20	147.50	0.96	87.87
[4]	1234.00	7.04	42.04	0.96	87.87
[5]	487.80	62.20	147.40	0.57	6.93
[6]	-40.32	61.70	41.84	0.57	6.93
[7]	1141.00	7.04	41.82	0.93	94.80
[8]	1071.00	7.04	33.34	0.93	94.80
[9]	16.91	6.74	14.51	0.93	94.80
[10]	31.97	65.60	17.05	0.93	94.80
[11]	101.40	64.10	31.83	0.93	94.80
[12]	1053.00	10.00	179.90	0.14	78.00
[13]	2778.00	9.70	179.00	100.00	11.23
[14]	2126.00	0.05	32.88	0.82	11.23
[15]	137.70	0.05	32.88	0.00	11.23
[16]	762.80	10.00	179.90	0.00	66.77
[17]	610.70	4.15	145.00	0.00	420.00

4.6 Analysis and comparison of all scenarios

The calculations and optimization work for different alternative scenarios have been carried out in last section. The main results of each scenario are summarized as in Table 18:

It is clear that the Scenario 1 of double flash cycle produces the lowest net power output but highest district heating capacity in contrast with the other scenarios. The highest net power output is from Scenario 3 which is pure ORC cycle with isobutane as the working fluid. But there's no district heating capacity supply in this system. The Scenario 2 is a hybrid flash and ORC cycle with isopentane working fluid. The maximum power output without heating supply of this system is 25,388 kW, and after optimization, the optimum power output is 22,378 kW with good heating capacity of 103,437 kW. Then the final scenario named Scenario 4 is designed as a combined flash and Kalina cycle. Similarly as Scenario 2, the maximum power output is 28,251 kW without heating capacity. Then the optimum system can produce 25,386 kW electricity and 102,435 kW heating power. Thus, both for Scenario 2 and Scenario 4, by sacrifice around 3MW power output, they can supply around 100 MW heating capacity. The thermal efficiency of power plant can increase considerably.

It is also obvious to see that Scenario 3 gives highest pure power efficiency as 8.46% but without heating capacity. Then Scenario 1 gives highest multiple thermal efficiency including power and heating. Therefore, they are all feasible at technical point of view. Since each scenario has its benefit, how to determine the most optimum one is also dependent on the economic analysis which also should take into account of the district heating system evaluation. A design and analysis of district heating system is thus performed in Chapter 5. The overall economic feasibility study will be carried out later in Chapter 6.

TABLE 17: Summary of overall results of Scenario 4

No.	Item description	Units	Optimum value
1	**High separation pressure**	**bar**	**10.00**
2	**Kalina cycle ammonia high pressure**	**bar**	**64.00**
3	**Ammonia steam quality**	**%**	**93.00**
4	Shaft power output	kW	27875.00
5	Topping flash cycle power output	kW	6477.00
6	Kalina cycle power output	kW	21398.00
7	**Total Net power output**	**kW**	**25386.00**
8	Pumping rating, cooling water	kW	449.80
9	Pumping rating of feed pump	kW	1427.00
10	Power of cooling tower fan	kW	612.00
11	Temperature of heat source brine for Kalina	$^{\circ}$C	149.80
12	Mass flow of heat source brine for Kalina	kg/s	486.80
13	Mass flow of Ammonia mixture	kg/s	94.80
14	Mass flow of cooling water	kg/s	2249.30
15	Condenser pressure	bar	0.08
16	Condenser cooling capacity	kW	122394.00
17	Flash cycle condenser area	m^2	544.3
18	Kalina cycle condensers area	m^2	17656.00
19	Cooling water inlet temperature	$^{\circ}$C	7.00
20	Cooling water outlet temperature	$^{\circ}$C	20.00
21	Minimum making up water flow rate	kg/s	54.21
22	Evaporator area	m^2	13922.00
23	Pre-heater area	m^2	89.11
24	Regenerator area	m^2	510.70
25	Discharge geothermal brine temperature	$^{\circ}$C	90.27
26	**District heating power capacity**	**kW**	**102435.00**
27	Heated water inlet temperature	$^{\circ}$C	5.00
28	Heated water outlet temperature	$^{\circ}$C	85.00
29	Heated water mass flow	kg/s	326.30
30	Heat exchanger area	m^2	3386.00
31	Total heat exchanger area	m^2	32722.30
32	**Thermal efficiency of power cycle**	**%**	**7.50**
33	**Thermal efficiency of multi-utility cycle**	**%**	**37.74**

TABLE 18: Summary of optimum results of each scenario

Item	Scenario 1	Scenario 2	Scenario 3	Scenario 4
W_{net} (kW)	**17,849.00**	**22,378.00**	**28,646.00**	**25,386.00**
$Q_{heating}$ (kW)	114,614.00	103,437	0	102,435.00
$T_{source,out}$ ($^{\circ}$C)	100.70	90.67	52.84	90.27
A_{total} (m^2)	5,943.00	22,257.00	39091.00	32722.30
$\eta_{thermal,power}$ (%)	5.27	5.99	8.46	7.50
$\eta_{thermal,multi}$ (%)	39.12	36.53	-	37.74

5 TECHNICAL FEASIBILITY STUDY OF DISTRICT HEATING SYSTEM FOR LHASA

5.1 Brief introduction

Geothermal district heating system connects geothermal hot water to heated buildings via a piping network. The main purpose of heating system is to supply adequate heat to consumers and maintain a comfortable indoor temperature while simultaneously saving energy. The benefit of geothermal district heating system is more profound and sustainable compared with the other energy source application. It is not only energy efficiency and economically viable but also environmentally friendly.

Outdoor temperature condition, general city building type, and main related factors of the district heating system are discussed and calculated. Two different sample buildings are taken into account to make detailed analysis using steady state and dynamic approaches programmed in Matlab to analyze the heating system performances. Based on the analysis results, the heat load and mass flow can be estimated for the whole city. Therefore the conceptual design of district heating system of Lhasa is carried out. As stated in Chapter 4, the heating capacity can be obtained from CHP power plant scenarios, which is around 110 MW. Therefore, a scenario of long distance district heating system from Yangbajain to Lhasa is proposed to fulfil the heating demand in Lhasa.

5.2 Outdoor temperature condition in Lhasa

Since the special geographic location of Lhasa with an elevation of 3658m, outdoor air temperature is lower than other places with the same latitude. The average temperature of the whole year is about 7.5ºC. Here the weather data of Lhasa were obtained from China Meteorological Bureau-Climate Information Center-Climate Data Office and Tsinghua University-Department of Building Science and Technology. The data indicate weather condition of Lhasa in 2005. The outdoor temperature of every hour in the whole year is analyzed for district heating system.

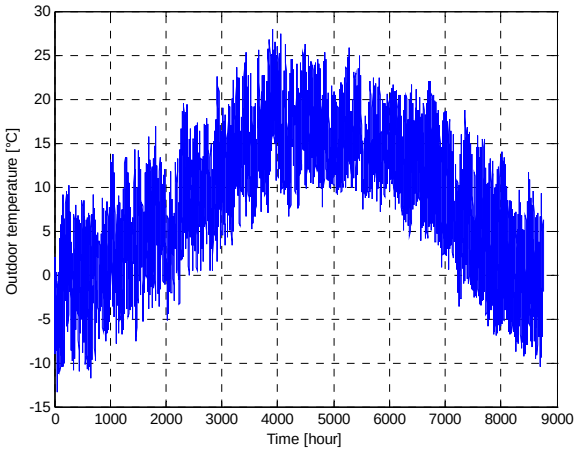

FIGURE 26: Outdoor temperature distribution

The plots of outdoor temperature against time are shown in figures on the right. Figure 26 indicates outdoor temperature distribution while Figure 27 shows duration curve all over the year from January 1st to December 31th in 2005, respectively. The lowest temperature of the year is -13.3ºC. And the coldest days just account for very small fraction.

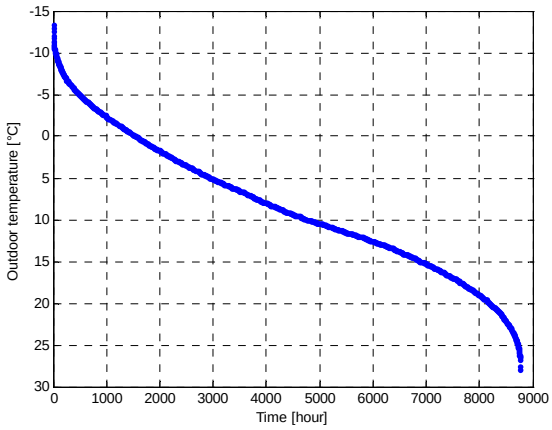

FIGURE 27: Outdoor temperature duration

5.3 Heat loss and thermal mass calculation

Heat loss is taken into account as the primary and important factor in district heating system. The methodology applied here is to make detailed calculation analysis of sample buildings' heat loss and heating performance. Based on the sample results, the estimation for the entire city can be performed.

5.3.1 Description of heated building in Lhasa

Cities and towns in Tibet are mostly developed around a temple as a centre, especially the capital city Lhasa. The old town of Lhasa has been developed around the Lhasa Jokhang Temple (Dazhao Si in Chinese) which is the oldest Buddhist temple in Tibet located in Barkor Street. The traditional residential buildings are mostly built by stones and local materials with commonly 2 or 3 stories. Since the liberation in 1959, the new buildings have been built gradually. In recent years, the energy efficiency buildings are developed very fast.

In this study, the two types of building will be both discussed for the heating system design and performance analysis. The traditional way of building is a response to Tibet's cold and dry climate, and the earthquake-prone ground. Since from at least the 7th century onwards until recently, the materials used for construction of housing in Lhasa have not changed much. Local stone, wood and earth are the basic materials, different qualities of which were used for different purposes. In nowadays, the new public housing is developing fast, the advent of modern construction technologies, particularly the availability of concrete and steel, has led to a decline of traditional building skills due to lack of demand.

The Figure 28 shows two different types of building in Lhasa. The traditional residential building in the front is made of local stone and timber with 2 or 3 stories. The modern energy efficiency buildings in nowadays and planned in future are concrete and steel structure. The common height of the new building is about 6 stories high. An example building is shown in Figure 28 behind the traditional building which is a lively comparison. These two typical building types are involved in the district heating system design. Based on the two sample building calculation, the entire city district heating system can be designed. Therefore, a typical residential building and a typical modern energy efficiency building are respectively taken as the sample building to calculate the heat loss and related factor to the space heating system analysis. It can be used to estimate the total heat loss of the city so as to predict overall heat demand and distribution system.

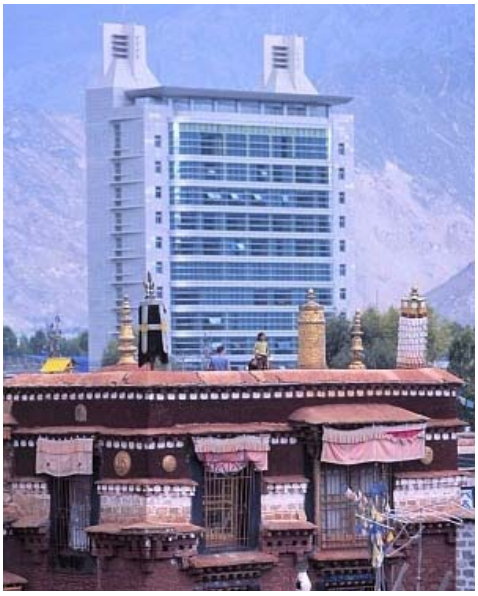

FIGURE 28: Different buildings in Lhasa

5.3.2 Main structure of traditional residential building

One of the most characteristic features of traditional Tibetan architecture is the battered wall (Figure 29). Besides giving Tibetan buildings a distinctive silhouette (Figure 30), the inward-sloping walls also provide extra stability in case of tremors. The sloping is created by the reduction in thickness from the ground floor wall to the top floor wall, with the inside wall remaining vertical. The walls on the ground floor, usually built from stone on shallow stone foundations, are extremely thick, often more than a meter. The walls get thinner and lighter towards the top of the building. The top floor of a house is commonly built from mud bricks, but wealthier houses would have used stone bricks for all floors. Between the meticulously-made outer and somewhat simpler inner faces, the wall core is filled with stone rubble and then rammed with mud, straw and other insulating materials. The masonry deserves special mention. Courses of large rectangular stones, roughly of equal size, are laid between layers of small flat stones. This technique, known as galetted rubble, gives the walls a greater flexibility in case of tremors and therefore adds to the

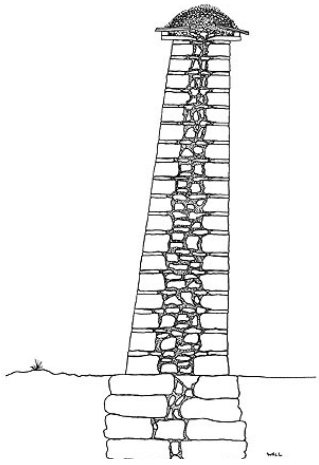

FIGURE 29: Section of traditional built wall

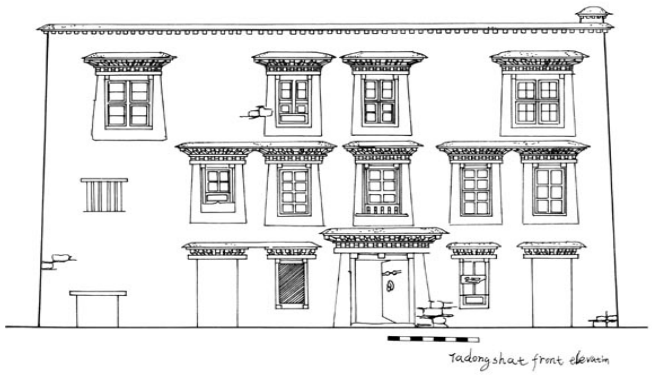

FIGURE 30: Traditional building front elevation

stability of a house. The top of a wall is sealed against rain by a cornice made from slate and wood, crowned by a mound of clay.

Ceilings, supported by a pillar-post construction, are built by placing wooden rafters between the central beams and the walls. The rafters support layers of pebbles and mud. The roofs are sealed either by stamped and oiled clay or water-absorbing sand known (Alexander and de Azevedo, 1998).

The structure of the sample traditional residential building is discussed below. The dimension of the building is $20 \times 8 \times 8$ (length $\times$ width $\times$ height). The main material of the construction is shown below in Tables 19 and 20. The thickness of wall here is taken to be 300mm as an equivalent value for further calculations.

TABLE 19: Roof structure and material of traditional sample building

Layer material	Thickness (mm)	Thermal conductivity (W/m.ºC)	Specific heat capacity (kJ/kg. ºC)	Density (kg/m^3)
Stamped and oiled clay	10	1.0	1.58	1600
Roof slate	150	1.80	0.60	1800
Chalk	20	4.64	0.86	2710

TABLE 20: External wall structure and material of traditional sample building

Layer material	Thickness (mm)	Thermal conductivity (W/m.ºC)	Specific heat capacity (kJ/kg. ºC)	Density (kg/m^3)
Stone with insulation material in middle	300	0.50	1.90	1900
Chalk	20	4.64	0.86	2710

5.3.3 Main structure of modern energy efficiency building

The typical modern building is energy efficiency type. The structure is concrete structure building with commonly about 6 stories. The dimension of the sample building is $30 \times 20 \times 18$m (length $\times$ width $\times$ height). The insulation material which is constructed on the outer external wall surface is polyurethanes (PU). The detailed construction materials of the building envelope are shown in Tables 21 and 22:

TABLE 21: Roof structure and material of modern sample building

Layer material	Thickness (mm)	Thermal conductivity (W/m.ºC)	Specific heat capacity (kJ/kg. ºC)	Density (kg/m^3)
Concrete with fine stones	40	1.51	0.92	2300
Polyurethanes insulation layer	60	0.037	1.38	50
Steel reinforced concrete board	150	1.74	0.92	2500
Cement mortar surface	20	0.93	1.05	1800

TABLE 22: External wall structure and material of modern sample building

Layer material	Thickness (mm)	Thermal conductivity (W/m.ºC)	Specific heat capacity (kJ/kg. ºC)	Density (kg/m^3)
Cement mortar outer surface	20	0.93	1.05	1800
Polyurethanes insulation layer	20	0.037	1.38	50
Abated Concrete	200	0.22	1.05	700
Cement mortar inner surface	20	0.93	1.05	1800

5.3.4 Reference condition and main assumptions

The reference design condition in this report is the Icelandic design method which is designed as 80/40, -15ºC systems. It means that district heating system is designed to maintain the desired indoor temperature, usually at 20 ºC, at -15ºC outdoor air temperature, with 80ºC supply temperature to radiators and 40ºC return temperature. It is emphasized that the reference return temperature is a function of radiator system in the buildings. In district heating system, every consumer has a different types and sizes of radiator, so the reference return temperature is assumed as an average of the whole radiator system's function. In this report, reference return temperature is also assumed to be 40°C. Thus, this temperature drop is somewhat larger than commonly used in hot water heating systems in most countries for maximum utilization of geothermal hot water. Then the radiator surface area is enlarged which result in larger temperature drop of the water flowing through.

Reference transmission effectiveness of the distribution system is specific to the system design. A district heating pipe heat transmission factor can be defined in a similar way as the heat exchanger effectiveness. Heat exchanger effectiveness of unity means that all the heat, which can be exchanged, has been exchanged. It is then logical to define the district heating pipe transmission effectiveness as the ratio between the heat transmitted and the heat put into the pipe relative to the ground temperature. Then the transmission effectiveness will be unity, if all the heat put into the pipe is transmitted (Valdimarsson, 1993). The reference transmission effectiveness of the piping system can be calculated from any operating conditions. In this report reference transmission effectiveness of the transmission pipe is assumed to be 0.95.

In the geothermal district heating network, part of geothermal water is used for supplying tap water, either consumed directly or used for heating of cold water in the heat exchangers. The consumption of the hot tap water does not depend on the outdoor temperature, but is a function of consumer's average behaviour. The tap water consumption is expected to have a periodic daily variation, with very low consumption during the night. The common amount of tap water use in the Reykjavik district heating system is 10 - 15% of the yearly average mass flow (Karlsson, 1982).

In this study the design outdoor temperature for heating system in Lhasa is -6ºC according to the Chinese Space Heating Standard. The design supply and return temperature of the geothermal heating system is the same as the referenced system which is 80/40 ºC. The design indoor temperature is 18°C according to the space heating system design standard in China. The hot tap water is also assumed as 10% of the total mass flow, neglecting its daily variations. The specific heat capacity of water was assumed to be constant over the system and its dependence on temperature has been neglected. The specific heat capacity for water, C_p = 4.186 kJ/(kg°C) is used here.

5.3.5 Main parameters calculation of the two types of sample buildings

In district heating system, the most important parameters of the building influence the heat demand and heating performance is the construction material and structure. Here the heat loss factor which is the overall heat transfer coefficient of the building is calculated as follows, as well as the thermal mass of the sample building which affects the dynamic heating performance analysis significantly.

Calculation for modern energy efficiency sample building

(1) Heat loss through the building envelope

For walls: the structure of the external wall has been shown in Table 23. The insulation layer is built on the outer surface of the wall. The detailed calculation has been taken in Excel file, the equation of the total heat transfer coefficient of the wall is as follows:

$$U_{wall} = u \cdot A = 1 \cdot A / \sum R = \frac{1 \cdot A}{R_i + R_o + x_c / k_c + x_{ins} / k_{ins} + + x_{sur} / k_{sur}} \tag{17}$$

where U_{wall} is the heat transfer coefficient, W/ºC;
u is the heat transfer coefficient per area, W/m^2. ºC;
A is the area of wall, m^2;
R is the heat resistivity, m^2 ºC /W;
R_i is the heat resistivity between indoor air and the wall which is 0.14 m^2 ºC /W;
R_o is the heat resistivity between outdoor air and the wall which is 0.07 m^2 ºC /W;
k_c is the thermal conductivity of abated concrete which is 0.22W/m ºC;
k_{ins} is the thermal conductivity of insulation material which is 0.037 W/m ºC;
k_{sur} is the thermal conductivity of cement mortar surface which is 0.93 W/m ºC;
x_c is the thickness of the concrete, m;
x_{ins} is the thickness of the insulation material, m;
x_{sur} is the thickness of the cement mortar surface, m.

Thus, the heat transfer coefficient of the walls is 1184.04 W/ ºC.

For windows: according to the Icelandic standard for the double pane window, the heat transfer coefficient per area is 3 W/m^2. ºC. The area of the window here is estimated as 20% of the whole external wall area. Then the total heat transfer coefficient is:

$$U_{window} = u_{window} \cdot A \tag{18}$$

Thus, the heat transfer coefficient of the windows is 1080 W/ ºC.

For roof: the calculation of heat loss factor for building roof is quite similar as the external wall. Table 22 shows the structure and material of the roof. According to the detailed calculation, the heat transfer coefficient of the roof is 305.22 W/ ºC.

For floor: the heat transfer coefficient per area for the roof is 0.3 W/m^2. ºC (according to Chinese design standard). Thus, it is:

$$U_{floor} = u_{floor} \cdot A \tag{19}$$

Thus, the heat transfer coefficient of the floor is 180 W/ ºC.

Finally the total heat transfer coefficient from the building envelope is:

$$U_{building} = U_{wall} + U_{window} + U_{roof} + U_{floor} = 2749.26 \text{W/ ºC} \tag{20}$$

The heat loss of the building through the envelope is

$$Q_{building} = U_{apartment} \cdot (T_i - T_o) = 2749.26 \times (18 - (-6)) = 65982.18 \text{W} \tag{21}$$

(2) Heat loss by infiltration

Infiltration is the leakage of outside air into the building through cracks by the windows and doors. The amount of the infiltration depends mainly on the tightness of windows and doors and on the outside wind velocity or the pressure difference between the outside and inside. Two methods can be used to estimate the volume of infiltration air into the heating area.

1. Crack length method

The base of this method is the perimeter of windows and doors, according to the following equation:

$$V = \sum l \cdot L \cdot n \quad (\mathrm{m^3/h}) \tag{22}$$

where l = the total length of crack (m);
L = infiltration of air volume through windows and doors per meter (m^3/(m h));
n = Correction factor of infiltration for different direction.

2. Air change method

This method is based on the air volume in a space for being replaced by outside air certain times per hour. This method is used here for calculating the infiltration. The Chinese heating code recommends 0.5-1.0 air changes per hour for residential buildings. One air change per hour is used in this paper and can be calculated in kJ/h according to:

$$Q_{\inf il} = C_p V \rho_d (T_i - T_o) \tag{23}$$

where C_p is the specific heat of air, 1.0056 kJ/kg.ºC;
V is the volume flow of infiltrated air, m^3/h;
ρ_d is the air density at the temperature T_o , 1.32 kg/m^3.

Using the air change method to determine V (m^3/h), gives:

$$V = nVh \tag{24}$$

where n is the air change times per hour, 0.5~1.0 / h, here 0.6 is selected;
V_h is the room volume, which is 10,800.00 m^3.

From Equation 11: Q_{infil} = 57.34 W.

(3) Total heat loss of the building

The total heat transfer coefficient k_l = 2751.65 W/ ºC.

Thus, the total heat loss is: $Q_{total} = Q_{envelope} + Q_{infil}$ = 66,039.53 W = 66.04 kW.

Thermal mass is a term used to describe the ability of building materials to store heat (thermal storage capacity). The basic characteristic of materials with thermal mass is their ability to absorb heat, store it, and at a later time release it. Adding thermal mass within the insulated building envelope helps reduce the extremes in temperature experienced inside the home, making the average internal temperature more moderate year-round and the home more comfortable to live in. It is also an important factor for analyzing the dynamic performance of building heating or cooling system. The following calculations, presented in Tables 23, 24 and 25 are for the present public sample building which is energy efficiency type.

TABLE 23: Thermal mass for external walls

Construction material	x (m)	A (m^2)	ρ (kg/m^3)	c (kJ/(kg °C))	C (kJ/°C)
Abated Concrete	0.20	1,800	2,500	1.05	945,000
Cement mortar surface	0.04	1,800	1,800	1.05	136,080
Polyurethanes insulation layer	0.02	1,800	200	1.38	9936
C_{total}	1091016				

TABLE 24: Thermal mass for roof

Construction material	x (m)	A (m^2)	ρ (kg/m^3)	c (kJ/(kg °C))	C (kJ/°C)
Concrete with fine stones	0.04	600	2,300	0.92	50,784
Polyurethanes insulation layer	0.06	600	50	1.38	2484
Steel reinforced concrete board	0.15	600	2,500	0.92	207,000
Cement mortar surface	0.02	600	1,800	1.05	22,680
C_{total}	282948				

TABLE 25: Thermal mass for floor

Construction material	x (m)	A (m^2)	ρ (kg/m^3)	c (kJ/(kg °C))	C (kJ/°C)
Concrete	0.20	600	2,500	0.90	270,000
Plywood	0.05	600	545	1.22	19,865
C_{total}	289,865				

Therefore, the total thermal mass of the building can be summarized as in Table 26:

TABLE 26: Thermal mass of modern sample building

Component	*C* (kJ/°C)
Roof	282,948
Floor	289,865
Walls	1,091,000
$C_{building}$	1,664,000

Thus, the time constant of the building τ_b can be calculated to be 167.96 hours.

Calculation for the traditional residential sample building

(1) Heat loss through the building envelope

For walls: The structure of the external wall has been shown in Table 21. The calculation of the wall here is simplified. The thickness is assumed as the same value as 300mm. The values of the material properties are also taken the average. The detailed calculation has been taken in Excel file, the equation of the total heat transfer coefficient of the wall is as follows:

$$U_{wall} = u \cdot A = 1 \cdot A / \sum R = \frac{1 \cdot A}{R_i + R_o + x_{stone} / k_{stone} + x_{chalk} / k_{chalk}} \quad (25)$$

where U_{wall} is the heat transfer coefficient, W/ºC;
u is the heat transfer coefficient per area, W/m^2 ºC;
A is the area of wall, m^2;
R is the heat resistivity, m^2 ºC /W;

R_i is the heat resistivity between indoor air and the wall which is 0.14 m^2 ºC /W;
R_o is the heat resistivity between outdoor air and the wall which is 0.07 m^2 ºC /W;
k_{stone} is the thermal conductivity of equivalent wall stone which is 0.50W/m ºC;
k_{chalk} is the thermal conductivity of chalk which is 4.64 W/m ºC;
x_{stone} is the thickness of the equivalent wall stone, m;
x_{chalk} is the thickness of the cement mortar surface, m.

Thus, the heat transfer coefficient of the walls is 616.18W/ ºC.

For windows: for the traditional building type, the heat transfer coefficient per area of window is estimated to be 3.5 W/m^2. ºC. The area of the window here is estimated as 20% of the whole external wall area. Then the total heat transfer coefficient is:

$$U_{window}=u_{window}: A \tag{26}$$

Thus, the heat transfer coefficient of the windows is 313.60W/ ºC.

For roof: the calculation of heat loss factor for building roof is quite similar as the external wall. Table 20 shows the structure and material of the roof. According to the detailed calculation, the heat transfer coefficient of the roof is 520.08 W/ ºC.

For floor: the heat transfer coefficient per area for the roof is 0.4 W/m^2 ºC (according to Chinese design standard). Thus, it is:

$$U_{floor} = u_{floor} \cdot A \tag{27}$$

Thus, the heat transfer coefficient of the floor is 240W/ ºC.

Finally the total heat transfer coefficient through the building envelope is:

$$U_{building} = U_{wall} + U_{window} + U_{roof} + U_{floor} = 1689.86\text{W/ ºC} \tag{28}$$

The heat loss of the apartment through the surroundings is

$$Q_{building} = U_{building} \cdot (T_i - T_o) = 1689.86 \times (18 - (-6)) = 40556.64\,\text{W} \tag{29}$$

(2) Heat loss by infiltration
The calculation is same as the one for present public building using the air change method. Hence, the heat loss by infiltration is Q_{infil} = 6.8 W;

(3) Total heat loss
The total heat transfer coefficient k_l = 1690.14 W/ ºC.

Thus, the total heat loss is: $Q_{total} = Q_{envelope} + Q_{infil}$ = 40,563.44 W = 40.56 kW.

Results of thermal mass calculations are presented in Tables 27, 28 and 29.

TABLE 27: Thermal mass for external walls

Construction material	x	A	ρ	c	C
	(m)	(m^2)	(kg/m^3)	(kJ/(kg °C))	(kJ/°C)
Stone with insulation material	0.30	576	1900	0.75	246240
Chalk	0.02	576	2710	0.86	26849
C_{total}	273,089				

TABLE 28: Thermal mass for roof

Construction material	x (m)	A (m^2)	ρ (kg/m^3)	c (kJ/(kg °C))	C (kJ/°C)
Stamped and oiled clay	0.01	160	1600	1.58	4045
Roof brick	0.15	160	1800	0.60	25920
Chalk	0.02	160	2710	0.86	7458
C_{total}	37,423				

TABLE 29: Thermal mass for floor

Construction material	x (m)	A (m^2)	ρ (kg/m^3)	c (kJ/(kg °C))	C (kJ/°C)
Brick	0.10	600	1800	0.60	64800
Plywood	0.05	600	545	1.22	19865
C_{total}	101,866				

Therefore, the total thermal mass of the building can be summarized as in table 30.

TABLE 30: Thermal mass for traditional sample building

Component	*C* (kJ/°C)
Roof	37,423
Floor	101,866
Walls	273,089
$C_{building}$	412,377

Thus, the time constant of the building τ_b can be calculated to be 67.77hours.

5.3.6 Summary of parameters calculation for two sample building

The main parameters used in district heating design and performance analysis are calculated in last two sections above, the summary is given in Table 31. The different structure and construction material of the buildings influence heat loss factor of the heat load requirement, especially the thermal mass. The heavy building like modern energy efficiency building sample has longer time constant than the traditional residential building. It will affect heating performance significantly. The detailed analysis is performed in the following sections.

TABLE 31: Summary of parameter calculations

Parameter	Symbol	Modern public building sample (A)	Traditional residential building sample (B)
Building dimension	$L \times W \times H$	$30 \times 20 \times 18$	$20 \times 8 \times 8$
Overall heat transfer coeff., W/ °C	k_l	2751.65	1690.14
Thermal mass, kJ/°C	C	1,664,000	412,377
Time constant, hour	τ_b	167.96	67.77

5.4 District heating system performance calculation principles

There are four main components in a district heating system, known as heat supple source, transmission pipeline and distribution network and building system. Some principles for the system design and performance are given below:

Building system is to transmit heat to the indoor air. There are many forms of building system such as radiator heating, floor heating and fan coil system. The most common and economical way is radiator system. The latter ones needs lower supply temperature which can be provided more easily. Here in this report this radiator system is applied and as direct connection with the distribution system, which means there's no heat exchanger in the building.

Heat loss of the heated building is mainly a function of an outdoor air temperature. By taking the outdoor temperature as primary influencing factor for the weather, the building heat loss is defined as:

$$Q_{loss} = k_l\left(T_i - T_o\right) \tag{30}$$

where Q_{loss} = heat loss, W;
k_l = overall heat transfer coefficient of building which is constant and only depends on building design, not on weather conditions, W/ ºC;
T_i = indoor temperature, ºC;
T_o = outdoor temperature, ºC.

Then, the relative heat loss from the buildings is obtained:

$$\frac{Q_{loss}}{Q_{loss0}} = \frac{T_i - T_o}{T_{i0} - T_{o0}} \tag{31}$$

Supply temperature of radiator system in steady state analysis:

$$T_s = T_g + \tau_0^{\dot{m}_0/\dot{m}}(T_1 - T_g) \tag{32}$$

The radiator model describes how heat is transferred from the district heating water to the building as a function of water mass flow through the radiator, supply temperature at the radiator inlet and indoor temperature. Then the district heating water return temperature is calculated by the performance of radiator systems in the buildings.

Radiator is the heat exchanger that transfers heat from the district heating network to the indoor air. According to Anon (1977), the relative heat duty of a radiator can be written as:

$$\frac{Q}{Q_0} = \left(\frac{\Delta T_m}{\Delta T_{m0}}\right)^{4/3} \tag{33}$$

Logarithmic temperature difference ΔTm is defined as:

$$\Delta T_m = \frac{\left(T_s - T_i\right) - \left(T_r - T_i\right)}{\ln\left(\frac{T_s - T_i}{T_r - T_i}\right)} = \frac{\left(T_s - T_r\right)}{\ln\left(\frac{T_s - T_i}{T_r - T_i}\right)} \tag{34}$$

Inserting Equation 34 into Equation 33, it becomes:

$$\frac{Q}{Q_0} = \left(\frac{\left(T_s - T_r\right)}{\ln\left(\frac{T_s - T_i}{T_r - T_i}\right)} \cdot \frac{\ln\left(\frac{T_{s0} - T_{i0}}{T_{r0} - T_{i0}}\right)}{\left(T_{s0} - T_{r0}\right)}\right)^{4/3} \tag{35}$$

The reference condition describes the efficiency of the radiator system to extract the heat from the district heating water. The reference return water temperature, at reference indoor temperature and reference supply temperature will be changed if effectiveness of radiator system is changed.

Return temperature in steady state analysis can be calculated by Equation 35 with iteration. According to Valdimarsson (1993) fastest convergence is obtained, when T_r inside logarithm is worked out:

$$T_{r,n+1} = \left(T_s - T_i\right) \cdot e^{-A} + T_i \tag{36}$$

Where A is:

$$A = \frac{T_s - T_{r,n}}{T_{s0} - T_{r0}} \cdot \ln\left(\frac{T_{s0} - T_{i0}}{T_{r0} - T_{i0}}\right) \cdot \left(\frac{T_{i0} - T_{o0}}{T_i - T_o}\right)^{3/4} \tag{37}$$

When outdoor temperature data is given, T_i is assumed to be constant and supply temperature is known, $T_{r,n+1}$ can be found iteratively from the Equation 36.

By assuming negligible heat capacity of the radiator itself, the relative heat flow from the radiator can be equated to the relative heat flow from the district heating water to the radiator. So, heat loss from the building and heat load from the district heating water in steady state analysis is equal all the time, assuming ideal controller:

$$Q_{supp} = Q_{loss} \tag{38}$$

$$mc_p\left(T_s - T_r\right) = k_l\left(T_i - T_o\right) \tag{39}$$

Mass flow is obtained directly from Equation 40:

$$m = \frac{k_l\left(T_i - T_o\right)}{c_p\left(T_s - T_r\right)} \tag{40}$$

Factor k_l can also be calculated from the reference conditions:

$$k_l = \frac{m_0 c_p\left(T_{s0} - T_{r0}\right)}{\left(T_{i0} - T_{o0}\right)} \tag{41}$$

Distribution piping network is the important part of the district heating system which is the connection of heat source and heat consumer. The new concept of the transmission effectiveness parameter which was introduced by Valdimarsson (1993) is a very useful factor to calculate the pipe network size and performance.

There must be some heat lost in the distribution system connecting the heat source and the buildings to be heated. The heat lost from the pipe goes into the surrounding ground and then goes to the air. The outdoor air temperature then influence the pipe heat loss, but with reduced intensity and delay. Therefore, it is assumed that heat is transferred from the pipe towards the ground, not the air above ground and ground temperature surrounding the pipe insulation has the undisturbed soil temperature. According to Valdimarsson (1993), the amount of heat lost from the pipe can be calculated by using pipe transmission effectiveness parameter. Assuming that the district heating pipe has a known performance at a certain operating condition, the pipe transmission effectiveness is defined:

$$\tau = \frac{T_s - T_g}{T_1 - T_g} = e^{-\frac{U_p}{mc_p}} \tag{42}$$

The reference value of pipe transmission effectiveness τ_0 can be calculated from the reference flow conditions:

$$\tau_0 = \frac{T_{s0} - T_g}{T_1 - T_g} = e^{-\frac{U}{m_0 C_p}} \tag{43}$$

From this, one obtains:

$$-\frac{U}{C_p} = m_0 \ln(\tau_0) \tag{44}$$

Parameters U and C_p is assumed to be constant all over the system. Substituting Equation 44, Equation 42 becomes Equation 45 and transmission effectiveness is found as a function of mass flow at operational condition:

$$\tau = \frac{T_s - T_g}{T_1 - T_g} = e^{\frac{m_0}{m}\ln(\tau_0)} \tag{45}$$

or,

$$\tau = \tau_0^{\frac{m_0}{m}} \tag{46}$$

For dynamic district heating system analysis, by assuming all heated parts of the building to be at uniform indoor temperature at all times, the building can be modelled as a heat capacity element. When the heating of building is turned off, the building does not cool down immediately due to stored energy. The building energy storage model is:

$$\frac{dT_i}{dt} = \frac{1}{C} Q_{net} = \frac{1}{C}\left(Q_{supp} - Q_{loss}\right) = \frac{1}{C}\left(m \cdot c_p \cdot \left(T_s - T_r\right) - k_l \cdot \left(T_i - T_o\right)\right) \tag{47}$$

All time derivatives equal to zero in steady state model and this equation is not used, but in dynamic modelling the equation plays a significant part (Lkhagvadorj, 2007).

5.5 Sample buildings heating system performance analysis

The two different sample buildings taking into account in this study have different heat loss factor and thermal mass. Therefore the heating performances for each building type are also different. As calculated in last section, the heat loss in principle is based on a function of the building's structure, its insulation characteristics, volume of building and local climate. Since the other features are fixed already, the only variable is the outdoor temperature. The figures below indicate the heat load of two sample buildings with similar shape.

The mass flow of hot tap water is assumed as 10% of the heating mass flow, according to the steady state calculations, the maximum hot tap water mass flow for modern and traditional sample building is 0.05kg/s and 0.03 kg/s, respectively. The maximum heat load for the modern and the traditional building sample is 86.12 kW and 52.90 kW respectively (Figures 31 and 32).

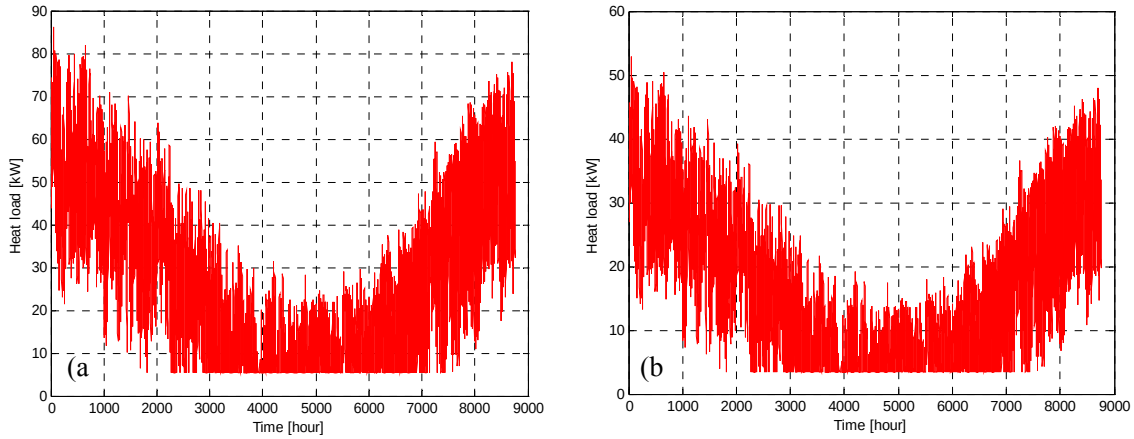

FIGURE 31: Heat load distribution of heating system for
(a Modern sample building, and (b Traditional sample building

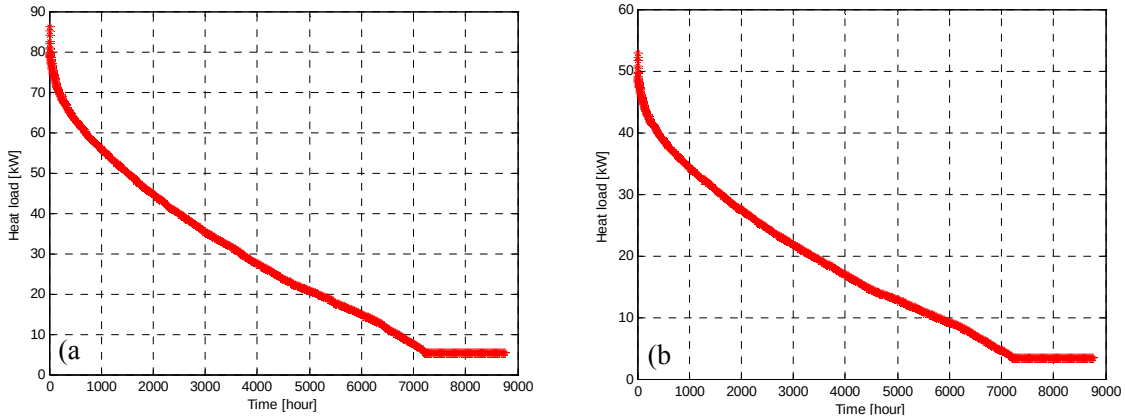

FIGURE 32: Heat load duration curve of district heating system for
(a Modern sample building, and (b Traditional sample building

5.5.1 Steady state approach analysis

When the district heating systems are assumed to be in steady state, it means that there is no heat accumulated in buildings. Therefore, indoor temperature is assumed to be constant. In this condition, the flow controller is assumed as an ideal one which adjusts the mass flow in such a way that the heat loss from building will be exactly supplied to the building at the same time. Thus, the mass flow will be considered unbounded.

The steady state model is set up in Matlab programme. The heat loss has been calculated as before which is only dependent on the outdoor temperature change. Here the hot tap water heating part will not be included in the analysis.

Results and analysis:
The steady state approach is performed for both sample buildings. The results have same trend for them. Therefore, here only illustrates the results for modern energy efficiency building sample as a representative for performance analysis.

(1) Heat load
As Figure 33 indicates, there is a linear relationship between heat load and the outdoor temperature. The heat load is decreasing as the outdoor temperature increases because there is not much heat load needed to maintain the required indoor temperature when outdoor temperature goes higher. From the graph below it indicates the heat load is heading towards zero even minus when outdoor temperature is closed to 18°C. However, it will not reach 18°C when the heat load becomes zero due to the effect of

building heat storage.

(2) Mass flow

Figure 34 shows the mass flow as a function of outdoor temperature. It is shown that the colder outside the more mass flow is needed, vice versa. That is because less heat duty is needed when the outdoor temperature is higher. The curve also shows the mass flow can increase sharply when the outdoor temperature decreases in the coldest days which means there needs quite a lot of energy input.

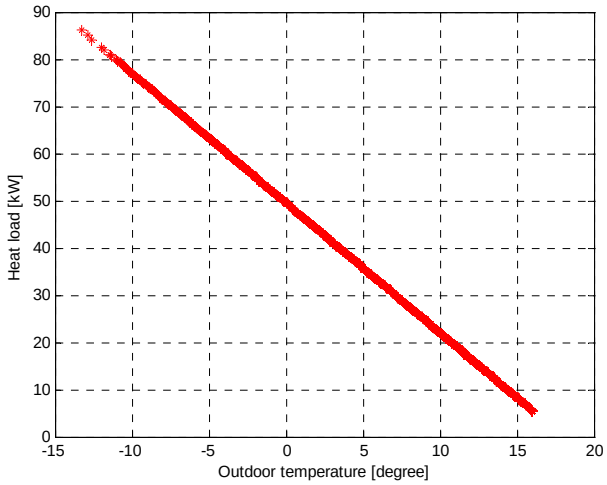

FIGURE 33: Heat load as a function of outdoor temperature

Figure 35 below shows the relative mass flow as a function of outdoor temperature. The transmission effectiveness factor has not been taken into account. The reference condition calculation is based on the Icelandic design outdoor temperature of -15°C. Therefore, the real condition in Lhasa, with the lowest temperature of -13.3°C during the coldest days, the relative mass flow is always less than 1.

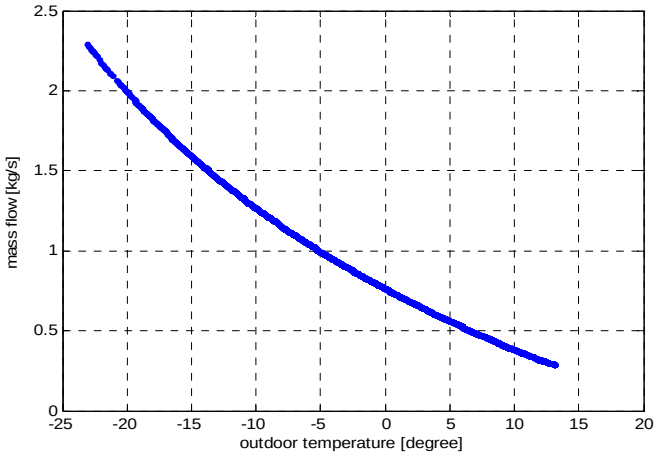

FIGURE 34: Mass flow rate as a function of outdoor temperature

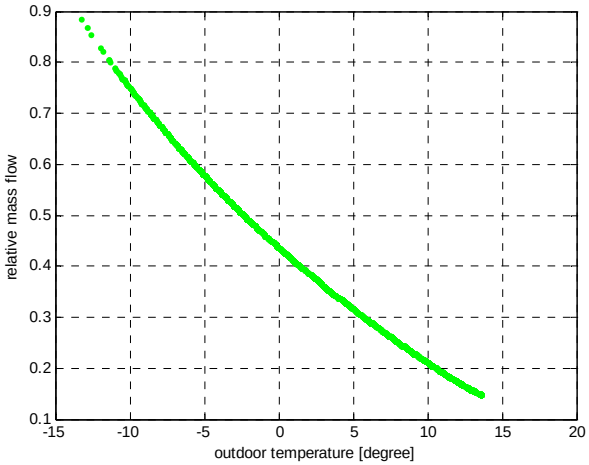

FIGURE 35: Relative mass flow rate as a function of outdoor temperature

(3) Supply and return temperature

For steady state analysis, to maintain the constant indoor temperature, the mass flow is not limited. Therefore the supply and return temperature of radiator is performed as shown in Figure 36. Supply and return water temperatures are shown as a function of outdoor temperature where the heat loss in the transmission pipe is included. It shows that return temperature is going higher while the outdoor temperature is going lower. That's because there are more mass flow transmitted to the radiator system to meet the higher heat demand.

(4) The relative values

Figure 37 shows the different relative values as a function of outdoor temperature. Compared to the reference condition, it shows clearly how the heat load, mass flow, supply and return temperature perform in the real case. The mass flow is the most sensitive parameter according to the changing of heat load.

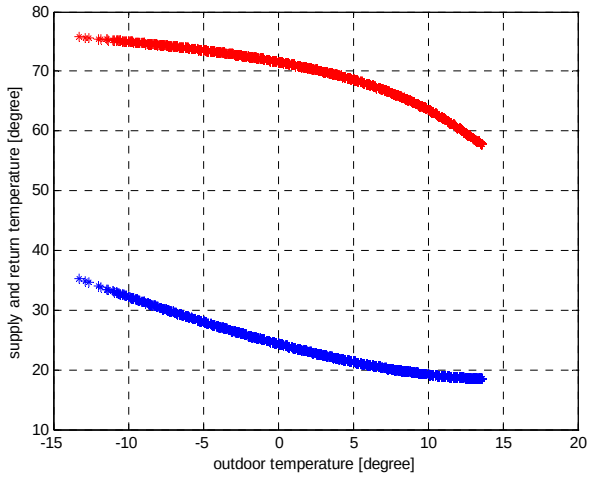

FIGURE 36: supply and return temperature as a function of outdoor temperature

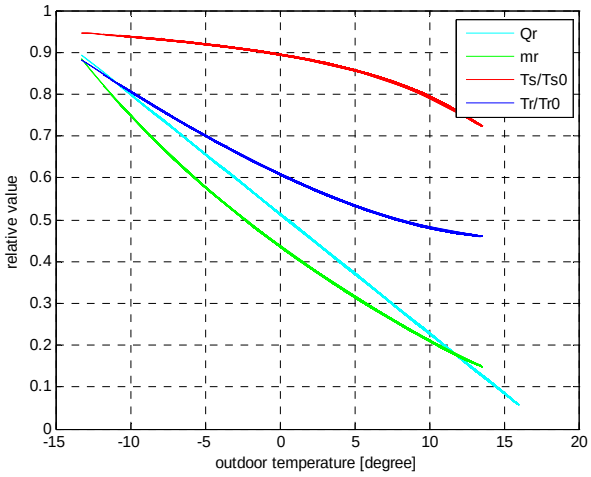

FIGURE 37: Relative values as a function of outdoor temperature

(5) The transmission effectiveness factor

Figure 38 and Figure 39 show the transmission effectiveness factor performance under steady state condition. It is obvious that the effectiveness is going lower when the mass flow of the transmission system decreases. That means less flow rate less effective transmission. The transmission system is more effective when it is colder.

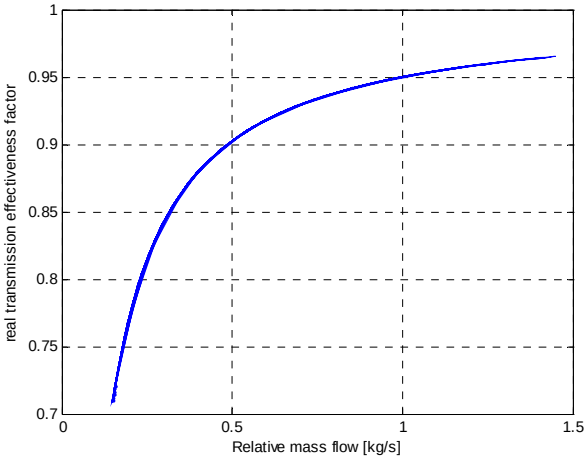

FIGURE 38: Transmission effectiveness factor as a function of relative mass flow

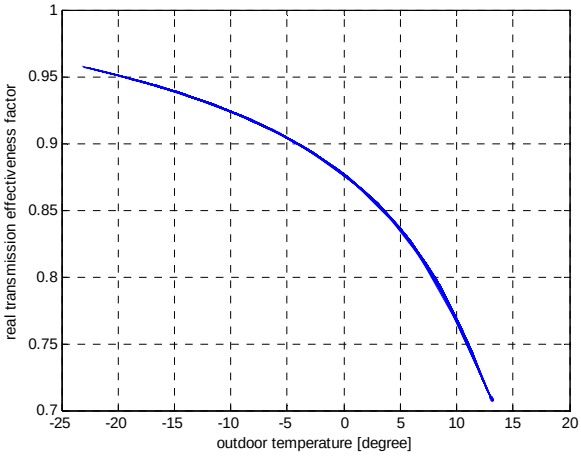

FIGURE 39: Transmission effectiveness factor as a function of outdoor temperature

5.5.2 Dynamic approach

The dynamic calculations are performed on the same sample buildings. By dynamic approach there assumed a limitation of mass flow of the transmission system, which means there must be some period that the indoor temperature couldn't keep the required value as 18°C in the real condition.

There are two important factors in dynamic calculation which are building heat loss factor k_l and building thermal mass C. The indoor temperature calculation is quite sensitive to the building thermal mass and building time constant. Building heat loss factor k_l for the modern energy efficiency sample building is calculated to be 2,751.65 W/°C. Building thermal mass is calculated to be 1,664,000 kJ/°C and building time constant is 167.96 hours. And k_l for traditional building sample is 1,690.14 W/°C, the thermal mass is 412,377 kJ/°C and building time constant is 67.77 hours.

In this report, ideal controller is assumed and used in the calculation. Tap hot water supply is also included. Indoor temperature calculation is based on the limited maximum mass flow at a specific

temperature which is called base temperature T_b. Therefore, for the outdoor temperature below the base temperature, the flow will be constant at the maximum value. The system can't provide the building with enough heat, so the indoor temperature starts to fall. The system performance above the base temperature is the same as in steady state.

The base mass flow can be determined by the base temperature, which is the important factor to determine the size of pipe and the cost of building system. The base mass flow is also the necessary mass flow needed to main a specific indoor temperature during a cold spell.

Results and analysis:
Since the different structures of two sample buildings result in the different heat loss factors and thermal mass, the dynamic system performances indicate correspondingly different. The results show that for modern building sample the base temperature T_b=2.5°C, while for traditional building T_b=1.1°C. For different base temperature, the following results are giving the comparison of two sample buildings' heating performance.

(1) Different temperature vs. time
According to the dynamic calculation programmed in MatLab, the base temperature is calculated for both samples that the indoor temperature falls to 16 °C once during the whole year of 2005 in Lhasa. Under base temperature conditions, the system supply temperature, return temperatures (i.e. only for heating and average of heating +hot tap water), indoor temperature and outdoor temperature distributions are shown in Figures 40 and 41, respectively. The temperatures are varying in dynamic way while the outdoor temperature is changing all year round.

It indicates that along with the change of outdoor temperature from Jan. 1 to Dec. 31 in 2005, each temperature behaves accordingly. In the central part of the graphs during summer time where outdoor temperature is assumed not higher than 18°C for calculation, there's only heating load for hot tap water. It shows that supply temperature goes down to around 60°C and average return temperature goes up to about 40°C. The calculation is based on temperature of each hour, the temperature in each day changes a lot in Lhasa, therefore, the temperatures are also changing correspondingly. The indoor temperature of each building is illustrated in detail in following figures.

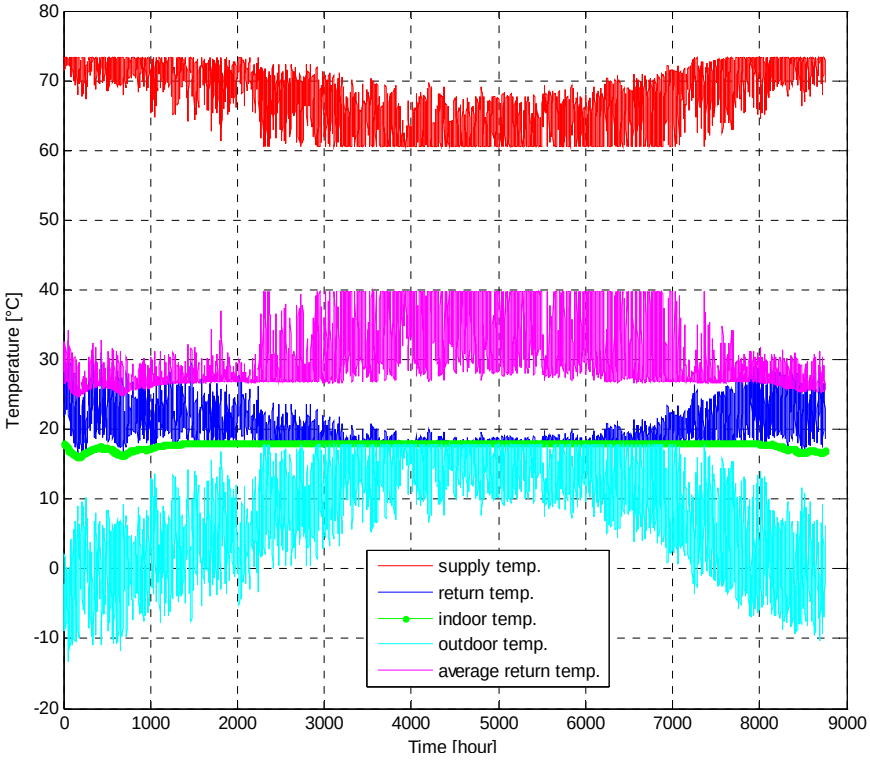

FIGURE 40: Temperatures performance for modern building sample

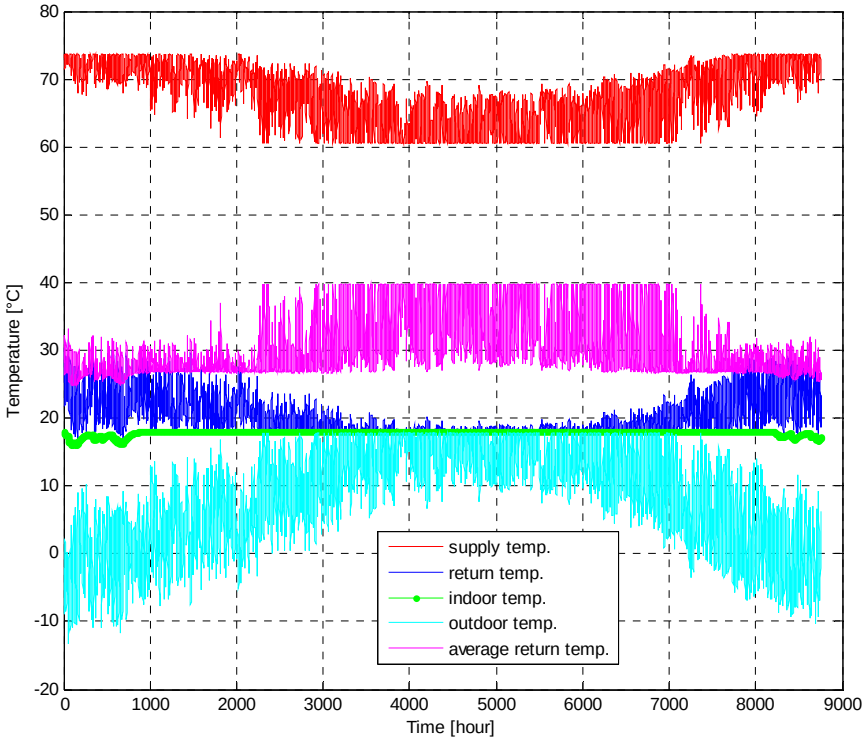

FIGURE 41: Temperatures performance for traditional building sample

(2) Indoor temperature

Compared with the steady state model, in dynamic model the indoor temperature will not be stable as the designed value of 18°C. The clear distribution diagrams for two sample buildings are shown below in Figure 42 and Figure 43 at respective base temperature. Because of the bigger thermal mass of modern building sample, the response of temperature change is slower than the traditional one. In first 50 days during winter, the indoor temperature changes are not as frequent as in traditional building. It can be seen in two ways that the positive view is the big thermal mass building can store more energy which will reduce the heating load peak which means saving energy, while the other view is the heavy building would also keep the low temperature for long time if the heating system is not well designed or the severe cold spell happens. In this analysis, there was no access to long term of 20 or 30 years weather data, so that the results from only one year shows that the degree days below designed temperature of 18°C is so long which is not acceptable.

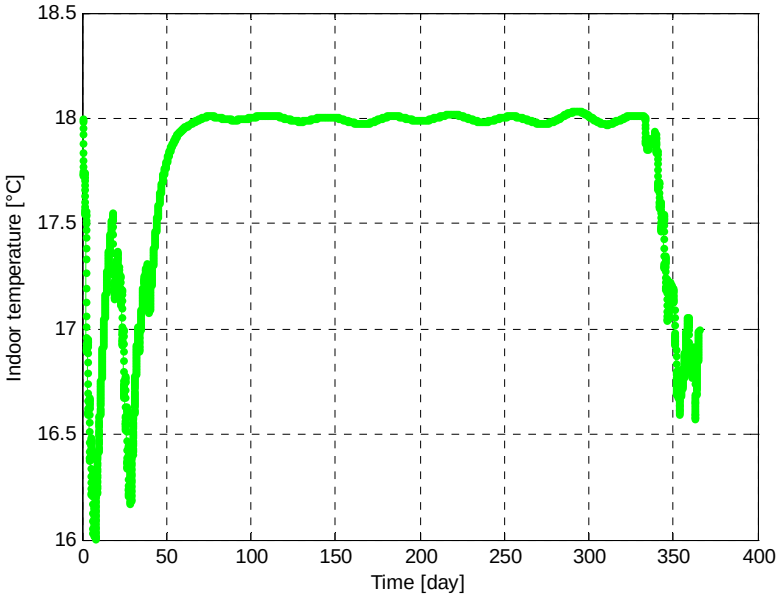

FIGURE 42: Indoor temperature performance for modern building sample

(3) Base temperature and indoor temperature analysis

The minimum indoor temperatures as a function of base temperature for ca+/-5°C interval around the base temperature of 2.5°C and 1.1°C are shown in Figure 44 and Figure 45. Both of them indicate that the lower base temperature selected the higher indoor temperature it can get. But it requires more heat load which means at the expense of energy consuming.

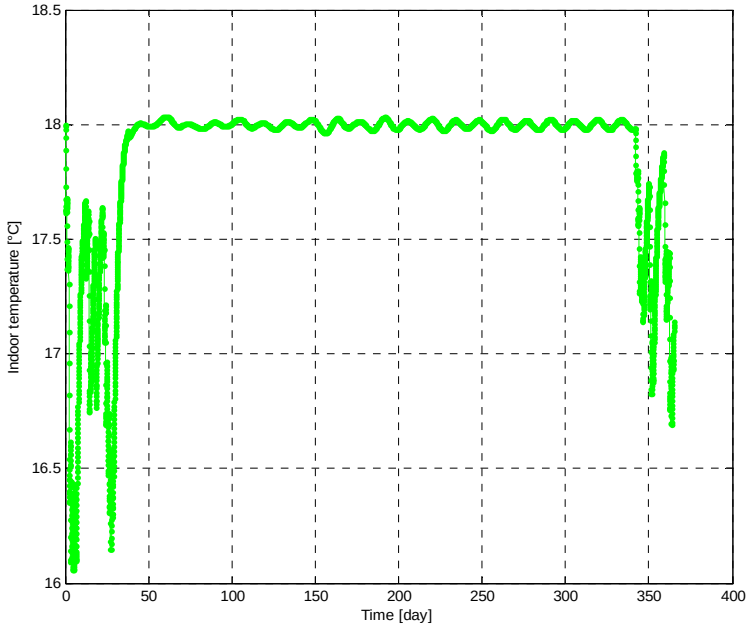

FIGURE 43: Indoor temperature performance for traditional building sample

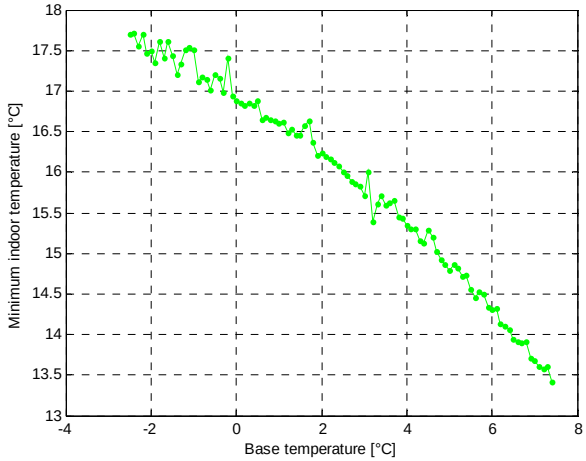

FIGURE 44: Minimum indoor temp. as a function of base temperature for modern building sample

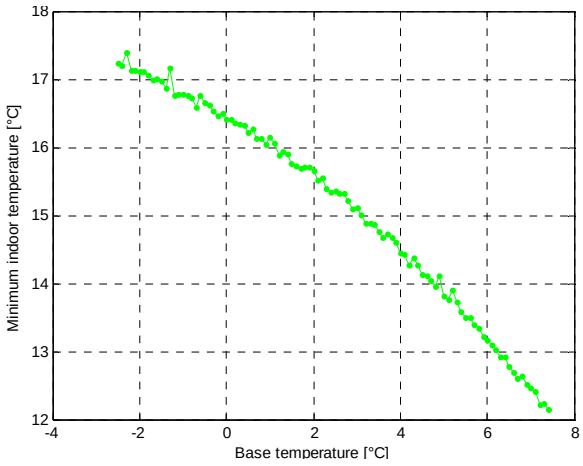

FIGURE 45: Minimum indoor temp. as a function of base temperature for traditional building sample

(4) Mass flow analysis

Mass flow of each sample building at the stated base temperature for the whole year is shown below in Figure 46 and Figure 47. The maximum flow rate for heating system of sample building is the bass mass flow. During summer time, there is only hot tap water supply. The maximum total mass flow of each system is 0.32kg/s and 0.23kg/s for modern and traditional sample respectively.

5.5.3 Summary and discussion of the performance analysis

The summary of the performance analysis results are shown below in Table 24. In steady state analysis, as the indoor temperature is assumed to be stable at 18°C, the heat load and the mass flow of hot supply water have to meet the maximum demand even it is just very short period. In dynamic analysis, by giving indoor temperature an acceptable temperature range of 16-18°C, the peak or severe cold period can be avoided. Therefore, the heat load and mass flow can be reduced to a medium value as shown in Table 32. It is obvious to see that for modern building, because of the big thermal mass, the base temperature is higher and the base heat load and mass flow can keep relatively smaller than that in traditional building case. That's the reason why this modern building can save more energy. Additionally, comparing the performance calculation of two sample building, it indicates that the modern building's big thermal mass plays significant part in reducing the peak load.

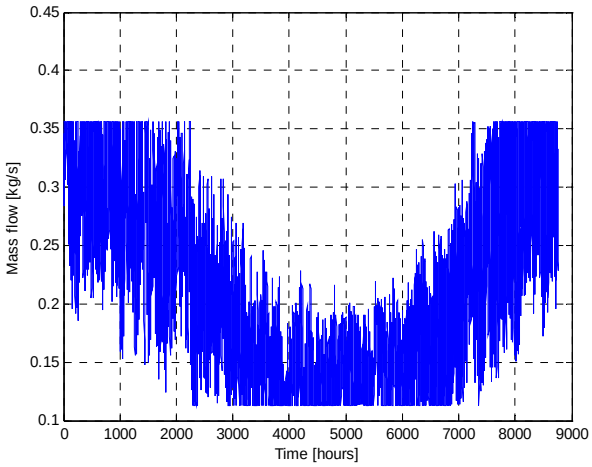

FIGURE 46: Total mass flow of heating and hot tap water for modern building sample

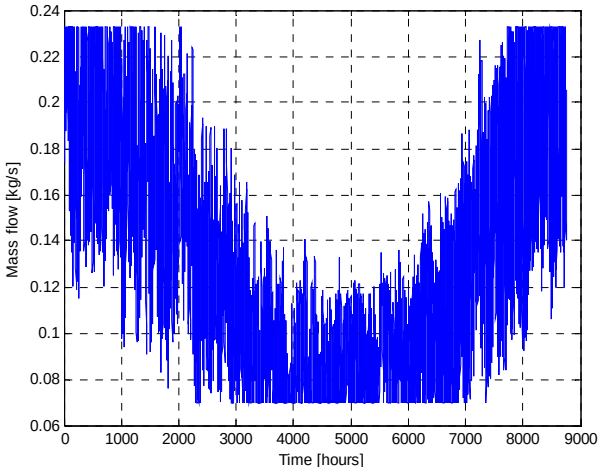

FIGURE 47: Total mass flow of heating and hot tap water for traditional building sample

TABLE 32: Summary of performance analysis results

Item	Modern building	Traditional building
Building dimension	30×20×18	20×8×8
Steady state analysis		
Maximum Heat load (kW)	86.13	52.90
Maximum Mass flow (kg/s)	0.51	0.31
Indoor temperature (°C)	18	18
Dynamic approach analysis		
Base temperature (°C)	2.5	1.1
Base heat load (kW)	48.15	31.94
Base mass flow (kg/s)	0.28	0.19
Total maximum mass flow(kg/s)	0.32	0.23
Indoor temperature (°C)	16-18	16-18

The base temperatures obtained in this dynamic analysis approach for both samples are based on the lowest acceptable indoor temperature, which is 16°C. Figure 48 and Figure 49 show indoor temperature duration curve according to different base temperature for each sample. In realistic design, for heating both modern buildings and traditional building, one reliable and uniform base temperature should be selected. From the figures below it is proved that T_b=-6°C is quite decent for both building type that the indoor temperature will be kept at designed temperature of 18°C. The heat load is 40.56

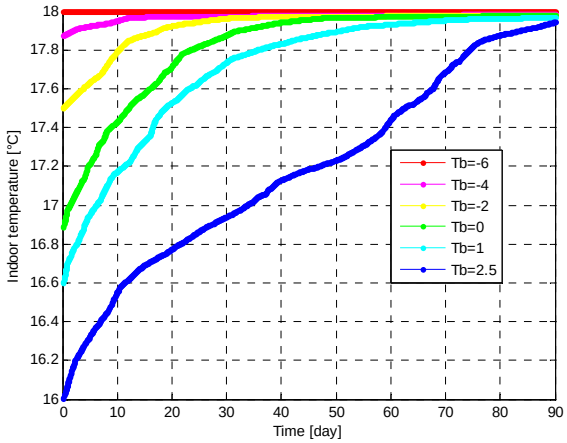

FIGURE 48: Indoor temp. duration curve based on different base temperature for modern sample

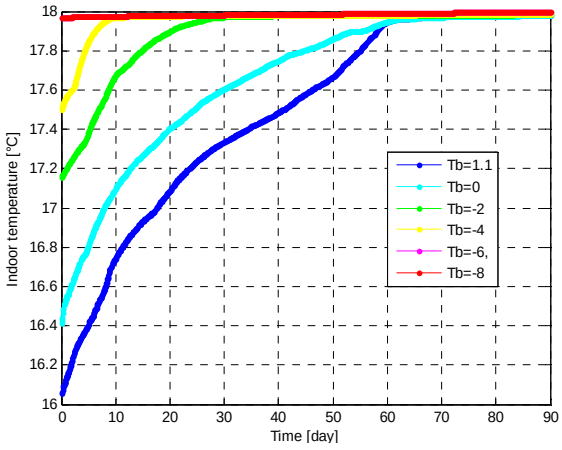

FIGURE 49: Indoor temp. duration curve based on different base temperature for traditional sample

kW for traditional building sample and 65.18 kW for modern building sample respectively based on this temperature. In addition, some different base temperatures can also be selected according to the level of comfort to be required.

5.6 Heat load estimation for the whole city

According to the data collected from city construction planning in Lhasa, the dimension of the city and population trend are shown in Table 33 below.

TABLE 33: City dimension and population of Lhasa

City scope	Total area (km^2)		Downtown area (km^2)	
	29,500		214.78	
City (1) and towns (7)	Lhasa city, Duilongdeqing, Qushui, Damei, Dangxiong, Nishui, Linzhou, Mozhugongka.			
Total population	2000 500,000	2005	2010 650,000	2015 765,000
City population	2000 200,000	2005 270,000	2010 300,000	2015 350,000~400,000
Construction land area (km^2)	55.69	60.58	66.54	72.5
Urbanization level	45%		60%	67.5%

According to the data above, the heat load and energy demand of the district heating system can be estimated. The urbanization level of Lhasa will be increased by 15% from 2000 to 2010. The population and construction area of Lhasa also will be increased significantly. The estimation of the heating system capacity will take all of the increase into account.

The dynamic model calculation in previous section gives different heat load values for the sample buildings, which are 40.56 kW for traditional one and 65.18 kW for modern one based on the base temperature of -6°C. For estimating the total heat demand, the sample building heat load could be converted to the specific heat load per area. Thus the average heat load of traditional building per area is estimated as 85 W/m^2 (normally with 2~3 stories), and for modern energy efficiency building is around 18 W/m^2 (normally with at least 6 stories).

At present, the total construction area of buildings is about 4 million m^2. The fractions of the traditional building and energy efficiency building are 75% and 25% respectively. Therefore, the heat load of the total city can be estimated as in Table 34. According to the city expansion and population development, the value in 2015 will be increasing to 320 MW roughly.

TABLE 34: Calculation of the overall heat load of Lhasa city

Building type	Calculations	Heat load (kW)
Traditional	$85 \times 4{,}000{,}000 \times 0.75$	255,000
Modern energy efficiency	$18 \times 4{,}000{,}000 \times 0.25$	18,000
Total	273,000	

5.7 Conceptual design of long distance geothermal district heating system for Lhasa

As designed in power generation section, the available heating capacity which can be supplied by three scenarios is roughly about 100-110 MW, with supply temperature of 85ºC. A cold water source from melted snow is used to be heated-up by discharge geothermal brine of the CHP plant which is also named as regeneration power plant. The mass flow of heated water is about 308.9, 326.3, and

342.3 kg/s from different power cycle scenarios. The long distance district heating system design schematic system diagram is shown in Figure 50.

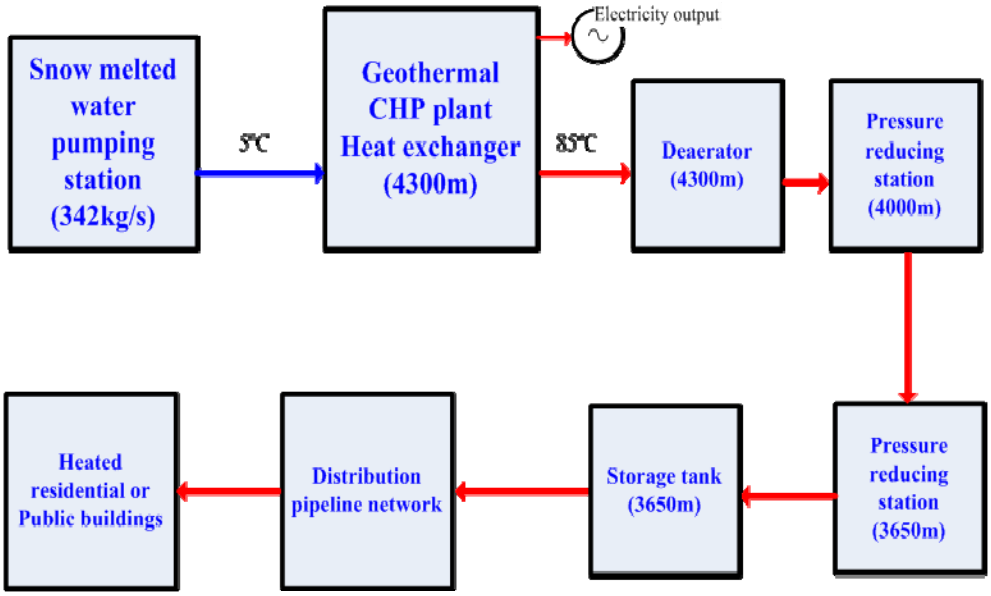

FIGURE 50: Schematic diagram of geothermal district heating system from CHP plant

The cold water been transmitted in the district heating system is from snow melted water tank which is built adjacent to power plant. The heat source is from the power plant discharge geothermal brine. The heat exchanger applied in the system is titanium plate heat exchanger due to the chemical feature of the geothermal brine. The snow melted water will be heated from 5 to 85ºC and then will be transmitted by pipeline to a storage tank which is built close to Lhasa city. From Yangbajain geothermal power plant to the storage tank, the distance is roughly measured to be 90050 m. The elevation decreases 600 m from 4300 to 3650 m. The big elevation difference results in the high pressure difference along the piping route. Therefore the design is to construct two pressure reducing stations to reduce transmission high pressure. The hot water from heat exchanger first goes to de-aerator to get de-aerated for preventing corrosion during transmission. Then it goes along the long distance pipeline to the storage tank before distributed to the heat consumers.

5.7.1 Transmission pipeline route design

According to the conceptual design of this long distance district heating system, the transmission pipeline starts from Yangbajain CHP plant at the elevation of 4300 m. Heated water will go through the pipe by gravity without any pumping cost to Lhasa city which is at 3650 m elevation. The pipeline is designed to be mostly underground laid along the railway and the highway route while some severe parts will be laid over ground if the condition is not available for underground laying. It is mostly river bed landscape rather than the hard rock or frozen earth, thus it is technically feasible. The pipeline is pre-insulated steel pipe. The rough pipeline route is shown in Figure 51.

The profile of this proposed pipeline is given in Figure 52. By figuring out 30 pots for designed the transmission route in Google earth, each point's altitude can be found as shown in Figure 52. The profile from Lhasa to Yangbajain is approximately linear. Therefore, the calculations and analysis of pressure and temperature drop of the pipeline is carried out based on this profile in this preliminary study.

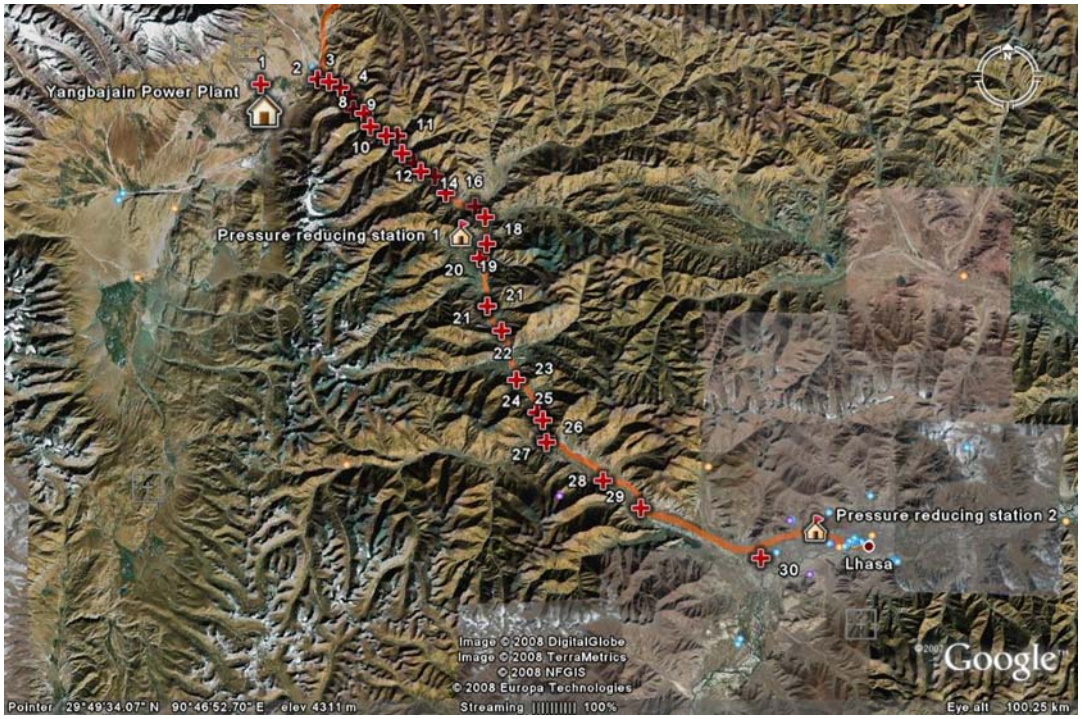

FIGURE 51: Proposed transmission route from Yangbajain CHP plant to Lhasa

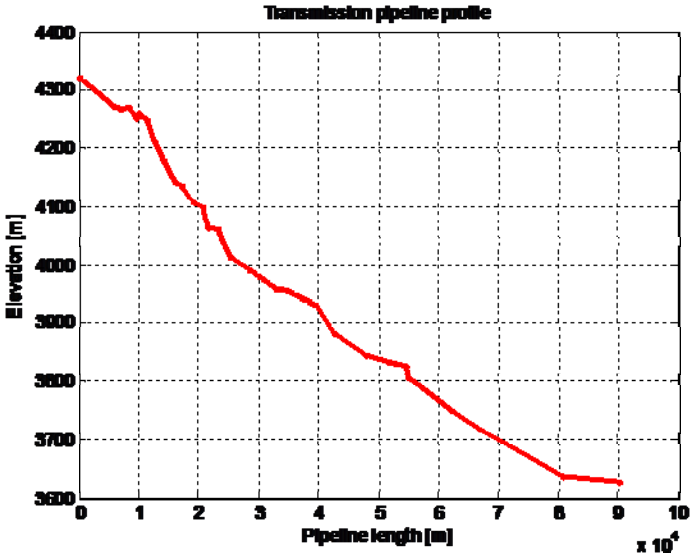

FIGURE 52: Transmission pipeline profile

5.7.2 Transmission pipeline calculation

(1) Pressure loss

The water flow pressure loss in pipeline is composed of elevation changes and wall friction two parts. The pressure along the pipeline can be calculated by the equation below:

$$P_B = P_A - \rho g \cdot (\Delta Z_{B-A} + f \cdot \frac{L}{D} \cdot \frac{v^2}{2g}) \quad (48)$$

where P_B= Pressure of pipeline outlet, Pa;
P_A= Pressure of pipeline inlet, Pa;
ΔZ_{B-A}= the change in pipe elevation from A to B, Z_B-Z_A, m;

f = Friction factor, based on the pipe roughness, pipe diameter, and the Reynolds number, can be obtained from engineer. handbooks, 2,3. For most applications, the value of the friction factor is between 0.015 and 0.0225. Here it is 0.016 which is calculated in EES;
v = Average flow velocity in m/s;
L = Pipe length in meters;
D = Pipe inner diameter in meters;
ρ = Heated water density in m^3/kg.
g = Gravity acceleration constant.

The pipeline model is set up in EES programme which is based on the proposed transmission route profile. The pressure loss calculation in gravity head curve is shown in Figure 53. The diameter for this pipeline is DN500, 508/630, and the thickness is 8.8 mm. It can sustain the highest pressure of 40 bar. The elevation changes are shown by the black dashed line, while the other curves indicate the pressure loss at different water flow rates. The red one represents the design water flow rate of 342.3 kg/s which can keep in good transmission condition at initial pressure. From the other results at lower flow rate of 300 kg/s and 250 kg/s, it is clear that if there's less flow rate in the pipeline, the pressure also reduce less. To keep the transmission pipeline at safe level, the pressure reducing stations are required along the pipeline.

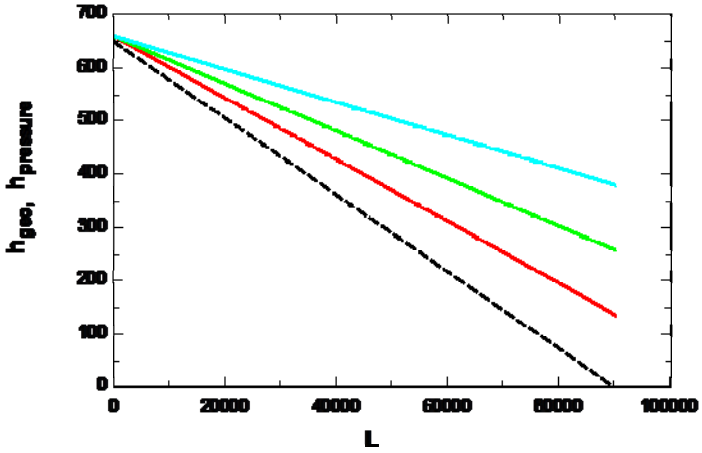

FIGURE 53: Transmission gravity head drop in pipeline

(2) Temperature loss
The temperature loss during transmission can be calculated as below:

$$T_2 = T_{outdoor} + (T_1 - T_{outdoor}) \cdot e^{(-\frac{k \cdot L}{\dot{m} \cdot C_p})} \quad (49)$$

where T_2 = transmission pipeline outtake temperature (i.e. distribution supply temperature), ºC;
$T_{outdoor}$ = outdoor temperature during pipeline working time, ºC;
T_1 = intake temperature of transmission pipeline from power plant, ºC;
k = coefficient of heat transfer from center of pipe to ambient air, in this case for DN500, 508/630 pipeline, is 0.8 W/mºC (Randlov, 1997);
L = transmission pipeline length, m;
m = transmission water mass flow rate, kg/s;
C_p = specific heat capacity, kJ/kg ºC, for water, it is 4187 kJ/kg ºC.

It is also calculated based on the designed pipeline route shown in Figure 54. The length is 90050 m from Yangbajain power plant to the storage tank. Therefore, the temperature at outlet of pipeline is 80.2ºC.

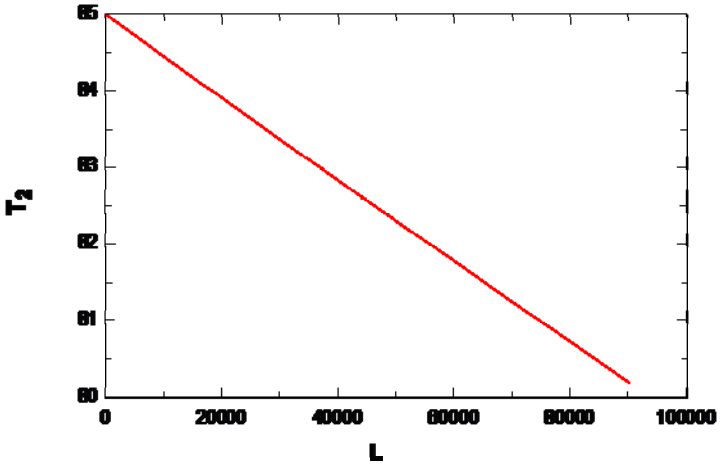

FIGURE 54: Temperature drop in the pipeline

5.7.2 Distribution network in Lhasa and building system in Lhasa

The distribution network of district heating system will be laid according to the city construction distribution map. The proposed distribution network is roughly shown in Figure 55. As stated in last chapter, the total heat capacity is about 110 MW which can supply total heated area of 1.6 million m^2 including 25% modern energy efficiency buildings and 75% traditional residential buildings. Therefore, the distribution mains will be laid in the primary streets to distribute to heat consumers.

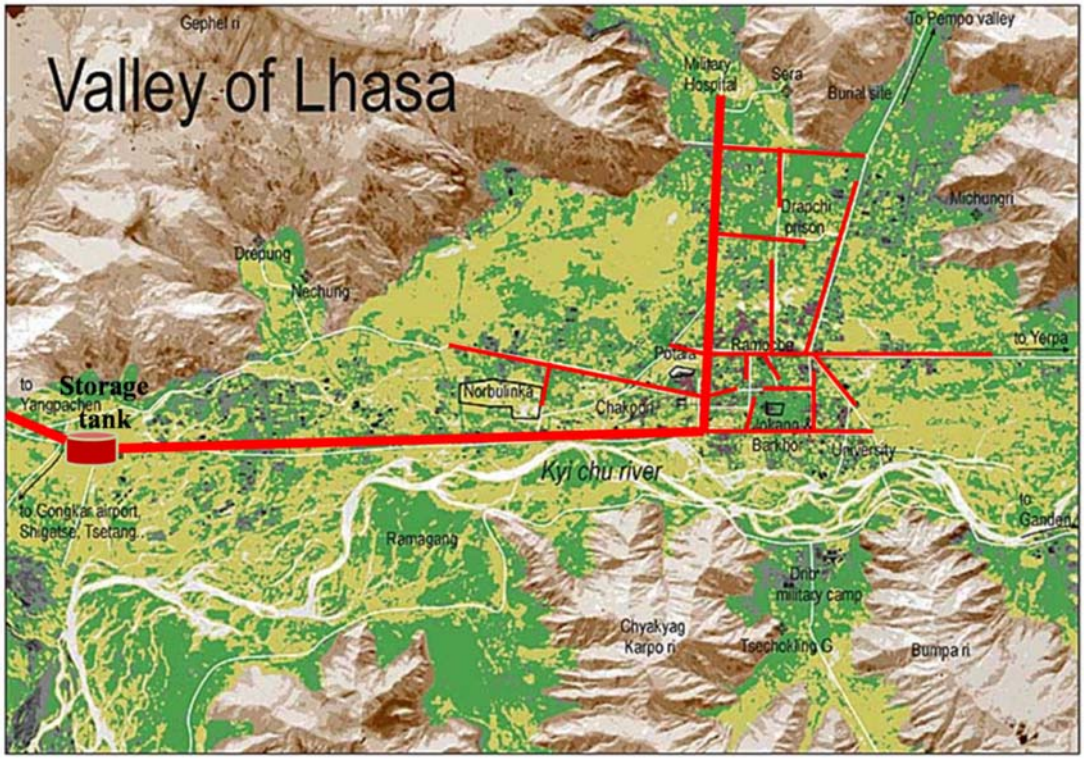

FIGURE 55: Proposed distribution network in Lhasa

5.8 Perspective scenario of heating system in Tibet

The district heating system designed in previous sections can be taken as the heating project's first stage since it will supply 40% of the entire heating load of Lhasa. For the rest demand, it can be met by using geothermal heat pump system. The discharge water from the designed long distance district heating system can be used as the low heat source of heat pump system by reducing the temperature to about 15ºC. Therefore, by assuming heat pump efficiency of 4, the total heat supply of geothermal heat pump system can yield around **48 MW**. It accounts for **18%** of the total heat load of the city. Due to the low population density of Tibet, the small scale solar heating system and close-loop ground source heat pump are also feasible to apply to fulfil the rest 22% of total area.

6. ECONOMIC FEASIBILITY STUDY FOR PROPOSED PROJECT

The aim of carrying out an economic feasibility study of different scenarios is to determine which one is the most financially viable. Every project is implemented with the same objective of getting positive returns from investment in the view of business investment. Financial viability analysis is significant factor to determine which alternative is finally selected. Engineering economic study is introduced to make this feasibility study. Some definition and principles are applied for all alternatives stated in the previous chapters including the power generation alternatives and the long distance district heating system.

6.1 Methodology and process

The economic evaluation and analysis for both power plant and district heating system is implemented by using engineering economic methodology. A PW (Present worth) value evaluation process is applied to determine the internal rate of return of a cash flow series, set up the ROR equation using PW relations. The present worth of costs or disbursements PW_D is equated to the present worth of incomes or receipts PW_R. That is, solve for i using:

$$PW_D = PW_R \tag{50}$$

The i value which makes the equation numerically correct is called i^*. It is the root of the ROR relation. To determine if the alternative's cash flow series is viable, compare i^* with the established MARR, where MARR is the minimum attractive rate of return defined by the investment company or market situation, etc:

If $i^* \geq$ MARR, accept the alternative as economically viable.

If $i^* <$ MARR, the alternative is not economically viable.

Rate of return (ROR) is known by several other names: internal rate of return (IRR), return on investment (ROI), and profitability index (PI). It is the rate paid on the unpaid balance of borrowed money, or the rate earned on the unrecovered balance of an investment, so that the final payment or receipt brings the balance or exactly zero with interest considered.

The PW-based procedure for sensitivity analysis and a graphical estimation of i^* value is as follows (Blank and Tarquin, 2002, *Engineering economy*):

- Draw the cash flow diagram;
- Set up the ROR relation in the form of Equation 50;
- Enter the cash flows onto the spreadsheet in contiguous cells;
- Develop the IRR function to display i^*;
- Use the NPV function to develop a chart of PW vs. i values. This graphically shows the i^* value at which PW=0.

For power plant project, there are 4 different alternative scenarios to compare. A method named Incremental IRR Analysis is applied to compare every two alternatives to figure out which one is more financially viable. This method is also based on the PW value evaluation, which is to make subtraction of the two alternatives represents a new alternative to find out if it is viable. The complete procedure by hand or computer for an incremental ROR analysis for two alternatives is as follows:

- Order the alternatives by initial investment or cot, starting with the smaller one, called A. The one with larger initial investment is in the column labelled B.
- Develop the cash flow and incremental cash flow series using the LCM of years, assuming reinvestment in alternatives.

- Draw an incremental cash flow diagram, if needed.
- Count the number of sign changes in the incremental cash flow series to determine if multiple rates of return may be present. If necessary, use Norstrom's criterion on the cumulative incremental cash flow series to determine if a single positive root exists.
- Set up the PW equation for the incremental cash flows in the form of Equation 50, determine Δi^*_{B-A} using trial and error by hand or spreadsheet functions.
- Select the economically better alternatives as follows:
  - If $\Delta i^*_{B-A} <$ MARR, select alternative A.
  - If $\Delta i^*_{B-A} \geq$ MARR, the extra investment is justified, select alternative B.

Therefore, the first step of the assessment is to estimate the total capital investment, the annual total cost, as well as annual total revenue of each alternative scenario. The annual total cost includes operation and maintenance cost (O&M) and annual capital cost. Every project has a certain lifespan. Hence a cash flow series during this lifespan can be tabulated. In the cash flow series, the annual expense equals the total annual cost substrate the depreciation cost since it is not real cash flow. By applying the PW evaluation method, the IRR value of each scenario can be figured out. Then by applying incremental ROR analysis method, the most financially feasible scenario can be found out. The evaluation for power plant system is carried out first, followed by the district heating system analysis.

In cost evaluation process, every component is estimated using related information available on the internet and from past publications all based on the local price indices in China or international standard indices. Estimating the cost of purchased equipment (including spare parts and components) is the first step in any detailed cost estimation. Two good methods can be used for cost estimation. The best cost estimates for purchased equipment can be obtained directly through vendors' quotations. The second is to use cost values from past purchase orders, and quotations from experienced professional cost estimators.

Annual O&M cost can be composed of cost for operating labor, maintenance labor, maintenance materials, auxiliary power input cost; while annual capital cost consists annual depreciation cost, interest rate and etc. The economic life span for both power plant and district heating system is 20 years. The price of electricity generated by geothermal power plant for accessing to grid is 0.41 yuan/kW in Tibet. The exchange rate of the Chinese yuan for the U.S. dollar is 7.0 yuan per dollar in this report.

6.2 Cost estimation and cash flow of proposed power plant scenarios

There are four different proposed power plant scenarios designed in Chapter 4. The economic evaluation is performed here by using the stated methodology and process. First of all, the cost estimation is made for each alternative including investment, operation and income cost. Then the evaluation analysis is performed based on the cash flow in their proposed life span. For all the alternatives, the drilling and related cost of all reinjection wells is included for sustainable development concern.

6.2.1 The CHP plant using double flash cycle (Scenario 1)

The first scenario designed is a CHP plant using double flash cycle. The main components of this plant are two turbo-generators, one condenser, cooling circulating pump, the cooling tower, and etc as shown in the schematic diagram in Figure 12 of Chapter 4. The cost estimates are listed in Tables 35 and 36.

TABLE 35: Estimated costs for purchased equipments of Scenario 1

Component	Rating (kW) /Area (m^2)	Unit cost (US$/kW)	Equipment cost (US$)
Steam turbo-Generator (HP)	6932	326	2,260,000
Steam turbo-Generator (LP)	12148	326	3,960,000
Cooling water circulation pump	630.4	428	270,000
Condenser ,water cooled	2859	280	801,000
Wet cooling tower	120069	11	1,321,000

The detailed calculation of total capital investment, annual total cost and annual total income are summarized as in Table 36. This is the basis for making a cash flow series to perform the economic analysis of the alternative.

TABLE 36: Summary of cost estimation for Scenario 1

Cost estimates	Cost (USD)
1. Fixed capital investment	19,580,000
A. Purchased Equipment Cost (PEC)	8,612,000
Steam turbo-Generator (HP)	2,260,000
Steam turbo-Generator (LP)	3,960,000
Cooling water circulation pump	270,000
Condenser	801,000
Wet cooling tower	1,321,000
B: Drilling and installation costs	10,968,000
Cost of drilling a deep wells and instruments (2500m x US$550/m) another one will be drilled 10 years later	1,375,000
Reinjection well drilling and instruments cost	3,025,000
Pumping and connection of the reinjection wells (20% of drilling cost)	454,000
Piping, valves and fittings (25% of PEC)	2,153,000
Instrumentation and control (45% of PEC)	3,875,000
Shipping (1% of PEC)	86,000
2. Construction related costs	2,153,000
Design and consultancy (5% of PEC)	431,000
Construction Cost (20% of PEC)	1,722,000
Commissioning and start up (3% of PEC)	258,000
Total capital investment	21,733,000
3. Annual O&M Costs	1,076,000
Labour cost(10 persons, 3000yuan/month)	51,000
Maintenance costs (1% of investment)	217,000
Operating cost (1% of investment)	217,000
Auxiliary electricity costs	591,000
4. Annual capital cost	1,518,000
Annual depreciation costs (Economic life span of 20 years)	1,087,000
Interest rate (5%)	431,000
Total annual cost	2,594,000
Total annual expense (Cash payment)	1,507,000
Annual income (Electricity sales at 0.41yuan/kWh)	8,782,000
Annual tax payment (3.4% of total income)	299,000
Annual revenue (Annual income - Tax)	8,483,000
Annual profit (Annual revenue-annual expense)	5,889,000
Recovery year	3.69

According to the cost estimation, the cash flow series can be made in the life span of the proposed project. The total investment cost is $21,733,000 at the beginning, and after 10 years, there will be another well drilled for ensuring the production at the cost of $1,375,000. The annual revenue after-tax is $8,483,000, and the annual expense is $1,507,000 as shown below in Figure 56.

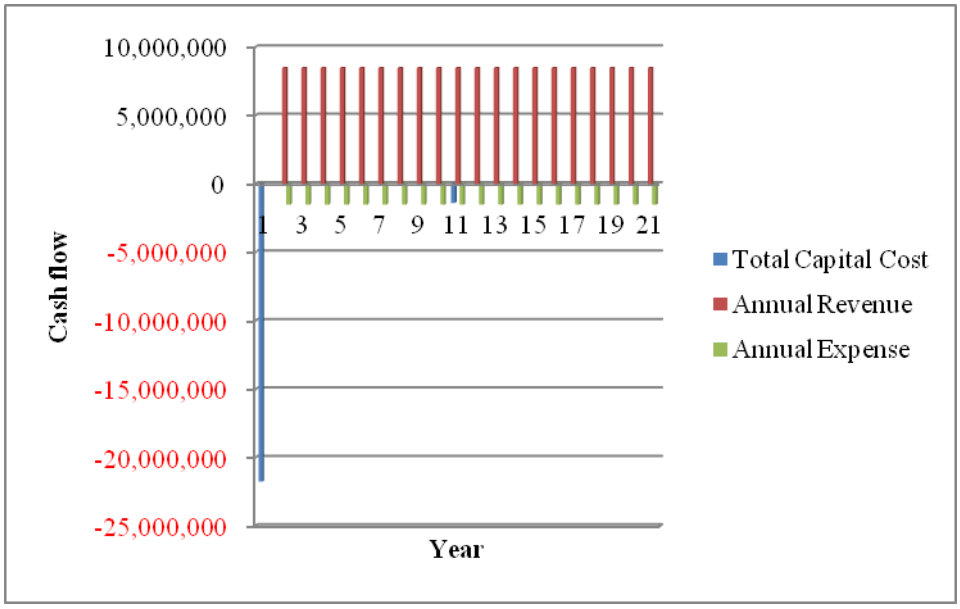

FIGURE 56: Cash flow of double flash power plant Scenario 1

6.2.2 Combined flash and ORC cycle using isopentane (Scenario 2)

The second scenario designed as a combined flash and ORC cycle with isopentane as the working fluid for bottoming ORC cycle. According to the thermodynamic calculation and optimization, it is feasible to supply the district heating for this system. The main components of this plant are two turbine-generators, one vaporizer, two condensers, and etc, as shown in the schematic diagram in Figure 15 of Chapter 4. The cost estimates are listed in Tables 37 and 38.

TABLE 37: Estimated costs for purchased equipments of Scenario 2

Component	Rating (kW) /Area (m^2)	Unit cost (US$/kW)	Equipment cost (US$)
Steam turbo- Generator (HP)	6107	326	1,991,000
Organic turbo- Generator (ORC)	17910	400	7,164,000
ORC Feed Pump	685	74	51,000
Cooling water circulation pump	328.5	820	269,000
Evaporator	7915	300	2,375,000
Condenser (HP)	495.4	280	139,000
Condenser (ORC)	9575	280	2,681,000
Wet cooling tower	125129	11	1,376,000

According to the cost estimation, the cash flow chart can be made for the life span of the proposed project. Figure 57 below shows the cash flow during 20 years lifetime.

TABLE 38: Summary of economic analysis for Scenario 2

Cost estimates	**Cost (USD)**
1. Fixed capital investment	32,444,000
A. Purchased Equipment Cost (PEC)	16,046,000
Steam turbo- Generator (HP)	1,991,000
Organic turbo- Generator (ORC)	7,164,000
ORC Feed Pump	51,000
Cooling water circulation pump	269,000
Evaporator	2,375,000
Condenser (HP)	139,000
Condenser (ORC)	2,681,000
Wet cooling tower	1,376,000
B: Drilling and installation costs	16,398,000
Cost of drilling a deep wells and instruments (2500m x US$500/m for each) another well drilled 10 years later	1,375,000
Reinjection well drilling and instruments cost	3,025,000
Pumping and connection of the reinjection wells (20% of drilling cost)	605,000
Piping, valves and fittings (25% of PEC)	4,012,000
Instrumentation and control (45% of PEC)	7,221,000
Shipping (1% of PEC)	160,000
2. Construction related costs	4,011,000
Design and consultancy (5% of PEC)	802,000
Construction Cost (20% of PEC)	3,209,000
Commissioning and startup (3% of PEC)	481,000
Total capital investment	36,455,000
3. Annual O&M Costs	1,568,000
Labor cost(10 persons, 3000yuan/month)	51,000
Maintenance costs (1% of investment)	365,000
Operation costs(1% of investment)	365,000
Auxiliary electricity costs	787,000
4. Annual capital cost	2,625,000
Annual depreciation costs (Economic life span of 20 years)	1,823,000
Interest rate (5%)	802,000
Total annual cost	4,193,000
Total annual expense (Cash payment)	2,370,000
Annual income (Electricity sales at 0.4yuan/kWh)	11,010,000
Annual tax payment (3.4% of income)	374,000
Annual revenue (Annual income - Annual Tax)	10,636,000
Annual profit (Annual revenue-Annual expense)	8,266,000
Recovery year	4.41

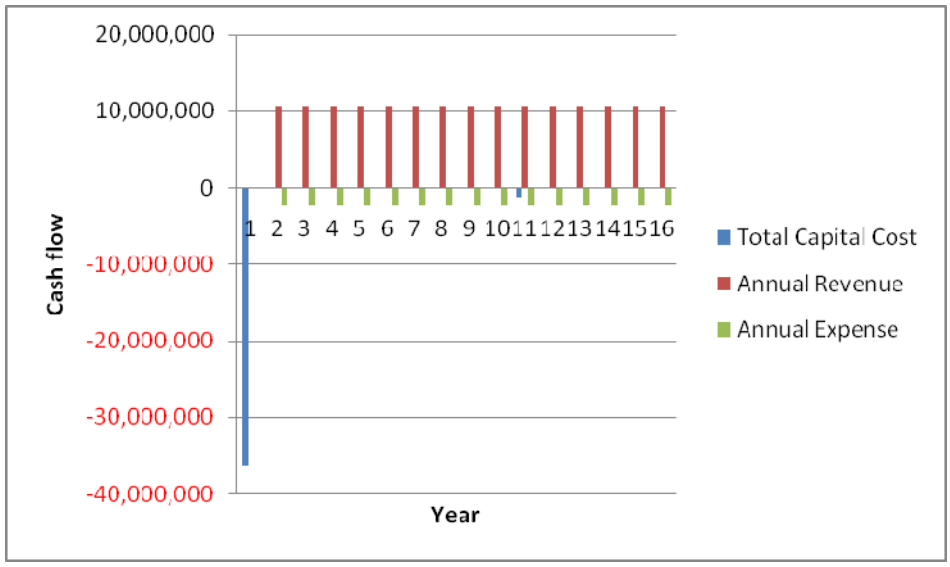

FIGURE 57: Cash flow of double flash power plant Scenario 2

6.2.3 ORC cycle using isobutane (Scenario 3)

The third scenario designed as a pure ORC cycle with isobutane as the working fluid. According to the thermodynamic calculation and optimization, there's no district heating capacity for this system. The main components of this plant are one turbo-generator, one vaporizer, one condenser, the cooling tower, and etc as shown in the schematic diagram in Figure 18 of Chapter 4. The cost estimates are listed in Tables 39 and 40, and the cash flow chart is in Figure 58.

TABLE 39: Estimated costs for purchased equipments of Scenario 3

Component	Rating (kW) /Area (m^2)	Unit cost (US$/kW)	Equipment cost (US$)
Organic vapour turbo- Generator (ORC)	34298	400	13,719,000
ORC Feed Pump	3669	23	84,000
Cooling water circulation pump	1015	324	329,000
Evaporator (ORC)	21230	300	6,369,000
Condenser (ORC)	17904	280	5,013,000
Wet cooling tower	193444	11	2,128,000

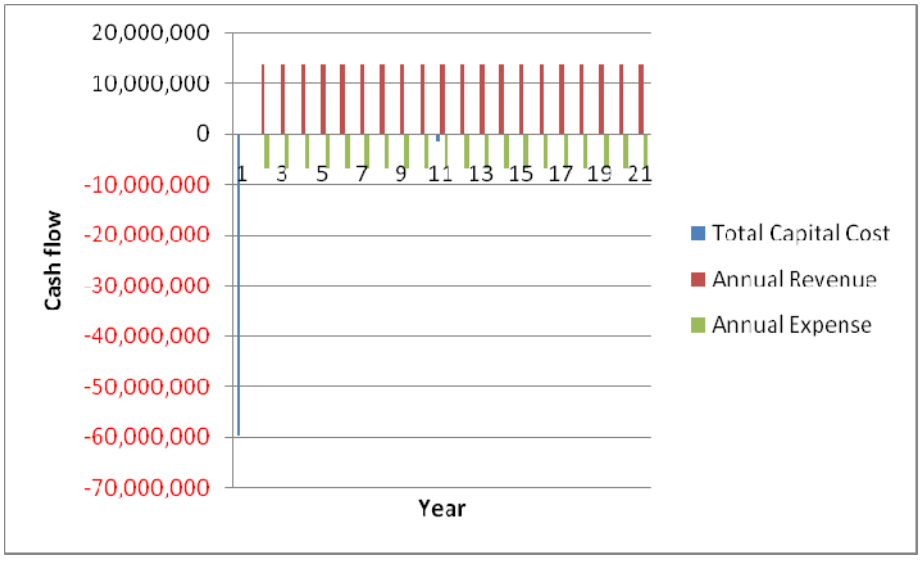

FIGURE 58: Cash flow of ORC power plant Scenario

TABLE 40: Summary of economic analysis for Scenario 3

Cost estimates	**Cost (USD)**
1. Fixed capital investment	51,667,000
A. Purchased Equipment Cost (PEC)	27,642,000
Organic vapor turbo- Generator (ORC)	13,719,000
ORC Feed Pump	84,000
Cooling water circulation pump	329,000
Evaporator (ORC)	6,369,000
Condenser (ORC)	5,013,000
Wet cooling tower	2,128,000
B: Drilling and installation costs	24,025,000
Cost of drilling a deep wells and instruments (2500m x US$550/m for each) another well drilled 10 years later	1,375,000
Reinjection well drilling and instruments cost	3,025,000
Pumping and connection of the wells (20% of drilling cost)	275,000
Piping, valves and fittings (25% of PEC)	6,911,000
Instrumentation and control (45% of PEC)	12,438,900
Shippping (1% of PEC)	276,000
2. Construction related costs	8,292,000
Design and consultancy (10 % of PEC)	2,764,000
Construction Cost (20% of PEC)	5,528,000
Commissioning and startup (3% of PEC)	829,000
Total capital investment	59,959,000
3. Annual O&M Costs	5,331,000
Labor cost(10 persons, 3000yuan/month)	62,000
Maintenance costs (1% of investment)	600,000
Operation costs (1% of investment)	600,000
Auxiliary electricity costs	4,069,000
4. Annual capital cost	4,380,000
Annual depreciation costs (economic life span of 20 years)	2,998,000
Interest rate (5%)	1,382,100
Total annual cost	9,711,000
Total annual expense (Cash payment)	6,713,000
Annual income (Electricity sales at 0.41yuan/kWh)	14,094,000
Annual tax payment (3.4% of income)	479,000
Annual revenue (Annual income - Annual Tax)	13,615,000
Annual profit (Annual revenue-Annual expense)	6,902,000
Recovery year	8.69

6.2.4 The CHP plant using hybrid flash and Kalina cycle (Scenario 4)

The last scenario designed as a hybrid flash and Kalina cycle. According to the thermodynamic calculation and optimization, it is also feasible to supply the heating capacity for district heating system. The main components of this plant are two turbo-generators, one vaporizer, two condensers, the cooling tower, and etc, as shown in the schematic diagram in Figure 19 of Chapter 4. The cost estimates are listed in Tables 41 and 42.

TABLE 41: Summary of economic analysis for Scenario 4

Cost estimates	**Cost (USD)**
1. Fixed capital investment	41,604,000
A. Purchased Equipment Cost (PEC)	21,723,000
Steam turbo- Generator (HP)	2,112,000
Ammonia vapor turbo- Generator (Kalina)	8,559,000
Feed Pump	26,000
Cooling water circulation pump	239,000
Evaporator	4,177,000
Regenerator	143,000
Brine heat exchanger	25,000
Condenser (HP)	152,000
Condenser (Kalina)	4,944,000
Wet cooling tower	1,346,000
B: Drilling and installation costs	19,881,000
Cost of drilling two deep wells and instruments (2500m x US$500/m for each) another well drilled 10 years later	1,375,000
Reinjection well drilling and instruments cost	3,025,000
Pumping and connection of the wells (20% of drilling cost)	275,000
Piping, valves and fittings (25% of PEC)	5,431,000
Instrumentation and control (45% of PEC)	9,775,000
Shipping (1% of investment)	217,000
2. Construction related costs	6,517,000
Design and consultancy (10 % of PEC)	2,172,000
Construction Cost (20% of PEC)	4,345,000
Commissioning and startup (3% of PEC)	652,000
Total capital investment	48,121,000
3. Annual O&M Costs	2,208,000
Labor cost(10 persons, 3000yuan/month)	51,000
Maintenance costs (1% of investment)	481,000
Operation cost (1% of investment)	481,000
Auxiliary electricity costs	1,195,000
4. Annual capital cost	4,578,000
Annual depreciation costs (Economic life span of 20 years)	2,406,000
Interest rate (5%)	2,172,000
Total annual cost	6,786,000
Total annual expense (Cash payment)	4,380,000
Annual income (Electricity sales at 0.4yuan/kWh)	12,490,000
Annual tax payment (3.4% of total income)	425,000
Annual revenue (Annual income - Annual Tax)	12,065,000
Annual profit (Annual revenue-Annual expense)	7,685,000
Recovery year	6.26

TABLE 42: Estimated costs for purchased equipments of Scenario 4

Component	Rating (kW) /Area (m^2)	Unit cost (US$/kW)	Equipment cost (US$)
Steam turbo- Generator (HP)	6477	326	2,112,000
Ammonia vapor turbo- Generator (Kalina)	21398	400	8,559,000
Feed Pump	1427	18	26,000
Cooling water circulation pump	449.8	531	239,000
Evaporator	13922	300	4,177,000
Regenerator	510.7	280	143,000
Pre-heater	89.11	280	25,000
Condenser (HP)	544.3	280	152,000
Condenser (Kalina)	17656	280	4,944,000
Wet cooling tower	122394	11	1,346,000

According to the cost estimation, the cash flow chart can be made for the life span of the proposed project. Figure 59 below shows the cash flow during 20 years lifetime.

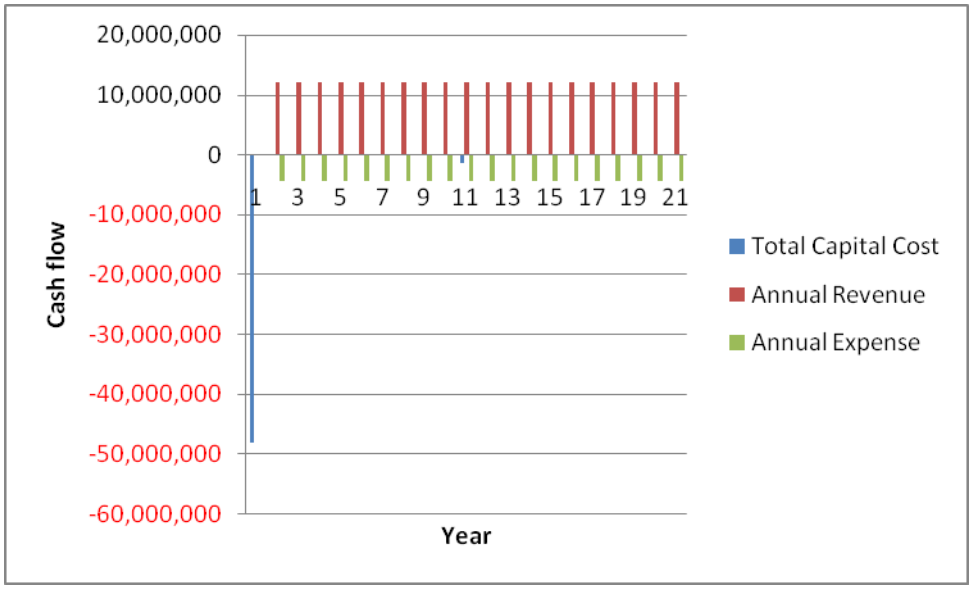

FIGURE 59: Cash flow of hybrid flash and Kalina cycle Scenario 4

6.3 Evaluation of all alternative scenarios using PW value method

Based on the cash flow series of each alternative, the IRR evaluation can be carried out. Figure 60 shows the curves of NPV value as a function of rate in the expected life span for all alternatives. It indicates the IRR results of all four alternative scenarios when NPV is equalized to zero. It is obvious that Scenario 1 designed as double flash cycle power system has the highest IRR as 31.84%,

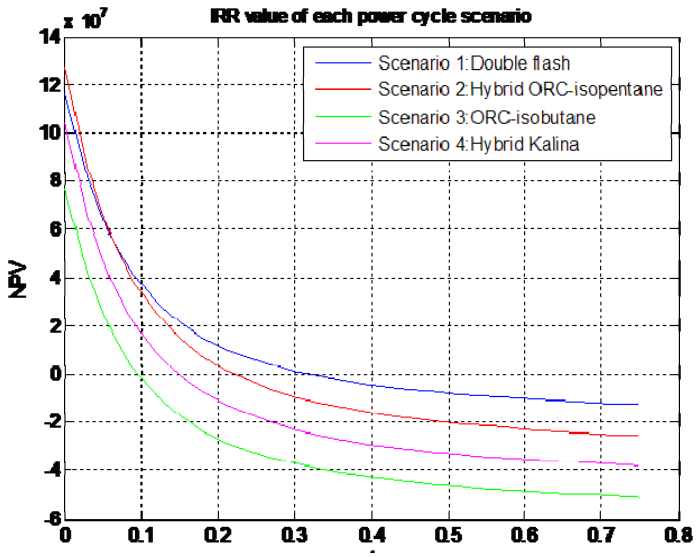

FIGURE 60: NPV as a function of rate of return of each scenario

followed by Scenario 2 as 22.15%, Scenario 4 as 14.86% and the last one Scenario 3 as 9.57%.

In a summary of cash flow series and IRR value for each alternative are shown in Table 43. The lowest total investment is from Scenario 1 and the highest revenue is from Scenario 2. The worst scenario is Scenario 3 since the IRR is the lowest and additionally it has not district heating supply capacity.

TABLE 43: Summary of cash flow series and main profitability results

Item	Cash flow (US$)			
	Scenario 1	Scenario 2	Scenario 3	Scenario 4
PV(0)	-21,733,000	-36,455,000	-59,959,000	-48,121,000
PMT(1-9)	6,976,000	8,266,000	6,902,000	7,685,000
PMT(10)	5,601,000	6,891,000	5,527,000	6,310,000
PMT(11-20)	6,976,000	8,266,000	6,902,000	7,685,000
FV	116,412,000	127,490,000	76,706,000	104,204,000
IRR	31.84%	22.15%	9.57%	14.86%

In incremental IRR principle, Scenario 1 and Scenario 2 are taken into the comparison assessment to figure out which one is more financially viable. The cash flow subtraction of two alternatives is performed to calculate the new IRR in Table 44 and Figure 61.

TABLE 44: Incremental IRR calculation of Scenario 1 and Scenario 2

Scenario 2 - Scenario 1				
Year	Net cash flow	Trial i	PW value (NPV)	IRR
0	-14,722,000	0	11,078,000	6.06%
1	1,290,000	0.01	8,557,000	6.06%
2	1,290,000	0.02	6,371,000	6.06%
3	1,290,000	0.03	4,470,000	6.06%
4	1,290,000	0.04	2,810,000	6.06%
5	1,290,000	0.05	1,354,000	6.06%
6	1,290,000	0.06	74,000	6.06%
7	1,290,000	0.07	-1,056,000	6.06%
8	1,290,000	0.08	-2,057,000	6.06%
9	1,290,000	0.09	-2,946,000	6.06%
10	1,290,000	0.1	-3,740,000	6.06%
11	1,290,000	0.11	-4,449,000	6.06%
12	1,290,000	0.12	-5,086,000	6.06%
13	1,290,000	0.13	-5,660,000	6.06%
14	1,290,000	0.14	-6,178,000	6.06%
15	1,290,000	0.15	-6,647,000	6.06%
16	1,290,000	0.16	-7,074,000	6.06%
17	1,290,000	0.17	-7,462,000	6.06%
18	1,290,000	0.18	-7,817,000	6.06%
19	1,290,000	0.19	-8,142,000	6.06%
20	1,290,000	0.2	-8,440,000	6.06%

The new IRR is calculated to be 6.06% which is much lower than the one Scenario 1 gives. In the same principle, Scenario 4 is definitely not as profitable as Scenario 1. Therefore, for only considering power generation economical viability, the Scenario 1 is the most economically feasible with the highest IRR value of 31.84%.

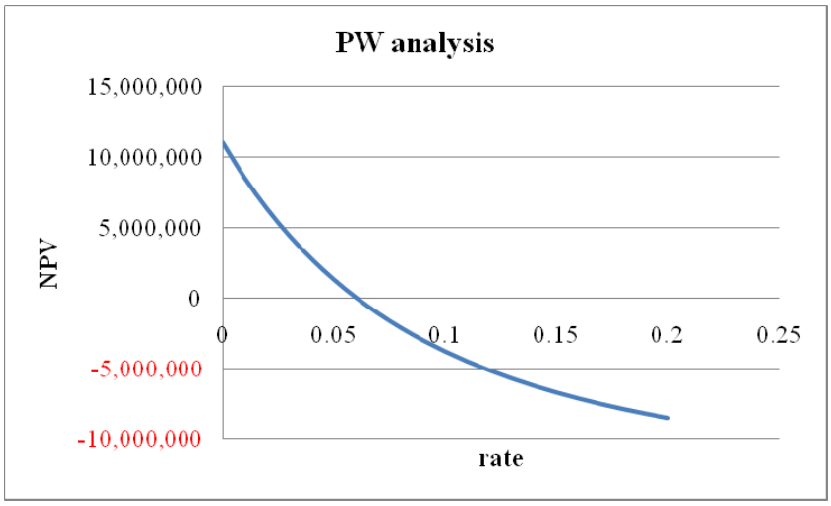

FIGURE 61: NPV as a function of rate of return in Incremental IRR analysis

6.4 District heating system economic analysis

A long distance district heating system is designed for Lhasa as detailed stated in Chapter 5. The heat capacity cannot cover the entire city of Lhasa which could meet 40% of the total demand. It's quite meaningful since it will be the first heating facility in Lhasa. The economic evaluation is vital for decision makers and related groups to figure out if the project is financially viable. The total investment cost and annual cost are estimated to make the economic analysis using PW value evaluation methods the same as the first part made for power generation assessment.

In a district heating system, the annual cost includes the annual investment cost and annual O&M cost. According to Valdimarsson (1993), the main annual cost factors are:

- Capital costs
- Pumping costs
- Maintenance
- Heat and water loss in the distribution system
- For a geothermal district heating system, the capital cost includes all the components investment cost which can be divided into three main parts:
- Supply system (well drilling and maintenance, pumps and accessories, or cogeneration power plant heat exchangers, etc)
- Distribution pipe network (construction the pipeline, pipes, connections, etc)
- Building system (radiator, pipes, control valves and accessories)

The annual O&M cost includes the pumping cost, maintenance (labour cost and repair) and heat and water loss in the distribution system. The labour cost is quite low in China, the repair work and heat water loss will not account a big proportion. The most costly part is the pumping cost in most cases. However, in this long distance geothermal district heating system, due to the big elevation difference from Yangbajain to Lhasa, there's no pumping cost. Instead, the pressure reducing stations are necessary.

6.4.1 Cost estimation

According to the pipeline calculation results, the appropriate diameter of pipeline is DN500, and the outer diameter and casing is 508/630mm. The pipe is selected as the pre-insulated standard steel pipe. The design maximum flow rate is 342kg/s, and the pipeline estimated length is 90050m. The estimated investment cost and annual cost are tabulated below. The life span of this geothermal district heating

system is 20 years as well.

In annual income estimates, as a new and first district heating system built in Lhasa, there's no ready standard to refer to. According to the local energy supply condition, comparing with other heating facilities in Tibet, using electricity heating the fee is about 55yuan/m^2, using diesel for heating it can be around 90yuan/m^2. Solar heating is more suitable for small households or remote area. The geothermal heating charge system is recommended to be differentially charged according to the function of building. It can be charged based on the heated area, therein for residential building it is 40yuan/m^2 and for public building it is 50yuan/m^2 (with no more than 3.5m height for each floor) as recommendation.

The estimates of total capital investment, the annual total cost, as well as annual total income are shown in Table 45. It is apparent that for this long distance district heating system, the investment cost is very high due to the long transmission pipeline construction. Although without pumping cost in annual cost, the recovery period is quite long. The detailed profitability evaluation is carried out in following section.

TABLE 45: Summary of economic analysis for Scenario 4

Cost estimates	Cost (USD)
1. Transmission capital investment	70,201,000
A. Purchased equipment cost (PEC)	39,378,000
Titanium heat exchanger	1,630,000
Pre-insulated Steel pipeline purchase cost (DN500, 90050m)	38,451,000
Pressure reducing valves(2 Sets)	350,000
Water source filter, deaerator and instruments	505,000
Electric control system	72,000
B. Installation cost	15,072,000
Total earth work and manual work of transmission pipeline	14,678,000
Installation all stations equipments	394,000
C. Construction related costs	15,751,000
Design and consultancy (5% of PEC)	1,969,000
Construction Cost (Cold water station, pressure reducing stations, 30% of PEC)	13,782,000
2. Distribution network capital investment (1.6million area)	8,800,000
3. Building system capital investment	32,000,000
Total capital investment	111,001,000
4. Annual O&M Costs	87,000
Labour cost (12persons, 3000yuan/month)	62,000
Pumping cold water cost	10,000
Maintenance costs	15,000
5. Annual capital cost	3,938,000
Annual depreciation costs (Economic life span of 20 years)	1,969,000
Interest rate (5% of PEC)	1,969,000
Total annual cost	4,025,000
Total annual expense	2,056,000
Annual income	9,943,000
Heating fee	9,714,000
Connection fee	229,000
Annual tax payment (3.4%)	338,000
Annual Revenue (Annual income - Annual tax)	9,605,000
Annual profit (Annual revenue -Annual expense)	7,549,000
Recovery year	14.70

6.4.2 PW value profitability evaluation

Based on the system cost estimation, a cash flow series is also performed as in Figure 62 for 20 years life span.

The profitability analysis is performed the same as the former alternatives. It is shown in Table 46.

The IRR calculation illustrates that the IRR equals to 3.13% (Figure 63). It reveals building this long distance district heating system is not so profitable.

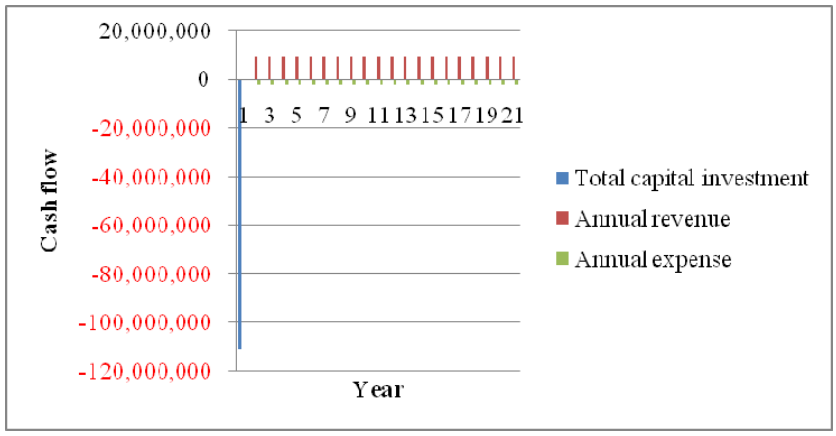

FIGURE 62: Cash flow series of district heating system

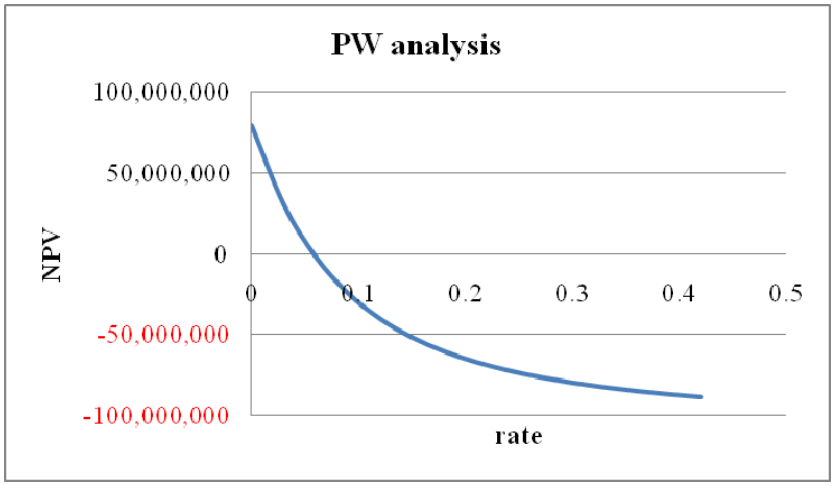

FIGURE 63: NPV as a function of rate of return of district heating system

TABLE 46: IRR calculation for district heating system

Trial i	PW value	IRR
0	39,979,000	3.13%
0.03	1,309,000	3.13%
0.06	-24,415,000	3.13%
0.09	-42,090,000	3.13%
0.12	-54,614,000	3.13%
0.15	-63,749,000	3.13%
0.18	-70,593,000	3.13%
0.21	-75,848,000	3.13%
0.24	-79,973,000	3.13%
0.27	-83,276,000	3.13%
0.3	-85,970,000	3.13%

6.5 CHP power plant combined economic analysis

As assessed in power cycle scenarios section, the most economic feasible alternative is **Scenario 1** designed as double flash cycle. In the view as an entire CHP power plant with the combination of power cycle and district heating system, By combining district heating system with the most profitable

double flash cycle, it yields integrally positive profitability. The evaluation is shown in Figure 64 and 65, and Table 47.

Therefore, the final IRR can be 8.92%. This evaluation is based on the pure commercial business consideration. It shows that only constructing power plant the IRR is 31.84%, and if combined with district heating system, the IRR is 8.92% since the profit for district heating system alone is very low as 3.13%. However, in reality, this kind of infrastructure project is normally subsidized by the central government. There will be no loan or just a small part. And for heating consumers the government will give substantial support. In this case, by assuming without paying loan interest of district heating system, the IRR can be raised to 10.78%. As the MARR of the company is defined to be 10%, then this entire project can be economically feasible.

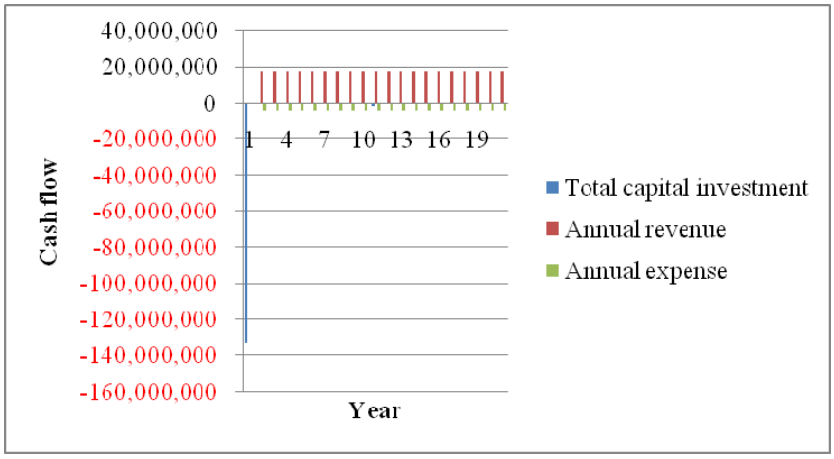

FIGURE 64: Cash flow of double flash CHP power plant

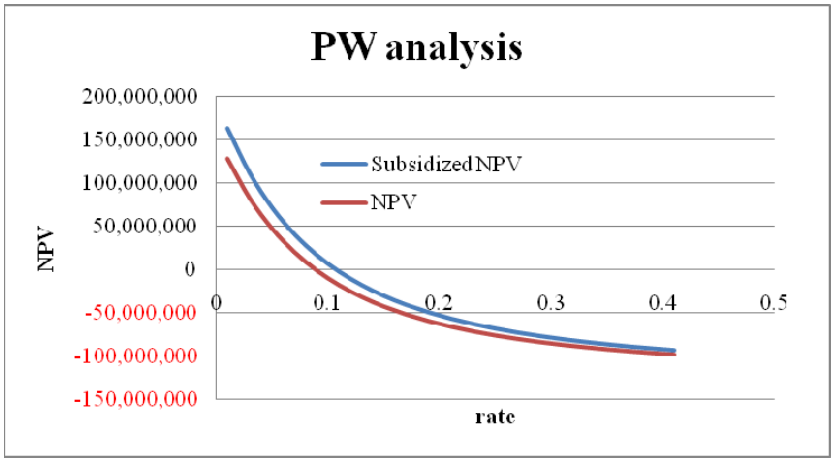

FIGURE 65: NPV as a function of rate of return for CHP plant

TABLE 47: IRR calculation for CHP and district heating system

Trial i	PW value	IRR
0.01	128,133,000	8.92%
0.03	82,338,000	8.92%
0.05	47,435,000	8.92%
0.07	20,445,000	8.92%
0.09	-723,000	8.92%
0.11	-17,551,000	8.92%
0.13	-31,105,000	8.92%
0.15	-42,157,000	8.92%
0.17	-51,277,000	8.92%
0.19	-58,885,000	8.92%
0.21	-65,300,000	8.92%

7. ENVIRONMENTAL CONCERN AND SUSTAINABLE DEVELOPMENT

Tibet Autonomous Region has unique features in geography, environment and ecology in China. It is the prime source of Asia's great rivers. It also has the world's most extensive and highest plateau, ancient forests, and many deep valleys untouched by human disturbances. But the ecological environment is very fragile at this high altitude over 4000m. Once it is damaged, the consequences can be probably irreversible. Due to the global warming and natural disasters, as well as the process of industrialization, the environmental concerns attract more and more attentions. Generally Tibet's current environmental conditions are fairly good, great care will need to be taken to protect the fragile ecology of the region. While very diverse, almost all of the ecosystem types in the Tibet Autonomous Region share one attribute - they are easily upset by over-exploitation to support human activity. The biggest challenge to Tibet's long term environmental quality is desertification driven by climate change. Experts say that average temperature on the Tibetan plateau have increased 1.5°C since 1970's, leading to drying out of lakes. More important, according to a 2001 report by the China Meteorological Administration, glacial melting in the unpopulated north and west of the Tibet has accelerated.

Under this background, the central government and local government has been making great efforts to protect environment. The new environmental policies emphasize more the sustainable development. Along with the infrastructure construction and economic development, the comprehensive and substantial contributions have been taken to protect local ecological environment. For instance, the government has spent around 1.2 billion Chinese yuan only on related to environmental protection during the construction Qinghai-Tibet railroad. The renewable energy utilization is essential to ensure the sustainable use of the Tibet's natural resources to provide a decent standard of living for its people. For long term development of geothermal resource, reinjection work is necessary and also profound. At present, due to the technical limits, the discharge geothermal fluid has not reached 100% re-injected. It has caused some pollution problems since the chemical characteristic. As well it may cause land sedimentation in the future. Therefore, in new project implementation, the reinjection must be fulfilled. The construction of transmission pipeline is as well a huge project. It is proposed to build underground as the same route of the railway. Similarly, the most attention should be paid to the environment and ecological system on the way.

8. CONCLUSIONS AND RECOMMENDATIONS

Based on the energy assessment and utilization status in Tibet, the proposed project of geothermal power generation and district heating system is designed and analyzed to investigate the technical and economical feasibility. The results show that all alternatives are technically feasible. Three of them are CHP cycle (i.e. including heating capacity), only Scenario 3 optimized as a pure ORC cycle double flash power cycle has no heating capacity. The power output of each scenario is about 18, 22, 29 and 25 MW, respectively. The thermal efficiency of each power cycle is 5.27%, 5.99%, 8.46%, 7.50%, respectively. Whereas, including heating capacity, it increases significantly to be 39.12%, 36.53%, and 37.74% for Scenario 1, 2 and 4. Therefore, Scenario 3 yields the maximum electricity at the highest efficiency of 8.46%, and Scenario 1 works at the maximum total thermal efficiency of 39.12% by producing both power and heating.

District heating system study is carried out based on the heating capacity of 114 MW from Scenario 1 which can supply 40% of the total heating demand of 273 MW. The heated water will be transferred to Lhasa via 90050 m long transmission pipeline with the diameter of DN500. The supply temperature is 85 $^{\circ}$C and the temperature drop along the pipeline is about 5 $^{\circ}$C.

The economic evaluation for all power cycles and district heating system shows that the most financially viable scenario is Scenario 1 as a double flash cycle with IRR of 31.84%, followed by Scenario 2, 4 and 3 with IRR value of 22.15%, 14.86% and 9.57% respectively. District heating system is low profitable since the high investment cost of long distance transmission pipeline with IRR of 3.13%. By combining the most financial feasible power cycle, the CHP power plant and district heating can get IRR of 8.92%. If considering the support from government, without loan interest payback, this IRR value can increase to be 10.78%, which means if MARR is 10% from the investment company, it is economically feasible.

In district heating system construction, it is recommended to develop other heating source to reduce the peak load during the severe period in winter, so that the distribution system of long distance heating system can be expanded. It would give better profitability. The other heating source is recommended to be ground source heat pump system, or in some cases, the oil or gas boiler can also be applied just for supplement the peak demand.

This research works out the optimum solution for CHP power plant in terms of technical and economical feasibility. Meanwhile, the environmental concern also should be emphasized all along. The fragile ecological and environmental conditions in Tibet urge more care when implementing such infrastructure projects especially the long distance district heating system. The construction of this project is not only an effort to improve local people's living standard, but also to prevent progressively deforestation. At the same time, the utilization of such renewable energy is also aiming for the sustainable development.

REFERENCES

Alexander, A., and de Azevedo, D., 1998: *The old city of Lhasa*. Report form a conservation project. 98-99. Website: *www.asianart.com/lhasa_restoration/report98/*

Bandoro S., R., 2006: *Thermodynamic analysis of preliminary design of power plant unit I Patuha, West Java, Indonesia.* Report 7 in: *Geothermal training in Iceland 2006*. UNU-GTP, Iceland, 83-119.

Bjornsson, O., 1980: *Cooling of water in geothermal pipes* (in Icelandic). Fjarhitun Engineering Ltd., Reykjavik, 4 pp.

Blank, L., and Tarquin, A., 2002: *Engineering economy* (5th edition). McGraw-Hill Science Engineering, US, 770 pp.

Center of Renewable Energy Development Beijing, Energy Research Institute Beijing, China, National Development and Reform Commission Beijing, China, China, 2005: *Biomass support for the China renewable energy law. Final report.* December 2005.

Ecological Improvement and Environmental Protection in Tibet, 2007: Website: *http://news.xinhuanet.com/zhengfu/2003-03/11/content_771404.htm*

Hepbasli, A., 2005: Thermodynamic analysis of a ground-source heat pump system for district heating. *Internat. J. of Energy Research*, *29,* 671–687.

Hui, R., 2007: *Electric power industry in China.* University of Wisconsin, Madison, North China Electric Power University, PSERC Tele-Seminar, Feb. 6th, 2007.

Hudson, R.B., 1988: *Electricity generation*. PB Power, Auckland, NZ.

Japanese International Cooperation Agency, 2006: *Yangbajain geothermal resource reservoir assessment and exploitation plan final report* (simplified version) *2*. JICA (in Chinese).

Karlsson, Th., 1982: *Geothermal district heating. The Iceland experience*, UNU-GTP, Iceland, report 4, 116 pp.

Lkhagvadorj, I., 2007: *District heating system design*. Department of Mechanical and Industrial Engineering, University of Iceland, in prep., 19 pp.

Nugroho, A.J., 2007: Evaluation of waste brine utilization from LHD unit III for electricity generation in Lahendong geothermal field, Indonesia. Report 17 in: *Geothermal training in Iceland 2007*. UNU-GTP, Iceland, 391-415.

Randlov, P., 1997: *District heating handbook*. European District Heating Pipe Manufacturers Association.

Valdimarsson, P., 1993: *Modelling of geothermal district heating systems.* University of Iceland, Faculty of Engineering, Reykjavik, Iceland, PhD thesis, 121 pp.

Wang H., Wei J., and Liu D., 2006: *Project proposal of district heating system by using Yangbajain power plant discharge geothermal brine in Lhasa*, *6* (in Chinese).

Weather Data Source in China, U.S. Department of Energy, Energy Efficiency and Renewable Energy, 2007: Website: *www.eere.energy.gov/buildings/energyplus/cfm/weather_data3.cfm/region=2_asia_wmo_region_2/country=CHN/cname=China*.

Zheng K., 2006: Giving full play to geothermal in renewable energy development in Tibet, China. *Proceedings of the 7th Asian Geothermal Symposium, July 25-26, 2006.*

Zhou S., Zhang X., 2005: *Prospect of briquetting biomass fuel by forest residues in Tibet of China*, Institute of Nuclear & New Energy Technology, Tsinghua University, Beijing, P.R .China.

NOMENCLATURE

A Heat transfer area, m^2
C Thermal mass of house, kJ/°C
C_p Water heat capacity, kJ/(kg °C)
D Pipe inner diameter in meters;
$h_{a,in}$ Enthalpy of the cold dry air (kJ/kg dry air), from psychometric chart;
$h_{a,out}$ Enthalpy of the hot dry air (kJ/kg dry air), from psychometric chart;
h_w Enthalpy of saturated liquid water, from steam table.
h_3 Enthalpy of the steam at inlet of the turbine, kJ/kg;
h_4 Enthalpy of the steam at actual outlet of the turbine, kJ/kg;
$h_{4,s}$ Isentropic enthalpy of the steam at outlet of the turbine, kJ/kg;
$h_{is,turb}$ Isentropic efficiency of the turbine;
k_l Overall heat transfer coefficient, W/ °C
k_p P-control parameter, kg/(s °C)
m Water mass flow, kg/s
m_0 Reference water mass flow, kg/s
P_{fan} Power input of cooling tower fan, kW
$P_{pumpcooling}$ Power input of circulating pump, kW
$P_{feedpump}$ Power input of feed pump of binary cycle, kW
Q Heat duty, W
Q_{loss0} Heat loss at reference conditions, W
Q_{loss} Heat loss, w
Q_{supp} Heat supply, W
T_1 Pipe inlet temperature (pumping station), °C
T_2 Return temperature at pumping station, °C
T_g Ground temperature, °C
T_i Indoor temperature, °C
T_{i0} Reference indoor temperature, °C
$T_{i\text{-}set}$ Desired indoor temperature in dynamic modeling, °C
T_o Outdoor temperature, °C
T_{o0} Reference outdoor temperature, °C
T_r Return water temperature, °C
T_{r0} Reference return water temperature, °C
T_s Water supply temperature, °C
T_{s0} Reference water supply temperature, °C
U Overall heat transfer coefficient, $W/(m^2\ °C)$
$U_{building}$ Heat transfer coefficient of one building, $W/(m^2\ °C)$
$U_{apartment}$ Heat transfer coefficient of one apartment, $W/(m^2\ °C)$
$V_{cooling}$ Volume flow rate of circulating cooling water, m^3/kg;
W_{actual} Actual power output of the turbo-generator, kW;
W_{shaft} Total shaft power output, kW;
W_{net} Total net power output, kW;
W_{hp} High pressure topping cycle power output, kW;
W_{ORC} ORC bottoming cycle power output, kW;
W_{Kalina} Kalina bottoming cycle power output, kW;
x Steam quality of water or working fluid, %
ΔT_m Logarithmic mean temperature difference, °C
ΔT_{m0} Logarithmic mean temperature difference at reference conditions, °C
ΔP Pressure difference, kPa;

Greek letters

$\eta_{turb.power}$ Thermal efficiency of power cycle;
$\eta_{turb.multi}$ Thermal efficiency of CHP power plant;
$\eta_{generator}$ Isentropic efficiency of the generator.
ω Ratio of water vapor to dry air in a particular height of air

τ_b Time constant;
τ Pipe transmission effectiveness
τ_0 Pipe transmission effectiveness at reference conditions
ρ Density, kg/m^3

Abbreviations used in text

ORC	Organic Rankine Cycle
NCG	Non-condensable gas
KCS34	Kalina Cycle System 34
O&M	Operation and maintenance
IRR	Internal rate of return
ROR	Rate of return
NPV	Net present value

Currency equivalents (May of 2008)
Chinese currency-yuan
US $1.00 = 7.00617Yuan
1.00 Yuan = US $0.14273
In this thesis, the rate US$1.00 = 7.00 yuan has been used.